



High Institute of Technology  
Benha University

**DYNAMIC BEHAVIOR OF TENSION LEG  
PLATFORMS SUBJECTED TO HYDRODYNAMIC  
FORCES**

by

**Amr Ramadan Ibrahim Ali El-gamal**  
(B.Sc., Civil Engineering Tech. Dept., B.H.I.T.)

A thesis submitted  
in partial fulfillment of the requirements for the degree of

**Master of Science in  
Civil Engineering Technology**

Supervised by

Dr. Ashraf M. Abou-Rayan  
Associate professor,  
Civil Engineering Tech. Dept.  
High Institute of Technology  
Benha University

Dr. Ayman A. Seleemah  
Associate professor,  
Structural Engineering Dept.  
Tanta University

**April 2011**

Copyright (©) 2011 by Amr Ramadan Ibrahim Ali El-gamal All rights reserved.  
Reproduction in whole or in part in any form requires the prior written permission of  
Amr Ramadan Ibrahim Ali El-gamal or designated representative.

The undersigned have examined the thesis entitled "**DYNAMIC BEHAVIOR OF TENSION LEG PLATFORMS SUBJECTED TO HYDRODYNAMIC FORCES**" presented by **Amr Ramadan Ibrahim Ali El-gamal** , a candidate for the degree of **Master of Science in Civil Engineering Technology** and hereby certify that it is worthy of acceptance.

Prof. Dr. El-Sayed Saad Abdel-Salam, Zagazig University

\_\_\_\_\_  
**Committee Chairperson**

Prof. Dr. Mohamad Abas Kotb, Alexandria University

\_\_\_\_\_  
**Examiner**

Dr. Ashraf M. Abou-Rayan, Benha University

\_\_\_\_\_  
**Thesis Advisor**

Dr. Ayman A. Seleemah, Tanta University

\_\_\_\_\_  
**Thesis Advisor**

Accepted for civil Engineering Technology Department:

Dr. Ahmed Hassan Abdel-Kareem

\_\_\_\_\_  
**Department Chairman**

Accepted for the Post Graduate Affairs:

Prof. Dr. Mohamad Anwer Rady

\_\_\_\_\_  
**Vice Dean for post graduate studies**

Accepted for the Institute:

Prof. Dr. Gamal Ismail Khalil

\_\_\_\_\_  
**Dean of the Institute**

## ABSTRACT

Among compliant platforms, the tension leg platform (TLP) is a hybrid structure which is generally used for deep water oil exploration. With respect to the horizontal degrees of freedom, it is compliant and behaves like a floating structure moored by vertical tubular members or “tethers”. These tethers are pretensioned due to the excess buoyancy of the platform, whereas with respect to the vertical degrees of freedom, it is stiff and resembles a fixed structure and is not allowed to float freely.

Dynamic analysis of squared and triangular TLP models under regular waves is presented, considering the coupling between surge, sway, heave, roll, pitch and yaw degrees of freedom. The analysis considers various nonlinearities produced due to change in the tether tension and nonlinear hydrodynamic drag force. The wave forces on the elements of the structure are calculated using Airy’s wave theory with Chakrabarti (1971) approaches and Morison’s equation, ignoring the diffraction effects. The nonlinear equation of motion is solved in the time domain using Newmark’s beta integration scheme.

Numerical studies are carried out in the time domain to examine the effect of change of wave parameters (wave height and wave period) and coupling effect in dynamic response of a square and a triangular TLP under a unidirectional surge wave force. Also, Numerical studies are conducted to compare the coupled response of a triangular TLP with that of a squared TLP and the effects of different parameters that influence these responses are then investigated. Computer MATLAB program is developed in this work for nonlinear dynamic analysis for both triangle and squared TLP. The program is capable of solving large displacement problem dynamically in the time domain.

## **ACKNOWLEDGEMENTS**

I would like to express my gratitude, respect and great appreciation to my supervisor, Dr. Ashraf M. Abou-Rayan, for his guidance, support and kindness. He has always been available to aid me in one way or another when difficulties seem insurmountable. It is such a great privilege to work under his supervision and to have him as my "academic father", who allowed me much freedom in defining the overall scope of this work, and yet, at the same time offered continued support, ideas and encouragement.

The same gratitude and appreciation is also due to my co-supervisor, Dr. Ayman A. Seleemah, for his support and kindness. His unique, cheerful way of teaching and conducting research has always been a source of inspiration.

Many useful and stimulating discussions with, my advisors played a role in the final development of the numerical models used in this thesis, and to them I owe my appreciation.

I am indebted to my brother, Eng. Mohammed Ramadan for his assistance in the development in some of computer programs.

Finally, to my family, I owe great thanks, for their help in typing part of the manuscript, and particularly for their support and understanding.

Amr Ramadan Ibrahim Ali

Benha University, H.I.T, Egypt

April 2011

# CONTENTS

	Page
<b>Abstract</b> .....	iv
<b>Acknowledgements</b> .....	v
<b>Contents</b> .....	vi
<b>List of Figures</b> .....	ix
<b>List of Tables</b> .....	xii
<b>Nomenclature</b> .....	xiii
<b>Abbreviation</b> .....	xix
<b>Chapter 1: Introduction</b> .....	1
1.1 Introduction .....	1
1.2 Platform Types .....	2
1.2.1 Platform Function .....	3
1.3 Platform Structural Types .....	4
1.3.1 Fixed Offshore Platforms .....	6
1.3.2 Compliant Offshore Platforms .....	8
1.3.3 Mobile Offshore Platforms .....	10
1.4 Literature Review .....	17
1.5 Aim of this Thesis .....	25
1.6 Organization of Dissertation .....	25
<b>Chapter 2: Hydrodynamic Loads</b> .....	27
2.1 Introduction .....	27
2.2 Theory of Linearized Gravity Waves .....	28

2.3	Surface Elevation Modification.....	36
2.4	Wave Force.....	39
2.4.1	Wave Force Regimes .....	40
2.4.2	Morison Equation .....	41
2.4.3	Modified Morison Equation.....	44
2.4.4	Modified Morison Equation for Inclined Cylinder .....	46
<b>Chapter 3:</b>	<b>TLP Dynamic Analysis .....</b>	<b>48</b>
3.1	Introduction .....	48
3.1.1	Structural Idealization and Assumptions .....	49
3.1.2	Mathematical Model of TLP.....	50
3.2	Development of a Rectangular tension leg platform.....	56
3.2.1	Draft Evaluation .....	56
3.2.2	Stiffness Matrix of the Rectangle TLP Configuration .....	56
3.2.3	Mass Matrix, $[M]$ .....	68
3.2.4	Structural Damping .....	73
3.2.5	Hydrodynamic Force Vector, $\{F(t)\}$ on Rectangular .....	73
3.3	Development of a triangular Tension Leg Platform.....	83
3.3.1	Draft Evaluation .....	83
3.3.2	Stiffness Matrix of the Rectangle TLP Configuration .....	83
3.3.3	Mass Matrix, $[M]$ .....	95
3.3.4	Structural Damping .....	100
3.3.5	Hydrodynamic Force Vector, $\{F(t)\}$ on Rectangular .....	101
3.4	Solution of Equation of Motion in Time Domain analysis .....	110

<b>Chapter 4: Case Study</b> .....	112
4.1 Introduction .....	112
4.2 Result and Discussions .....	117
4.2.1 Response of Square TLP .....	118
4.2.2 Response of Triangular TLP .....	120
<b>Chapter 5: Conclusions and Recommendations</b> .....	134
5.1 Introduction .....	134
5.2 Conclusions .....	135
5.3 Recommendations .....	137
<b>References</b> .....	138
<b>Appendix A: Newmark's <math>\beta</math> method</b> .....	143
<b>Appendix B: Program Flow Chart</b> .....	145
<b>Vita</b> .....	147



## LIST OF FIGURES

	Page
Figure 1.1: 1,2) Conventional fixed platforms; 3) compliant tower; 4,5) Vertically moored tension leg and mini-tension leg platform; 6) Spar; 7,8) Semi-submersibles; 9) Floating production, storage, and offloading facility; 10) Sub-sea completion and tie-back to host facility. <a href="http://www.mms.gov">www.mms.gov</a> .....	5
Figure 1.2: The scheme of steel jacket platform <a href="http://www.mms.gov">www.mms.gov</a> .....	11
Figure 1.3: The scheme of steel tower platform <a href="http://www.mms.gov">www.mms.gov</a> .....	12
Figure 1.4: The scheme of steel gravity platform <a href="http://www.paroscreennc.com">www.paroscreennc.com</a> .....	13
Figure 1.5: The scheme of concrete gravity platform <a href="http://www.ogp.org.uk">www.ogp.org.uk</a> .....	13
Figure 1.6: The scheme of free standing tower <a href="http://www.offshore-technology.gov">www.offshore-technology.gov</a> .....	14
Figure 1.7: The scheme of guyed tower <a href="http://www.offshore-technology.gov">www.offshore-technology.gov</a> .....	14
Figure 1.8: The scheme of tension leg platform.....	15
Figure 1.9: The scheme of drilling ships <a href="http://www.offshore-technology.gov">www.offshore-technology.gov</a> .....	16
Figure 1.10: The scheme of jack-ups <a href="http://community.webshots.com/album/126570186zwqfus">http://community.webshots.com/album/126570186zwqfus</a> .....	16
Figure 1.11: Six degree of freedom of offshore structure .....	17
Figure 2.1: The wave propagation for linear wave theory .....	35
Figure 2.2: The ranges of suitability for various theories .....	35
Figure 2.3: The comparison of vertical distribution of horizontal water particle velocity for (A) Airy which is limited to MWL,(B)Extrapolation of linear wave theory,(C) Stretching of linear wave theory and (D) Modified linear wave theory "Chakrabarti" .....	37

Figure 2.4: Wave force on a vertical cylinder .....	43
Figure 2.5: A flexible cylinder .....	45
Figure 2.6: Sketch of wave loading on an inclined cylinder .....	47
Figure 3.1: Wind and wave spectra relative to the fixed and TLP structures (Kareem, 1987).....	53
Figure 3.2: The global and local coordinate system of TLP .....	53
Figure 3.3: The rectangular TLP (plan and elevation) .....	57
Figure 3.4: The Surge displacement in a rectangular TLP.....	61
Figure 3.5: The Sway displacement in a rectangular TLP .....	61
Figure 3.6: The Roll displacement in a rectangular TLP .....	64
Figure 3.7: The Pitch displacement in a rectangular TLP .....	66
Figure 3.8: The Yaw displacement in a rectangular TLP.....	69
Figure 3.9: The triangular TLP (plan and elevation).....	84
Figure 3.10: The Surge displacement in a triangular TLP .....	87
Figure 3.11: The Sway displacement in a triangular TLP .....	87
Figure 3.12: The Roll displacement in a triangular TLP .....	89
Figure 3.13: The Pitch displacement in a triangular TLP .....	94
Figure 3.14: The Yaw displacement in a triangular TLP.....	98
Figure 4.1: Layout of the studied square TLP .....	115
Figure 4.2: Layout of the studied Triangular TLP .....	116
Figure 4.3: Surge response of square TLP for (a) wave period = 8 sec; (b) wave period = 10 sec; (c) wave period = 12.5 sec; (d) wave period = 15 sec .....	123

Figure 4.4: Heave response of square TLP for (a) wave period = 8 sec; (b) wave period = 10 sec; (c) wave period = 12.5 sec; (d) wave period = 15 sec .....	124
Figure 4.5: Pitch response of square TLP for (a) wave period = 8 sec; (b) wave period = 10 sec; (c) wave period = 12.5 sec; (d) wave period = 15 sec .....	125
Figure 4.6: Response Spectrum for pitch motion of square TLP for different wave periods (wave height = 8.0m) .....	126
Figure 4.7: Tether tension force response of square TLP for (a) wave period = 8 sec; (b) wave period = 10 sec; (c) wave period = 12.5 sec; (d) wave period = 15 sec .....	127
Figure 4.8: Phase plane for coupled motion of square TLP (a) Wave period = 10 sec; (b) Wave period = 15 sec .....	128
Figure 4.9: Surge response of triangular TLP for (a) wave period = 8 sec; (b) wave period = 10 sec; (c) wave period = 12.5 sec; (d) wave period = 15 sec .....	129
Figure 4.10: Heave response of triangular TLP for (a) wave period = 8 sec; (b) wave period = 10 sec; (c) wave period = 12.5 sec; (d) wave period = 15 sec .....	130
Figure 4.11: Pitch response of triangular TLP for (a) wave period = 8 sec; (b) wave period = 10 sec; (c) wave period = 12.5 sec; (d) wave period = 15 sec .....	131
Figure 4.12: Tether tension force response of triangular TLP for (a) wave period = 8 sec; (b) wave period = 10 sec; (c) wave period = 12.5 sec; (d) wave period = 15 sec .....	132
Figure 4.13: Phase plane for coupled motion of triangular TLP (a) Wave period = 10 sec; (b) Wave period = 15 sec .....	133

## LIST OF TABLES

	Page
Table 1.1: Different types of offshore structures.....	5
Table 2.1: The linear theory different relationship.....	38
Table 2.2: Asymptotic forms of hyperbolic functions.....	34
Table 4.1: Geometric properties of the square TLP and load data.....	113
Table 4.2: Geometric properties of the triangular TLP and load data.....	114
Table 4.3: Calculated natural structural periods for different analysis cases (in seconds) for the four-legged tension leg platforms .....	114
Table 4.4: Calculated natural structural periods for different analysis cases (in seconds) for the three-legged tension leg platforms .....	114

## NOMENCLATURE

$\phi$ : Fluid velocity potential

$u$ : Fluid velocity component in x-direction

$w$ : Fluid velocity component in z-direction

$\eta$ : Distance between MWL and free surface level

$\vec{v}$ : Total velocity vector

$\nabla F$ : Fluid gradient function

$\vec{n}$ : Unit normal vector associated with gradient function

$P_n$ : Pressure

$\lambda$ : Wave length

$d$ : Water depth

$k$ : Wave number

$\omega$ : Wave angular frequency

$c$ : Wave celerity

$D$ : Diameter of structure

$A_s$ : Cross-sectional area

$g$ : Gravity acceleration

$\rho$ : Water weight density

$C_m$ : Inertia coefficient

$C_d$ : Drag coefficient

$U_c$ : Current velocity

$T$ : Wave period

$H$ : Wave height

$W$ : Platform weight

$2a$ : Square platform length

$2b$ : Square platform width

$Pl$ : Triangle platform length

$r_x$ : Platform radius of gyration in x-directions

$r_y$ : Platform radius of gyration in y-directions

$r_z$ : Platform radius of gyration in z-directions

$r_i$ : The location of the mass center with respect to the platform- fixed coordinate system

$j_{ii}$ : Moments of inertia in I- direction

$j_{ij}$ : Products of inertia in I- direction

$[M_a]$ : Structure added mass matrix

$D_c$ : Diameter of columns

$H_C$ : Center of gravity above the sea level

$\gamma$ : Tether stiffness

$L$ : Tether length

$D_p$ : Diameter of pontoon

$D_r$ : Draft distance

$\zeta$ : Damping ratio

$\{x\}$ : Structural displacement vector

$\{\dot{x}\}$ : Structural velocity vector

$\{\ddot{x}\}$ : Structural acceleration vector

$[M]$ : Structure mass matrix

$[C]$ : Structure damping matrix

$[K]$ : Structure stiffness matrix

$\{F_o(t)\}$ : Hydrodynamic force vector

$M$ : Mass of the body

$F_B$ : Total buoyancy force

$T_i$ : Total instantaneous tension in the Tether

$T_o$ : Initial pre-tension in the tether

$S_a$  : Length of the pontoon between the inner edges of the columns in the x-direction

$S_b$ : Length of the pontoon between the inner edges of the columns in the y-direction

$[c_s]$ : Structure damping mass matrix

$[B]$ : Radiation damping matrix

$[c_H]$  :Hydrodynamic drag damping and is included in the force vector

$[c_w]$ : Aerodynamic damping

$\{\phi_n\}$ : Mode shapes vector

$\omega_n$  : Structure's natural frequencies

$A$ : Cross-sectional area of the tether

$E$ : Young's Modulus of the tether

$\Delta T_1$ : The increase in the initial pre-tension due to the arbitrary displacement given in the surge degree of freedom

$\Delta T_2$ : The increase in the initial pre-tension due to the arbitrary displacement given in the sway degree of freedom

$\Delta T_3$ : The increase in the initial pre-tension due to the arbitrary displacement given  
in the heave degree of freedom

$\Delta T_4$ : The increase in the initial pre-tension due to the arbitrary displacement given  
in the roll degree of freedom

$\Delta T_5$ : The increase in the initial pre-tension due to the arbitrary displacement given  
in the pitch degree of freedom

$\Delta T_6$ : The increase in the initial pre-tension due to the arbitrary displacement given  
in the yaw degree of freedom

$x_1$ : Arbitrary displacement in the surge degree of freedom.

$x_2$ : Arbitrary displacement in the sway degree of freedom.

$x_3$ : Arbitrary displacement in the heave degree of freedom.

$x_4$ : Arbitrary displacement in the roll degree of freedom.

$x_5$ : Arbitrary displacement in the pitch degree of freedom.

$x_6$ : Arbitrary displacement in the yaw degree of freedom.

$\delta_x$  : The angle between the initial and the displaced position of the tether for unit  
displacement given in the surge direction

$\delta_y$  : The angle between the initial and the displaced position of the tether for unit  
displacement given in the sway direction

$U_v$ : Body velocity in surge direction

$U_x$ : Body velocity in heave direction

$FI_{ic}$ : Inertia surge force on columns

$FI_{icj}$ : Inertia surge force on column j



$F1_{cd}$ : Drag surge force on columns

$F1_{dcj}$ : Drag surge force on column j

$F1_{ip}$ : Inertia surge force on pontoons

$F1_{ipj}$ : Inertia surge force on pontoon j

$F1_{dp}$ : Drag surge force on pontoons

$F1_{dpj}$ : Drag surge force on pontoon j

$F1_1$ : Total surge force on TLP

$F3_c$ : Heave force on columns

$F3_{cj}$ : Heave force on column j

$F3_{ip}$ : Inertia heave force on pontoons

$F3_{ipj}$ : Inertia heave force on pontoon j

$F3_{dp}$ : Drag heave force on pontoons

$F3_{dpj}$ : Drag heave force on pontoon j

$F3_1$ : Total heave force on TLP

$MH_{ip}$ : Inertia moment on pontoons due to surge force

$MH_{ipj}$ : Inertia moment on pontoon j due to surge force

$MH_{dp}$ : Drag moment on pontoons due to surge force

$MH_{dpj}$ : Drag moment on pontoon j due to surge force

$MH_p$ : Total moment on pontoons due to surge force

$MH_{ic}$ : Inertia moment on columns due to surge force

$MH_{icj}$ : Inertia moment on column j due to surge force

$MH_{dc}$ : Drag moment on columns due to surge force

$MH_{dcj}$ : Drag moment on column j due to surge force

$MH_c$ : Total moment on columns due to surge force

$MH$ : Total moment on TLP due to surge force

$MV_{ip}$ : Inertia moment on pontoons due to heave force

$MV_{ipj}$ : Inertia moment on pontoon j due to heave force

$MV_{dp}$ : Drag moment on pontoons due to heave force

$MV_{dpj}$ : Drag moment on pontoon j due to heave force

$MV_p$ : Total moment on pontoons due to heave force

$MV_c$ : moment on columns due to heave force

$MV_{cj}$ : moment on column j due to heave force

$MV_c$ : Total moment on columns due to heave force

$MV$ : Total moment on TLP due to heave force

$F_{5I}$ : Total pitch moment on TLP

## **ABBREVIATION**

TLP: Tension Leg Platform

FPS: Floating Production System

GPS: Global Position System

ISSC: International Ship Structure Conference

PSDF: Power Spectral Density Function

MWL: Mean Water Level

SWL: Still Water Level

MSL: Mean Sea Level

*To the memory of my father,  
a humble teacher,  
who had always encouraged me to dream;  
and to my mother,  
who with constant love and care,  
taught me how to persevere  
and turn the dream into a reality.*

# Chapter 1

## INTRODUCTION

### 1.1 Introduction

A significant part of the world oil and natural gas reserves lies beneath the sea bed. The drilling and production operation to exploit this offshore oil and gas supplies is generally done from offshore platforms.

In 1947, the first steel platforms were installed for offshore in the Gulf of Mexico, in 20 ft (6 m) of water. The structures were supported by a large number of small piles, driven at varying depths and directions. In 1955, a platform was constructed in approximately 100 ft (30.5 m) of water. The maximum water depth for offshore platforms construction was extended to 225 ft (68.6 m) by 1965 and to 474 ft (144.5 m) by 1975. In 1975, the Hondo platform was installed by Exxon in 850 ft (259 m) of water in the Santa Barbara channel of California. This was followed in 1978 by Shell's Cognac platform in the Mississippi Canyon area in the Gulf of Mexico. Since then several offshore platforms were installed in the Gulf of Mexico in water depths greater than 900 ft (274 m).

It is expected that pile-supported platforms will be limited to a maximum water depth of 1200-1500 ft (366-457 m), primarily owing to the cost of fabrication and certain installation constraints. However, new types of platforms such as guyed towers and tension leg platforms, which are designed to move with forces applied by wind, wave and current, rather than rigidly resist them, offer promise of extending platform capability significantly.

The first guyed tower, used as a drilling and production platform, Lena, was installed by Exxon in 1000 ft (305 m) of water in the Gulf of Mexico in 1983. It is a slender, bottom supported tower laterally braced by cable stays. This type of structures is cost effective in 2000-2500 ft (609.9-762 m) of water.

The first tension leg platform used as a drilling and production platform was installed by Conoco in 485 ft (147.8 m) of water in the North Sea in 1984. This structure

is a floating platform supported by submerged buoyant members and held in place by vertical moorings, making the platform less sensitive to water depths. It is believed that this type of platform can be cost effective in water depths exceeding 3000 ft (914.4 m).

Until 1986 over 3500 platform structures were standing in the offshore waters of more than 35 countries. Although, most of these platforms have successfully withstood the forces of nature, there have been major damages and some catastrophic failures. Off the Louisiana coast alone, in the two-year period between 1957 and 1959, there was an estimated damage of about 200 million dollars in Losses of 10 drilling, production and pipeline facilities. These resulted from two major hurricanes, the Hilda and Betsy. In 1980 the Alexander Kielland, a semi- submersible rig, failed and sank in the Norwegian sector of North Sea, killing the entire crew of 123 on board. Another accident involving the floating platform, Ocean Ranger killed all the crew on board in 1982. These accidents reflect inadequacy in the design and analysis or in the operational procedures adopted. The rules for the design and analysis have been continually modified to reflect increased understanding of the situation. However, there are several areas that still require more understanding and need more reliable analytical models. The assessment of hydrodynamic loads is one such area. These loads result primarily from the effects of water currents and wave actions. The effect of current is relatively easy to assess. However, the action of waves is significantly more complex, and difficult to analyze. The difficulty lies both in modeling the wave motion itself, and in accounting for the irregular nature of the waves in a real ocean.

## **1.2 Platform Types**

Offshore platforms consist broadly of two components: (1) facilities for drilling and production operations, often called topsides, and (2) the supporting structure and its foundation. The topsides define the function of the platform. Included in the topside plant are the drilling rigs and associated equipment, oil and/or gas-processing equipment, transportation pumps and/or compressors, utilities and living quarters. Most major platforms also have a helideck for helicopters. The second component of an offshore platform, and the one that defines its type, is the supporting structure. Such structures

must secure the topside facilities against environmental loads, providing safe and protected area for equipment and personnel to work.

The arrangement of structures and employment of production facilities at a specific location are influenced by reservoir capacity, production rate, field size, field shape, environmental conditions, and water depth. Other factors affecting the selection of an offshore platform are availability of construction materials, proximity and capability of fabrication facilities, availability of installation equipment, and equipment considerations such as capital cost, time to start up, and operating and maintenance costs.

Platform types are classified in two groups according to their function and structural supports as:

### **1.2.1 Platform Function**

Because the platform supports the operating function for which it is required, the function dictates the basic configuration of a platform.

#### **1.2.1.1 Drilling Platforms**

Structures that provide lateral support to one or more wells drilled with a mobile drilling rig are normally referred to as well protector platforms. These are undoubtedly the most common platforms in service today. Generally found in water depths less than 150 ft (45.7 m), these structures are small, often straight-sided, and normally sized to fit within the drilling slot of a submersible or jack-up drilling rig.

There are usually three or four pile structures with minimum size decks, they provide only minimum production facilities, if any, and their wells are most frequently connected by pipe lines to nearby production facilities.

#### **1.2.1.2 Production Platforms**

Some owners prefer to separate drilling operations from production operations because of safety considerations. The production platform is connected by bridge or pipeline to the drilling platform.

### **1.2.1.3 Self-Contained Drilling and Production Platforms**

Many structures are designed to serve the combined functions of drilling platforms and production platforms, these structures contain the wells and all the required drilling equipment and supplies, and provide the required space for production facilities. The standard self-contained platform is typically a two-deck, eight-pile, and template-type structure with provisions for 12-24 wells. The drilling rig is generally installed on the upper deck, and the basic production facilities are placed on the lower deck, separated from the wellhead area by a firewall.

### **1.3 Platform Structural Types**

Offshore platforms are usually divided into two general categories (Table 1.1), (Figure 1.1), fixed and compliant platforms. Fixed types are traditional structures, extend to the seabed and remain in place by their weight or by piles driven into the soil, in the sense that its deformation under lateral loads is small, but it is located into the sea water. Unlike fixed, compliant platforms are more responsive to external effects and their movements are controlled by mooring systems. They are designed to move under lateral forces, so that the effects of these forces are mitigated. Compliant platforms are used in deep water, where the stiffness of a fixed platform decreases while its cost increases, and they are the only technical solution in very deep water (>500 m).

The increase in cost of fixed offshore structures with depth of water encouraged the development of compliant- type structures. The key idea behind their installation is the minimization of the resistance of the structure to environmental loads by making the structure flexible.



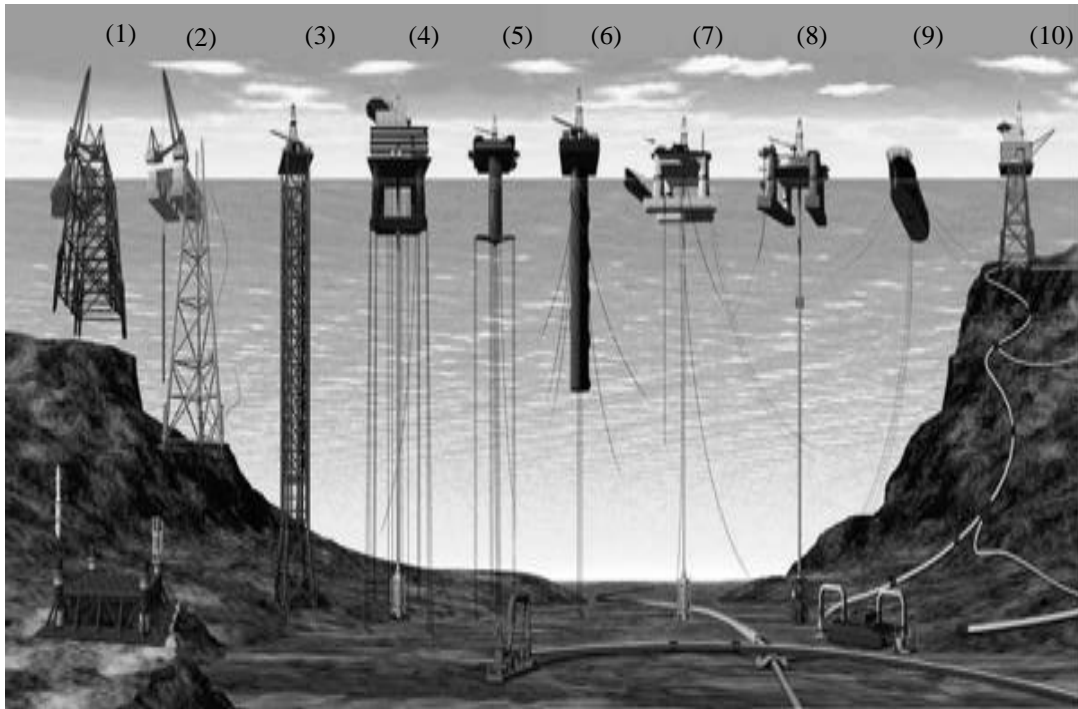


Figure 1.1: 1,2) Conventional fixed platforms; 3) compliant tower; 4,5) Vertically moored tension leg and mini-tension leg platform; 6) Spar; 7,8) Semi-submersibles; 9) Floating production, storage, and offloading facility; 10) Sub-sea completion and tie-back to host facility. ([www.mms.gov](http://www.mms.gov))

Table 1.1: Different types of offshore structures.

Classification	Type	Function	Control mooring
Fixed offshore platform	Steel jacket -Steel tower -Steel gravity - Concrete gravity	production	-
Compliant offshore platform	Free standing tower -Guyed tower - Spar tower -Tension leg platform(TLP)	production	Anchor wire pipe tethers
Mobile offshore platform	Drilling ship - Jack up -Semi submersible	Exploration and drilling	Wire DP-legs

### **1.3.1 Fixed Offshore Platforms**

#### **1.3.1.1 Steel Jacket**

This is a space frame that extends from the sea bottom to above the water surface. Piles are driven through the legs of the jacket into the sea floor (Figure1.2). These transfer vertical loads to the soil and fix the structure in place against lateral loads from wind, Waves, currents and collisions with ships or ice bergs. The bending stiffness of the piles contributes to the lateral stiffness of the structure and thus they are rigidly connected to the structure and are placed as far away from each other as possible. Steel jackets are normally used in shallow to moderate deep waters (from 20 to 100 m), but they have been used up to 500 m of water. Their natural period ranges from 1 to 5 seconds. The natural period of the jacket type structure increases with the increase in water depth until it becomes close to the period of the peak wave energy which leads to a large dynamic magnification.

#### **1.3.1.2 Steel Tower**

It is a large jacket where the piles cannot be inserted in the legs mainly for economical reasons (Figure1.3). In fact, too long piles are too expensive. So, when the platform is located in deep waters, the jacket becomes very heavy and the piles cannot be as long as the legs. They become skirt piles inserted in sleeves around the outside of the legs. In this way, the legs are plugged and normally sufficient to ensure resistance of the buoyancy. This is very convenient from both economical and construction aspects.

#### **1.3.1.3 Steel gravity platforms**

This type of structure is rarely used. It uses its own weight to counter the lateral actions due to wind and waves that tend to overturn the platform, the weight is used as a stabilizing force (Figure1.4). The real reason for using gravity platforms is the nature of the soil, when it is of solid rock, it is impossible to drive piles into it, so the gravity solution is the only possible one. Normally, gravity platforms are concrete platforms, but in some cases a steel solution can be adopted, in relation with several factors, mainly economic considerations. Normally, the structure has a certain number of large tanks, flooded by water or by crude oil, to ballast the platform and provide the necessary weight

to counter overturning lateral forces. An important feature of all the gravity platforms is that they can be removed for demobilization or re-use.

#### **1.3.1.4 Concrete Gravity Platforms**

They are the hugest and most impressive structures ever built. In this platform, the steel structure supporting the deck is totally or partially replaced by a concrete structure of large dimensions (Figure1.5). It consists of cluster of oil storage tanks surrounding hollow, tapered concrete legs that extend above the water line to support a steel deck. Concrete gravity platforms are used when some particular circumstances are present:

- a. Economical factors: in some cases, the construction of a very large concrete structure can be cheaper than the construction of a steel structure;
- b. Ecological factors: a concrete platform can be very huge, so as to concentrate onboard some industrial treatments of the crude and to allow a great stocking capacity in the ballast cells;
- c. Construction conditions: the pile driving operation for a steel jacket needs usually 5 to 10 days; in the North Sea it is rare to have such a period of fine weather; the installation in the oil field of a concrete gravity platform, complete with its deck, requires a shorter period (1 to 2 days);
- d. Decommissioning aspects: concrete gravity platforms can be decommissioned and eventually re-used;
- e. Soil conditions: when the soil is made of rock it is impossible to drive piles into it: the gravity solution is then the only one possible;
- f. Geographical conditions: the presence of calm and deep waters not far from the oil field is an important factor for the construction phases.

These structures can reach a height of 400 m and weigh more than 800000 ton.

### **1.3.2 Compliant Offshore Platforms**

#### **1.3.2.1 Free Standing Towers**

They are classical towers but so slender that their structural behavior is similar to that of a compliant structure with large sway displacements and high oscillating period (Figure 1.6).

#### **1.3.2.2 Guyed Towers**

It consists of a uniform cross section held by several guy lines (anchor cables) supported by clump weights resting on the sea floor (Figure 1.7). Under normal operating loads, the clump weights remain on the sea floor forming a mooring system. Under severe environmental loads, the clump weights are lifted off the sea floor. Therefore, the tower acts as pinned tower at its base and absorbs the loads by swaying back and forth without overloading the guy lines. Guyed tower platforms are used for water depth of about 660 m.

#### **1.3.2.3 Spar Towers**

These platforms are composed of a large steel tube as substructure directly supporting the deck and topsides. The tube is ballasted so as its floating stable equilibrium position is vertical (including topsides), and moored by tensioned risers and by mooring lines (catenaries). On the lateral surface of the large vertical cylinder there are helicoids, installed to counter vortex-shedding.

#### **1.3.2.4 Tension Leg Platforms (TLP)**

The TLP is basically a floating structure moored by vertical tubular member, or "tethers". These tethers are pretensioned due to the excess buoyancy of the platform. As, the platform translates horizontally, the horizontal component of the pretension in the tethers tends to force the platform back to its original position (Figure 1.8). The TLP is compliant in horizontal plane, but quite rigid in the vertical direction. The TLP has a six degree of freedom, shown in Figure 1.11. The concept of TLP has been in existence since the early 1970's.

A TLP is composed of 4 principal parts: the foundation template, the tethers, the hull and the deck. Some TLPs (e. g. Heidrun) have a concrete hull. TLPs are very large structures, able to host great payloads. So, they are used for great fields and can host some refining processes and have a good storage capacity TLP can be used from 150 m of water depth on, and theoretically there is no limit of water depth for their use. The restoring force is given by extra buoyancy; this is obtained deballasting the TLP hull once the tethers installed. TLPs can be reused.

The long periods of vibration associated with the compliant structures prevents dynamic amplification of the response due to first order waves, since there is little or no energy associated with the wave forces for long periods. While these long periods of vibration remove any concern associated with dynamic amplification of first order wave loads, wind loads and second order non-linear wave loads can be of importance.

Most of the energy associated with wind loading occurs at periods of about 40 seconds and longer, and as a result, dynamic amplification of the response due to wind loads may be of prime importance in estimating the response of compliant structure to environmental loads. The cost for other offshore structures will rise more rapidly than that of TLP in deep-water reservoirs. The TLP is essentially advantageous for the following reasons:

1. It attracts a lesser impact of the wave loading due to its compliant nature and hence can operate even in rough sea.
2. The natural frequencies in the main or soft degrees of freedom (surge, sway and yaw) are well below the wave frequencies, thus avoiding the occurrence of resonance and reducing the horizontal motion and hence loading on the tether platform system.
3. It is less expensive than the bottom-supported structures, especially in deep seas.
4. It can be easily dismantled, installed and transported according to site requirements. Where, the change in the water depth essentially requires a change in the tether length.
5. It is much safer in a seismically active zone compared with any other fixed platform.

6. Because of the restrained vertical motion of the TLP, it is quite convenient to monitor and maintain the risers, oil wells and tethers.
7. A particularly attractive feature of the TLP is the ability to shift any resonance outside the frequency region of the active wave energy.

### **1.3.3 Mobile Offshore Platforms**

#### **1.3.3.1 Drilling Ships**

Like all the mobile systems, drilling ships are used mostly for the drilling phase, but they can be used, at least temporarily, also as Floating Production System (FPS). A drilling ship is, as its name indicates, a common ship equipped with a drilling system (a derrick tower) (Figure1.9). It is maintained in its position by a system of mooring catenaries, eventually assisted by servo-motors and GPS positioning.

#### **1.3.3.2 Semi-Submersibles**

As their name indicates, these are special ships, normally composed of two pontoons, some columns and a deck. The deck is equipped for all the drilling operations. A semi-submersible is a complete platform that can navigate as it is furnished of motors. Once in place, its positioning is provided by a system of catenaries normally controlled by a GPS system. Recently a concrete semi-submersible has been constructed.

#### **1.3.3.4 Jack-Ups**

These are special mobile platforms, normally used for the drilling operations (Figure1.10). They are triangular barges, completely equipped for the drilling operations and disposing of three or four truss legs. These legs can be lifted or lowered by motors. When the legs are lifted, the jack-up can navigate just as a common ship. Once arrived on the field, the jack-up lowers the legs so as to be fixed in the drilling place and it lifts itself at the right height above the sea level.

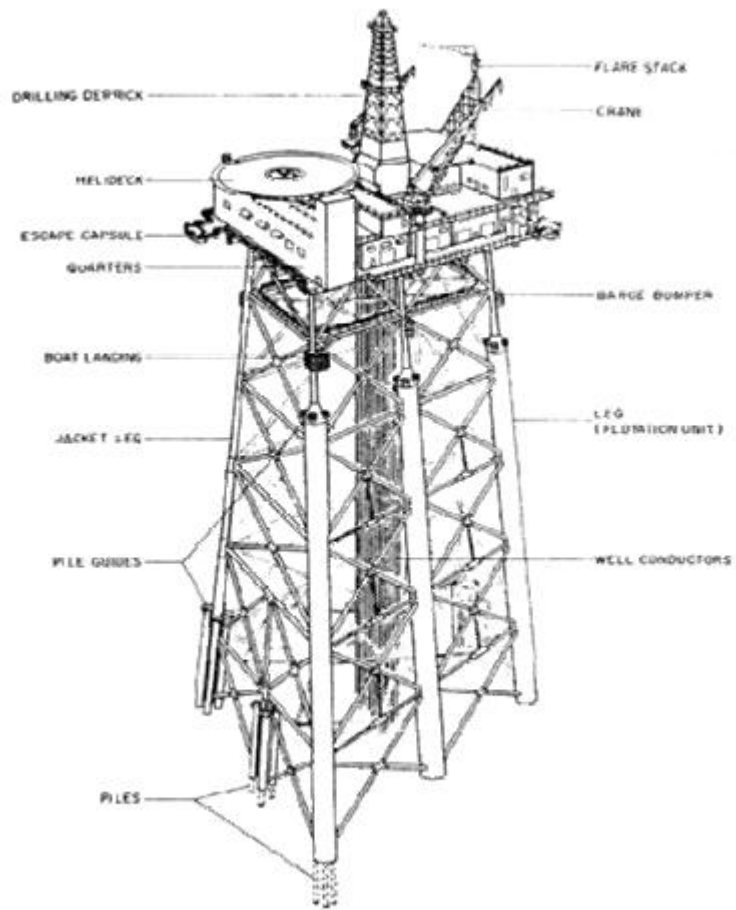


Figure 1.2: The scheme of steel jacket platform ([www.mms.gov](http://www.mms.gov))

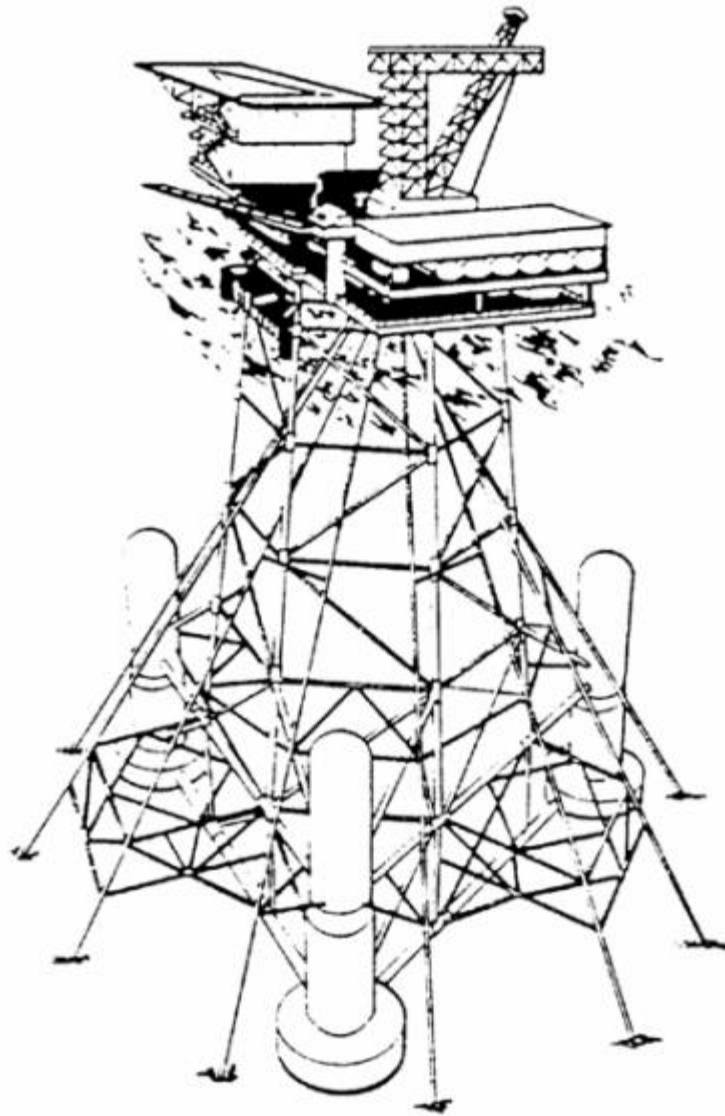


Figure 1.3: The scheme of steel tower platform ([www.mms.gov](http://www.mms.gov))





Figure 1.4: The scheme of steel gravity platform ([www.paroscreen.com](http://www.paroscreen.com))



Figure 1.5: The scheme of concrete gravity platform ([www.ogp.org.uk](http://www.ogp.org.uk))

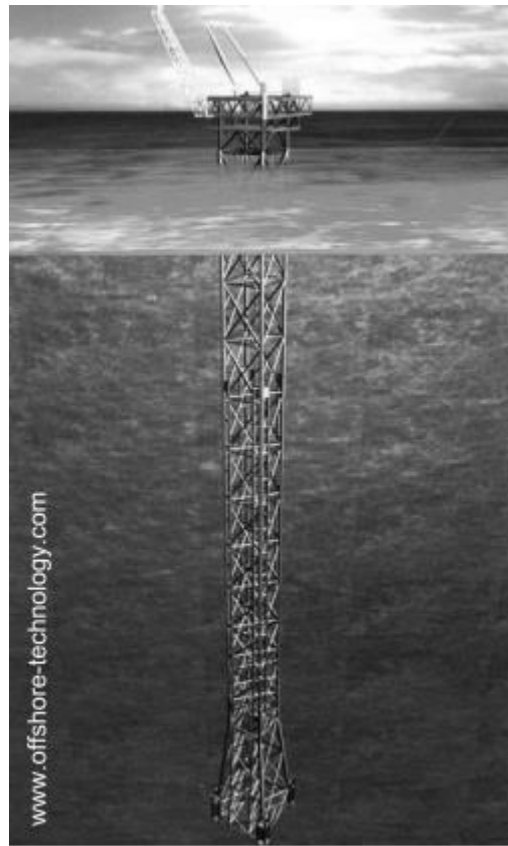


Figure 1.6: The scheme of free standing tower ([www.offshore-technology.gov](http://www.offshore-technology.gov))

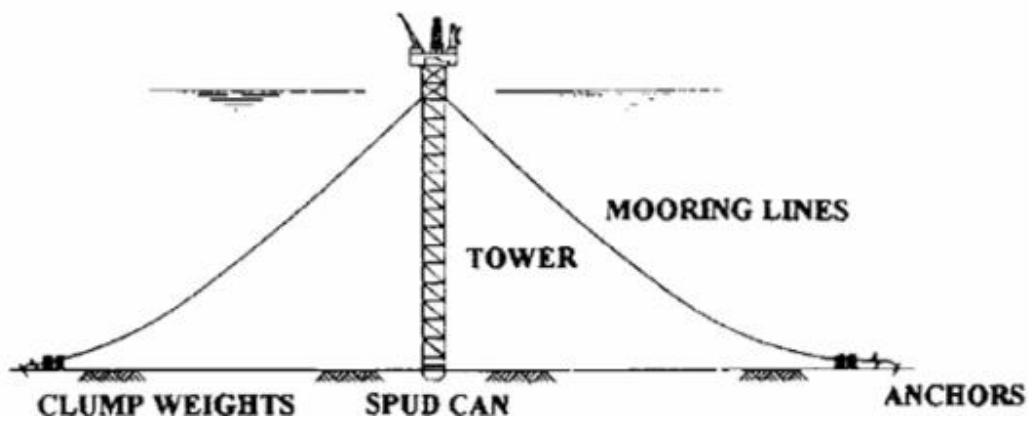


Figure 1.7: The scheme of guyed tower ([www.offshore-technology.gov](http://www.offshore-technology.gov))

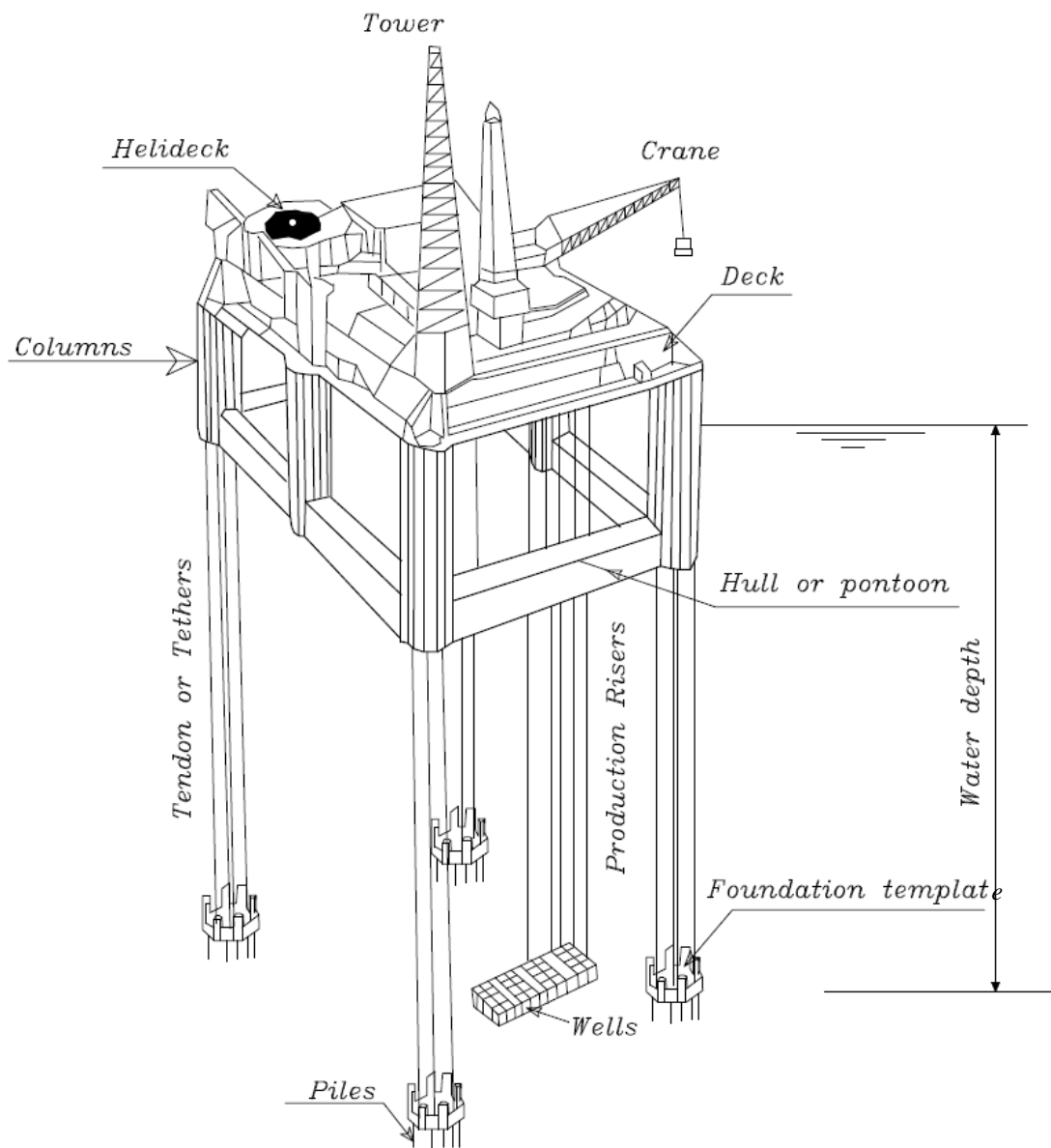


Figure 1.8: The scheme of tension leg platform



Figure 1.9: The scheme of drilling ships ([www.offshore-technology.com](http://www.offshore-technology.com))



Figure 1.10: The scheme of jack-ups  
(<http://community.webshots.com/album/126570186zwqfus>)

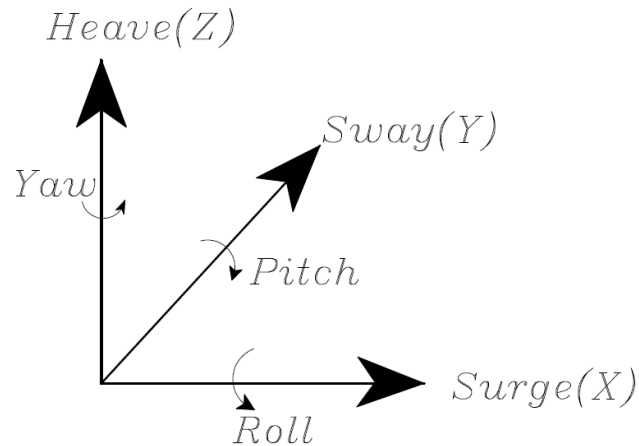


Figure 1.11: Six degree of freedom of offshore structure.

#### 1.4 Literature Review

Since the original concept of the TLP put forward. Most of the literature available is on conventional square (four-legged) TLPs. Paulling and Horton, 1970, reported a method of predicting the platform motions and tether forces due to regular waves using a linearized hydrodynamic synthesis technique. Each member was assumed to be cylindrical in shape with cross-sectional dimensions small in comparison to both the length of the cylinder and the wave length.

Also, a number of studies has been made on the dynamic behavior of TLP platforms under both regular and random waves (Taudin, 1978; Denis and Heaf, 1979; Tan and De Boom, 1983). The majority of these studies deal with the two dimensional behavior of the platform. The hydrodynamic interactions between adjacent or intersecting members were neglected. The drag term was linearized and the free-surface effect was neglected. The results agreed well with experimental model results. The motions and tensions due to regular waves were shown to vary in a linear fashion with wave amplitude.

Angelides et al., 1982, considered the influence of hull geometry, force coefficients, water depth, pre-tension and tether stiffness on the dynamic responses of the

TLP. The floating part of the TLP was modeled as a rigid body with six degrees of freedom. The tethers were represented by linear axial springs. Wave forces were evaluated using a modified Morison equation on the displaced position of the structure considering the effect of the free sea surface variation.

Faltinsen et al., 1982, developed a comprehensive theoretical model for the behavior of a TLP and verified such model using test program. The basic outline of the model included:

- (i) The velocity potential solution for first- and second-order hydrodynamics, except for the slender members which were modeled with Morison's equation,
- (ii) Morison's theory and Newman's approximation to calculate drift forces,
- (iii) The large deflection three-dimensional finite element theory with forces from Morison's equation which was used for the tethers,
- (iv) The short-crestedness of waves, and
- (v) The wind and current. The origin for the Mathieu-type instabilities was the presence of a constant plus a time-dependent restoring force for surge, sway and yaw. The amplitudes of oscillations due to the Mathieu-type instabilities depended on the damping in the system and the relative importance of the time-dependent restoring term compared to the constant restoring term.

Lyons et al., 1983, presented comparisons between the results of hydrodynamic analyses and two sets of large-scale model test results for the wave-induced motion responses of TLPs. The results of analyses and tests showed good agreement for surge motions although discrepancies were observed for the tether tension responses at certain wave frequencies. Linear wave theory was used and hydrodynamic interference between members was neglected. The nonlinear damping was linearized by assuming an effective linear damping, which would dissipate the same amount of energy at resonance as the nonlinear damping.

Teigen and Navig, 1983, presented the response of a TLP in both long-crested and short-crested waves through model tests. It was concluded that the low-frequency part of the horizontal response looked enlarged in tests carried out in long-crested seas,

compared to tests carried out in short-crested seas, irrespective of the actual shape of the directional distribution.

Few investigations, however considered all the six degrees of freedom of the platform in describing its dynamic behavior (Morgan and Malaeb 1983; Chandrasekaran and Roy 2005). They presented phase space studies of offshore structures subjected to nonlinear dynamic loading through Poincare maps for certain hydrodynamic parameters.

Morgan and Malaeb, 1983, investigated the dynamic response of TLPs using a deterministic analysis. The analysis was based on coupled nonlinear stiffness coefficients and closed-form inertia and drag-forcing functions using the Morison equation. The time histories of motions were presented for regular wave excitations. The nonlinear effects considered in the analysis were stiffness nonlinearity arising from coupling of various degrees of freedom, large structural displacements and hydrodynamic drag force nonlinearity arising from the square of the velocity terms. It was reported that stiffness coupling could significantly affect the behavior of the structure and the strongest coupling found to exist between heave and surge or sway.

Spanos and Agarwal, 1984, used a single degree-of-freedom model of a TLP and calculated wave forces at the structure's displaced position using the Morison equation. It was shown that by numerically integrating the equation of motion, the calculation of wave forces, on the displaced position of the structure, introduces a steady offset component in the structural response for either deterministically or stochastically described wave fields. The formulation did not involve any velocity-squared type of terms, and yet an offset component was found to be present.

Vickery, 1988, studied the importance of wind load on TLP through using different two numerical models and through an experimental scale model study carried out in a wind – wave flume. The numerical models included a full diffraction analysis and effect of the second – order, non-linear wave drift force.

Bhattacharjee, 1990, studied the applicability of the state space method for modeling idealized three degree of freedom of TLP. Jain, 1990, investigated the relative importance of different types of nonlinearities on the dynamic response of TLP and focused on the nonlinear effect of evaluating the wave forces up to the free surface using different approximation method, and TLP hull model with time varying tendon forces is

subjected to regular wave with and without current, the effect on calculating the wave kinematics up to mean sea level or up to the actual free surface making use of various extrapolation or stretching techniques are discussed.

Ahmad et. al, 1990, studied the effect of the variable submergence on the maximum tether tension force on TLP with change in wave incidence angle. The study was carried out on coupled and uncoupled model. Jain et.al, 1990, studied the effect of wind load on the dynamic response on TLP where the sea state was characterized by Pierson-Moskowitz spectrum.

Kareem and Li, 1992, presented the response of a TLP to wave drift forces. The wave drift forces on TLP are contributed to second- order potential and viscous wave loading effect, the fluctuations in wave surface elevation, and the influence of platform's displaced position on the wave excitation.

Li et al., 1993, presented the second – order double- frequency wave loads on ISSC TLP in regular waves. Huse and Utnes, 1994, presented an experimental investigation on hydrodynamic spring damping of TLP columns as influenced by the presence of current and waves, and by the variation of radius of curvature at the lower edge of the columns. They also compared the numerical calculations of the damping in calm water with the experiment.

Mekha et. al, 1994, studied the nonlinear effect of evaluating the wave forces on a TLP up to the wave-free surface. Several approximate methods were evaluated for regular and irregular wave forces, with and without current, and compared to Stoke's second-order wave theory. The tethers were treated as massless springs providing axial and lateral stiffness at their connection with the hull.

Lee, 1994, presented the analytical solution of the coupling problem of a 2D tension leg structure interacting with a monochromatic linear wave train. Fluid-induced drags, including form drag and inertia drag, on linearly elastic tension legs had been considered in the study. The nonlinear form drag was then replaced by a linear drag according to Lorentz's hypothesis of equivalent work. Analytical solutions showed that the inertia drag on tension legs was negligible compared to that due to the evanescent waves caused by the wave–structure interaction. However, the form drag on the legs altered the



structural motion and, consequently, the wave field, especially when wave periods were close to the structure's resonant frequency.

Hahn, 1994, reported the effects of wave stretching on realistic representations of the wave forces that act on offshore structures. The structures considered were modeled as linear, cantilever, stick-like systems. The lateral responses of such systems to wave forces, computed from water particle kinematics calculated by using the standard and stretching approaches, were examined. The results showed that the effects of stretching on the governing wave forces and the resulting structural responses were small, indicating that they could be ignored in design practice. It was also shown that the action of stretching could not materially influence the governing excitation and the corresponding structural response.

Duggal and Niedzwecki, 1995, presented results from a large-scale experimental study of the interaction of regular and random waves with a long, flexible cylinder, exhibiting the dynamic characteristics of a TLP riser or tether in approximately 1000 m of water depth. Regular wave conditions were chosen to provide a large range of Keulegan–Carpenter numbers. Classification of the transverse response in regular waves showed similarities with results obtained by previous investigators with oscillating flow on rigid cylinders. For high Keulegan–Carpenter numbers, the response became more irregular, with response at harmonics of the incident wave frequency and at several natural frequencies of the cylinder.

Natvig and Vogel, 1995, focused on design of future TLPs should be on the aspects of the platform geometry that affects tether loading and on the tether system itself. Their experience with a four-legged TLP has shown that the indeterminate tether system implies some very heavy cost items. The new concept of a three-legged TLP, which is statically determinate, will not require complicated devices and the foundations can be placed with larger tolerances without affecting tether behavior. The main aspect of three-legged TLP is that all tethers share approximately the same loads despite weather directions. With the near-equal load sharing of the three-legged TLP, the maximum load level in one group is less, thus requiring less tether cross section material than that of a four-legged TLP. Studies indicate that 12 tethers are feasible for a three-legged TLP

whilst 16 would be required for a four-legged equivalent TLP. This is thus an important area for savings since tethers are important cost items.

Munkejord, 1996, presented a conceptual analysis of the triangular TLP behavior and then compared the results with data from model tests. The objective was to verify maximum tether tension, maximum platform offset, and minimum air gap and tether fatigue. Aker and Saga Petroleum developed the concept of a triangular TLP, which has enabled significant savings in main steel for both hull and deck due to fewer main element intersections and effective force distributions. Munkejord, 1996, summarized the design features for the triangular TLP of Aker as a statically determinate system with effective distribution of dynamic loads and fixed-length tethers. They stated that no design cases where TLP sustained a maximum storm with one tether missing were reported. No tether tension measurements required day-to-day operation and increased tolerances for the position of the foundation and increased draught and heel tolerances.

Ahmad, 1996, investigated the coupled response of a TLP to random waves characterized by a long-crested sea surface spectrum. The response analysis was based on a simulation, which duly considered various nonlinear effects, such as relative velocity squared drag force, variable added mass due to variable submergence with the passage of waves and nonlinearity due to large excursion. It also accounted for variable tension in tethers due to variable submergence, variable buoyancy and vertical wave forces. The power spectral density function (PSDF) of the coupled heave and tether tension showed the energy distribution with respect to frequencies and proved to be an important informative tool for the preliminary design under the long-crested sea state. Variable submergence was found to be a major source of nonlinearity enhancing the surge and heave responses, which in turn introduced tether tension fluctuations.

Ahmad et.al, 1997, dynamic response studies of a tension leg platform (TLP) are carried out in time domain to investigate the influence of non-linearities due to the hydrodynamic drag force, variable cable tension, variable submergence, long excursions and fluctuating wind together with the effect of coupling. The sea state is characterized by Pierson Moskowitz spectrum while the fluctuating wind has been estimated using Emil Simiu's wind spectrum which is meant for the compliant offshore structures. Random wind and waves are modeled by Monte-Carlo simulation. Power spectral

density functions (PSDF) are plotted to highlight the wind-induced dynamic responses of the structure.

Jain, 1997, Dynamic response analysis of a TLP to deterministic first order wave forces is presented, considering coupling between the degrees-of-freedom surge, sway, heave, roll, pitch and yaw. The analysis considers nonlinearities produced due to changes in cable tension and due to nonlinear hydrodynamic drag forces. The wave forces on the elements of the pontoon structure are calculated using Airy's wave theory and Morison's equation ignoring diffraction effects. The nonlinear equation of motion is solved in the time domain by Newmark's beta integration scheme. The effects of different parameters that influence the response of the TLP are then investigated. Like change in tether tension force and damping ratio.

Lee and Wang, 2000, investigated the dynamic behavior of a TLP with a net-cage system with a simplified two-dimensional modeling. They found that there is a close relationship between the dynamic behavior of the platform and the net-cage features.

Chandrasekaran and Jain, 2002a; 2002b, investigated the structural response behavior of the triangular TLP under several random sea wave loads and current loads in both time and frequency domains. They studied the effect of coupling of stiffness coefficients in the stiffness matrix and the effect of variable submergence of the structure, due to varying water surface, on the structural response of the triangular TLP.

Tabeshpour et. al, 2004, studied the effect of added mass fluctuation on the heave response of the TLP by using perturbation method both for discrete and continuous models. Bhattacharya et. al, 2004, investigated coupled dynamic behavior of a mini TLP giving special attention to hull-tether coupling.

Tabeshpour et. al, 2005, studied an analytical heave vibration of TLP with radiation and scattering effects for undamped systems where the effect of structural and radiation damping on the response of the structure was not considered so that the amplitude of the heave motion was over estimated.

Ketabdari and Ardakani, 2005, developed a computer program to evaluate the dynamic response of sea-star TLP to regular wave forces considering coupling between different degrees of freedom.

Tabeshpour et.al, 2006, nonlinear dynamic analysis of TLP is carried out in both time and frequency domains. The time history of random wave is generated based on Pierson-Moskowitz spectrum and acts on the structure in arbitrary direction. The hydrodynamic forces are calculated using the modified Morison equation according to Airy's linear wave theory. The power spectral densities (PSDs) of displacements, velocities and accelerations are calculated from nonlinear responses. The focus of the paper is on the comprehensive interpretation of the responses of the structure related to wave excitation and structural characteristics. As an example a case study is investigated and numerical results are discussed.

Chandrasekaran et.al, 2007, focuses on the response analysis of triangular tension leg platform (TLP) for different wave approach angles varying from 0 through 90 and its influence on the coupled dynamic response of triangular TLPs. Chandrasekaran et.al, 2007b, Dynamic analysis of two triangular TLP models at water depths 1200 and 527.8m is performed under regular waves along with impulse load acting at an angle of 45 degrees at the TLP column.

Kurian et. al, 2008a, developed a numerical study of the effect for determining the dynamic responses of square TLPs subjected to regular and random wave, with available theoretical and experimental results. Also, parametric studies have been made varying parameters such as water depth, pretension, wave angle and position of center of gravity. Kurian et. al, 2008b, developed a numerical study of the effect for determining the dynamic responses of square and triangular TLPs subjected to random wave, with available theoretical. They found that the responses of triangular TLP are much higher than that of square TLP.

Joseph et.al, 2009, presents a new geometric configuration which could be a better alternative to an existing configuration. A 3-column mini TLP is designed and its platform-mooring coupled dynamic behavior is investigated and compared with an existing 4-column mini TLP.

Y. M. Low, 2009, presents the formulation for the linearization in all six degrees-of-freedom. Y. M. Low, 2010, developed a simple method for incorporating setdown in the extreme response prediction of the airgap.

Chan K. Yang, M. H. Kim, 2010, developed a numerical study of the transient effect of tendon disconnection on global performance of an extended tension leg platform (ETLP) during harsh environmental conditions of Gulf Of Mexico (GOM).

### **1.5 Aim of The study**

In this study, dynamic analysis of squared and triangular model TLP to regular waves is presented, considering the coupling between surge, sway, heave, roll, pitch and yaw degrees of freedom. The analysis considers various nonlinearities produced due to change in the tether tension and nonlinear hydrodynamic drag force. The wave forces on the elements of the structure are calculated using Airy's wave theory with Chakrabarti (1971), approaches and Morison's equation, ignoring the diffraction effects. The nonlinear equation of motion is solved in the time domain using Newmark's beta integration scheme.

Numerical studies are carried out in the time domain to examine the effect of change of wave parameters (wave height and wave period) and coupling effect on dynamic response of a square and a triangular TLP under a unidirectional surge wave force. Also, Numerical studies are conducted to compare the coupled response of a triangular TLP with that of a squared TLP and the effects of different parameters that influence these responses are then investigated. Computer MATLAB program is developed in this work for nonlinear dynamic analysis for both triangle and squared TLP which is capable of solving large displacement problem dynamically in the time domain.

### **1.6 Organization of the Present Study**

This thesis consists of five chapters, after this introductory chapter, Chapter 2 presents a review of the basic equations of ocean wave propagation using linearized gravity waves theory. It also includes a short review of the wave force representation using Morison equation.

Chapter 3 describes the equations of motion being utilized in modeling tension leg platform. Detailed derivation of the equations of squared and triangular tension leg

platform are presented. The time integration scheme and the iterative solver of a system of nonlinear equations using Newmark beta method are also provided.

Chapter 4 presents the studied model for both squared and triangular TLP. The chapter also presents the obtained results for both of square and triangular TLPs. A general view on all discussions and comments on the results are also presented in this chapter.

Chapter 5 presents the conclusions of this thesis along with recommended future work that may improve the applicability of the proposed method.

## Chapter 2

### HYDRODYNAMIC LOADS

#### 2.1 Introduction

The oceans have been an important part of our life for centuries, providing various natural sources. They have also provided a continuous challenge to human by the enormous forces contained in the waves. The waves in a severe storm may devastate coastal villages and wreck ships, harbors, lighthouses and other important structures, causing great damages. However, the same waves if harnessed properly can be everlasting sources of energy. Attempts to fully understand the complex phenomena of wave dynamics have been only partially successful. An accurate and improved analysis of the highly irregular wave dynamics has become even more important with the increased interest in natural offshore resources.

Ocean waves are the result of energy input into the ocean through natural phenomena; primarily wind, through a complicated process in which the momentum of the wind passing over the sea surface is transferred into wind waves, which develop with time and space. This type of ocean wave is random in nature, and typically has period in the range of 1 to 20 seconds. Large storm waves lengths around 600 meters. It is these wind-generated waves which are of the most importance in the evaluation of the wave loads on offshore structures. Although wind-generated waves are extremely certain, simplification can be made so that the waves may be adequately described using mathematical models. Also tidal forces and occasionally earthquakes, are free surface phenomena, with a continual exchange of kinetic and potential energy as the fluid particles oscillates about the mean level of fluid surface. The longest period waves are those associated with tides, which are caused by the gravitational pull of the sun and the moon. Tides have periods in the range of 12 to 24 hours, and height of the order of 10 meters.

## 2.2 Theory of Linearized Gravity Waves

The motion of water waves is a complex phenomenon. Even in its most simple form, after numerous simplifying assumptions, only an approximate solution can be obtained (Airy, 1845, Dean and Dalrymple, 1984, Chakrabarti, 1987). In a strict sense, water waves propagate in a viscous fluid medium, over an irregular bottom of varying permeability. Fortunately, the main body of the fluid motion is nearly irrotationally, except for a "thin boundary layer" near the bottom and the surface. Also, the water can be considered incompressible for all practical purposes. These conditions imply that a velocity potential exists for the main body of the fluid, and the objective of any wave theory is to solve for this potential function.

The linear wave theory has been developed for long-crested waves. These are deterministic waves that are propagating in one direction. And the wave crests are "long enough" so that the fluid has no motion in the direction of the wave crest. Thus the flow can be considered essentially two-dimensional, and restricted to the x-z plane of propagation.

Since the flow is irrotational, a velocity potential  $\phi$ , can be defined and the velocity component in the x and z directions are given as

$$u = \frac{\partial \phi}{\partial x}, w = \frac{\partial \phi}{\partial z} \quad (2.1)$$

The introduction of  $\phi$  into the continuity equation for two-dimensional incompressible flow is defined as

$$\nabla \cdot \bar{v} = 0 \quad (2.2)$$

Or,

$$\nabla \cdot \nabla \phi = 0 \quad (2.3)$$

Or,

$$\frac{\partial u}{\partial x} + \frac{\partial w}{\partial z} = 0 \quad (2.4)$$

The velocity potential  $\phi$  pertaining to fluid region can be determined through 2-D Laplace equation



$$\nabla^2 \phi = \frac{\delta^2 \phi}{\delta x^2} + \frac{\delta^2 \phi}{\delta z^2} = 0 \quad (2.5)$$

The governing equation for the gravity wave is obtained as a solution for  $\phi$  in Eqn. (2.5), subject to the appropriate boundary conditions. In the above,  $x$  denotes the positive direction of wave propagation,  $z$  is positive upward, and the origin is fixed at the still water level (SWL).

The sea bottom is assumed to be a rigid, impenetrable, horizontal boundary for the mathematical derivation. This results in the condition of "no flow across the rigid boundary".

$$z = -d \Rightarrow \frac{\delta \phi}{\delta z} = 0 \quad (2.6)$$

where,  $d$  is the local water depth.

The boundary condition at the sea surface is more complex in nature, and most text present only the final equation, without explaining how it was arrived. The kinematic free surface boundary condition states that a particle lying on the free surface at one instant of time would continue to remain on the free surface. Mathematically it implies that if the free surface of a wave is described by  $F(x,z,t) = z - \eta(x,t) = 0$ , where  $\eta(x,t)$  is the displacement of the free surface about the SWL ( $z = 0$ ). Then,

$$\frac{DF(x,z,t)}{Dt} = \frac{\delta F}{\delta t} + u \frac{\delta F}{\delta x} + w \frac{\delta F}{\delta z} \Big|_{F(x,z,t)=0} = 0 \quad (2.7)$$

Or,

$$\frac{\delta F}{\delta t} + \bar{v} \cdot \nabla F = 0 \quad (2.8)$$

Thus,

$$\bar{v} \cdot \bar{n} = \frac{-\delta F / \delta t}{|\nabla F|} \Big|_{F(x,z,t)=0} \quad (2.9)$$

Where,

$$|\nabla F| = \sqrt{\left(\frac{\delta F}{\delta x}\right)^2 + \left(\frac{\delta F}{\delta z}\right)^2} \quad (2.10)$$

Where,  $\bar{n}$  is the unit normal vector associated with the gradient function  $\nabla F$  as

$$\bar{n} = \frac{\nabla F}{|\nabla F|} \quad (2.11)$$

on substituting  $F(x,z,t) = z - \eta(x,t) = 0$ , on Eqn.(2.9) the kinematic boundary condition at the free surface is

$$z = \eta(x,t) \Rightarrow \bar{v} \cdot \bar{n} = \frac{-\delta\eta/\delta x}{\sqrt{(1+(\delta\eta/\delta x)^2)}} \quad (2.12)$$

Where, the unit normal to the surface  $F(x,z)$  is given by

$$\bar{n} = \frac{(-\delta\eta/\delta x)i + 1k}{\sqrt{(1+(\delta\eta/\delta x)^2)}} \quad (2.13)$$

Thus,

$$\bar{v} \cdot \bar{n} = \frac{(-\delta\eta/\delta x)u + w}{\sqrt{(1+(\delta\eta/\delta x)^2)}} = \frac{(\delta\eta/\delta t)}{\sqrt{(1+(\delta\eta/\delta x)^2)}} \quad (2.14)$$

Carrying out the dot product this leads to

$$z = \eta(x,t) \Rightarrow w = \frac{\delta\eta}{\delta t} + u \frac{\delta\eta}{\delta x} \quad (2.15)$$

Substituting  $\frac{\delta\phi}{\delta z} = w$  in the above, the kinematic free surface boundary condition can

be represented as

$$z = \eta(x,t) \Rightarrow \frac{\delta\phi}{\delta z} = \frac{\delta\eta}{\delta t} + u \frac{\delta\eta}{\delta x} \quad (2.16)$$

Which means that the velocity of the free surface equal to the particle velocity normal to the free surface (kinematic condition).

The free surface, such as the water-air interface cannot support pressure variations, neglecting surface tension effects. Across the interface thus, the free surface responds in

order to maintain the uniformity in pressure. A complicating factor in the wave equation is that the upper boundary is not known apriori, applying the Bernoulli equation with

$P_n = \text{constant}$  is applied, on the free surface

$$z = \eta(x, t) \Rightarrow \frac{\delta\phi}{\delta t} + \frac{1}{2} \left[ \left( \frac{\delta\phi}{\delta x} \right)^2 + \left( \frac{\delta\phi}{\delta z} \right)^2 \right] + \frac{p_n}{\rho} + gz = C(t) \quad (2.17)$$

Usually, the  $P_n/\rho$  term is absorbed in the constant  $C(t)$ , replacing the latter by a new constant  $CI(t)$ . Thus, the problem is to find a solution to  $\phi(x, z, t)$  which satisfies the boundary condition specified by Eqns.(2.16) and Eqns.(2.17) at  $z = \eta$

$$z = \eta(x, t) \Rightarrow \frac{\delta\phi}{\delta t} + \frac{1}{2} \left[ \left( \frac{\delta\phi}{\delta x} \right)^2 + \left( \frac{\delta\phi}{\delta z} \right)^2 \right] + gz = 0 \quad (2.18)$$

Which means that the pressure at the free surface is constant and equal to zero (i.e, atmospheric pressure) (dynamic condition).

The difficulties associated with the free surface boundary conditions are that they are non linear and are valid only at  $z = \eta$ , which is unknown. To linearize the boundary conditions, it is assumed that the wave height is very small relative to wave length ( $H \ll \lambda$ ) neglecting the nonlinear terms in Eqn. (2.16) lead to,

$$u \frac{\delta\eta}{\delta x} \approx 0 \quad (2.19)$$

And in Eqn. (2.17, 2.18) lead to,

$$\left[ \left( \frac{\delta\phi}{\delta x} \right)^2 + \left( \frac{\delta\phi}{\delta z} \right)^2 \right] \approx 0 \quad (2.20)$$

Next, the boundary conditions are applied at  $z = 0$  instead of  $z = \eta$ . Simplifying the boundary conditions to

From Eqn. (2.16)

$$z = 0 \Rightarrow \frac{\delta\phi}{\delta z} = \frac{\delta\eta}{\delta t} \quad (2.21)$$

and from Eqn. (2.18)

$$z = 0 \Rightarrow \frac{\delta\phi}{\delta t} + g\eta = C_1(t) = 0 \quad (2.22)$$

$$\Rightarrow \eta = -\frac{1}{g} \left( \frac{\delta\phi}{\delta t} \right)_{z=0}$$

(2.23)

The solution to this simplified boundary value problem is (Dean and Dalrymple, 1984)

$$\phi(x, z, t) = \frac{\pi H}{kT} \frac{\cosh[k(z+d)]}{\cosh(kd)} \sin(kx - \omega t) \quad (2.24)$$

So from Eqn. (2.23) and Eqn. (2.24) lead to

$$\eta = \frac{H}{2} \cos(kx - \omega t) \quad (2.25)$$

Where,  $H$  is the wave height,  $T$  is the wave period,  $k=2\pi/\lambda$  is the wave number,  $\lambda$  is the Wave length,  $(\omega) = 2\pi/T$  is the wave angular frequency,  $c = \omega/k$  is the wave celerity. The frequency and wave number are related for linear waves by the dispersion equation

$$\omega^2 = gk \tanh(kd) \quad (2.26)$$

Or,

$$c^2 = \frac{g}{k} \tanh(kd) \quad (2.27)$$

Where,  $g$  is the gravity acceleration.

The independent wave parameters are the local water depth,  $d$ , wave height,  $H$ , and anyone of the following four parameters:  $\omega, k, \lambda$  or  $T$ . Furthermore, waves become unstable and break (Stokes, 1847) when either the crest angle exceeds 120 degrees or the following ratio of wave height to length is exceeded:

$$\frac{H}{\lambda} \geq 0.142 \tanh(kd) \quad (2.28)$$

Once the velocity potential  $\phi$  is obtained the three fundamental unknowns of the flow field, namely velocity, pressure and acceleration along with other parameters of interest, may be evaluated as listed in Table (2.1).

Further, the dynamic pressure under a surface wave at a depth  $z$  below the SWL is in table where the first term on the right hand side denotes the hydrostatic pressure due to the water head up to the still water, and the second term represents the dynamic pressure due to wave motion. The dynamic pressure term has the same sign as the hydrostatic pressure under a trough and the opposite one under a crest it is interesting to note the action of surface waves on a fully submerged. Neutrally buoyant body due to this dynamic pressure effect it would experience a net downward force under a wave crest and an upward force under the trough. This fact is used to advantage in the design of

semisubmersibles. Where, the change in the vertical forces on the columns due to variable submergence is canceled by the opposing force on the submerged hulls, at the design wave frequency.

To summarize, the assumptions of the linear wave theory are stated. The amplitude  $H/2$  is small relative to the wave length  $\lambda$ , the pressure contribution from the term  $(u^2 + w^2)/2g$  is negligible, the local water depth  $d$  is uniform, the fluid is considered inviscid and irrotational. In addition, the fluid is incompressible and unstratified or homogeneous, the deflection force associated with the earth's rotation, the Coriolis force is negligible. Surface tension effects are negligible, the bottom is smooth and impermeable, and the sea level atmospheric pressure can be considered uniform.

Dimensionless parameters are frequently used to characterize a wave train. The wave height is expressed in terms of  $(H/gT^2)$ , the wave steepness  $H/\lambda$  or the relative height  $H/d$ . the water depth expression in terms of depth parameters  $(d/gT^2)$  or  $(kd)$  or the relative depth  $d/\lambda$ , for steeper waves in shallow water the ursell number  $U=H \lambda^2/d^3$  is often used as Figure (2.2).

It is useful to note that depending upon the relative measure of water depth and wave length two extreme conditions of shallow and deep water can be described. The parameter  $(kd)$  specified the ranges over which certain approximations are applicable which appears in the denominator for the velocity potential, is defined as

$$\cosh(kd) = \frac{e^{kd} + e^{-kd}}{2} \quad (2.29)$$

By Taylor series expansion

$$e^{kd} = 1 + kd + \frac{(kd)^2}{2} + \dots \quad (2.30)$$

$$e^{-kd} = 1 - kd + \frac{(kd)^2}{2} + \dots$$

Therefore, for small  $kd$  lead to

$$\cosh(kd) = 1 + \frac{(kd)^2}{2} \quad (2.31)$$

And for large  $kd$  the term  $e^{-kd}$  becomes quite small that lead to

$$\cosh(kd) = \frac{e^{kd}}{2} \quad (2.32)$$

The shallow and deep water ranges corresponded to  $kd < \pi/10$  and  $kd > \pi$  respectively, and over these ranges approximate expressions may be substituted for hyperbolic functions used to obtain flow field velocities as show in Table (2.2)

Table 2.2: asymptotic forms of hyperbolic functions

functions	$kd < \pi/10$	$kd > \pi$
Sinh(kd)	Kd	$e^{kd/2}$
Cosh(kd)	1	$e^{kd/2}$
Tanh(kd)	kd	1

Substituting these into the last relation, we obtain the simplified expressions that summarized in Table (2.1).

So we can divide the water depth to three categories as:

- 1) Shallow water waves:  $(1/25) > (d/\lambda)$ ;  $0.0025 > d/gT^2$
- 2) Intermediate water waves:  $(1/25) < (d/\lambda) < (1/2)$ ;  $0.0025 < d/gT^2 < 0.08$
- 3) Deep water waves:  $(1/2) < (d/\lambda)$ ;  $0.08 < d/gT^2$

It is not Uncommon (in engineering application) to use linear theory over a wider range. Figure (2-2) shows the ranges of suitability for various theories.

As waves start to become large compared to their length, the second- order terms present in Eqn. (2.17) and Eqn. (2.18) become increasingly important. The inclusion of these terms in a stockes-type perturbation solution indicates that for  $H/\lambda$  larger than approximately 0.006 and  $H/d < 0.03$ , the wave profile changes from the sinusoidal from given in the linear solution. The Stokes waves tend to have relatively long shallow troughs and sharper peaks. As  $H/\lambda$  becomes even larger, the waves finally break. This breaking limit is reached when  $H/\lambda$  approaches.

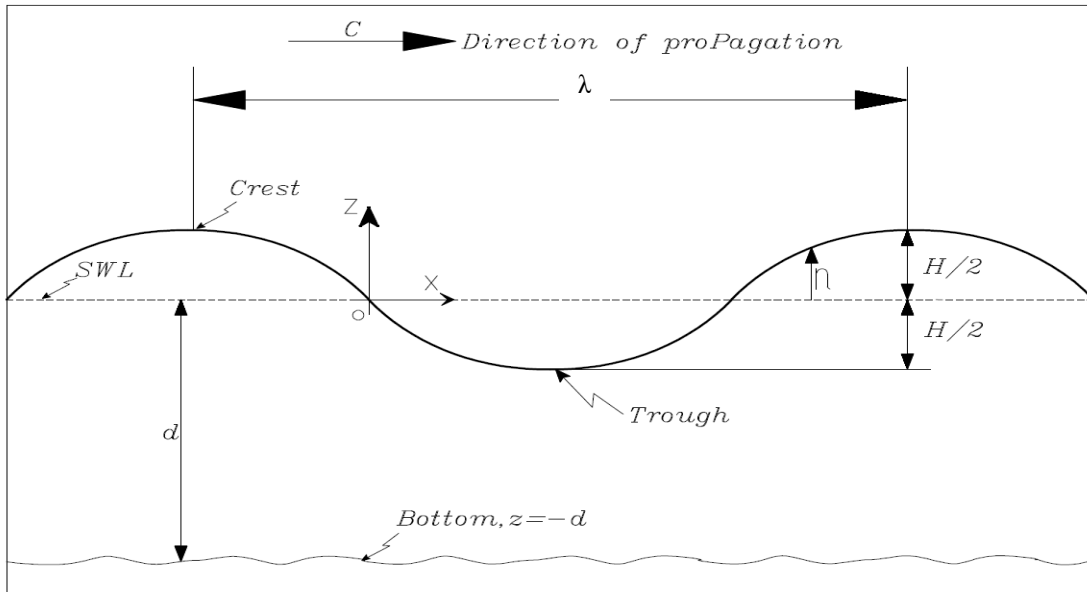


Figure 2.1: the wave propagation for linear wave theory

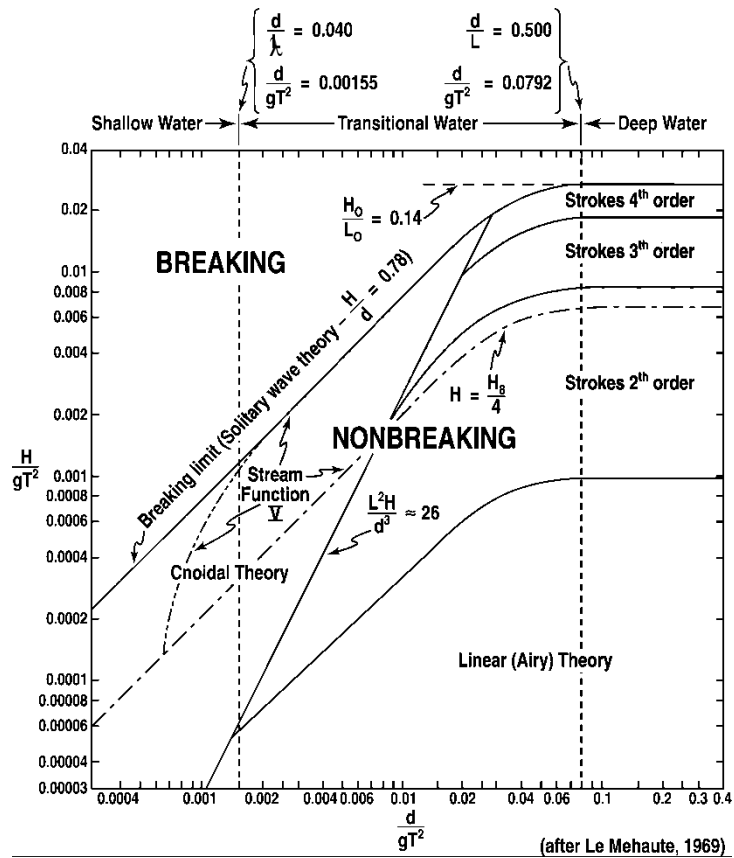


Figure 2.2: the ranges of suitability for various theories (Bhattachargee, S.,1990).

### 2.3 Surface Elevation Modification

Similar to the velocity potential, the expression for the water particle kinematics consists of the amplitude at the surface; the variation with depth given by attenuation in the form of a hyperbolic function; and a factor dependent on time and position of the particle. For the extreme wave condition where the wave height is large, the effect of the variable free surface elevation needs to be considered. As shown in Eqn. (2.24) the depth Factor  $\frac{\cosh[k(z+d)]}{\cosh(kd)}$  decays rapidly from still water level (MSL) to the sea floor and the wave kinematics near the water surface have a significant importance on the total wave force applied to the structure. To compute the hydrodynamic forces, the water particle kinematics has to be known at all positions of the structure. Linear wave theory however, can only evaluate the water particle kinematics up to the MSL to overcome this limitation. Several extrapolation methods have been suggested to evaluate the water particle kinematics between the MSL and the wave free surface. Some of the methods are (Jain, 1997):

- (a) **Hyperbolic Extrapolation:** This method, suggested by Hogben simply extends the water particle kinematics above the MSL in a hyperbolic manner. This, extrapolation has been proved to overestimate the forces on the structure and to be very conservative.
- (b) **Linear Extrapolation:** This method, used by Nwogu and Irani computes the water particle kinematics beyond the MSL by expanding the expression in a Taylor's series and neglecting second order and higher order terms. This method also leads to an over estimation of the total force.
- (c) **Stretching methods:** This is the most recommended method when the free surface effect is to be taken in to account in the analysis. These methods shift the water particle kinematics profile from the MSL to the free surface. Thus, the water particle kinematics decays exponentially between the wave surface and the sea bed. Meeler's approximation and Chakrabarti approximation have been suggested. Wheeler, 1969, replaced the term  $(z+d)$  in the numerator of hyperbolic extrapolation function by  $(z + d) d / (d + \eta)$  so that the crest and



trough have the same particle velocity as Eqn. (2.24). Chakrabati, 1971, replaces the term  $d$  in the denominator of the hyperbolic function by  $(d + \eta)$ .

(d) **Uniform Extrapolation:** This method, used by Eatoek, Taylor et. al, assumes that the water particle kinematics in the crest region above the MSL are equal to their corresponding values at MSL.

It is worth mentioning that Jain, 1997, showed that the Chakrabarti, 1971, approximation is better than other approximations and its results are very close to experimental values. Therefore, this approximation will be utilized in the current study.

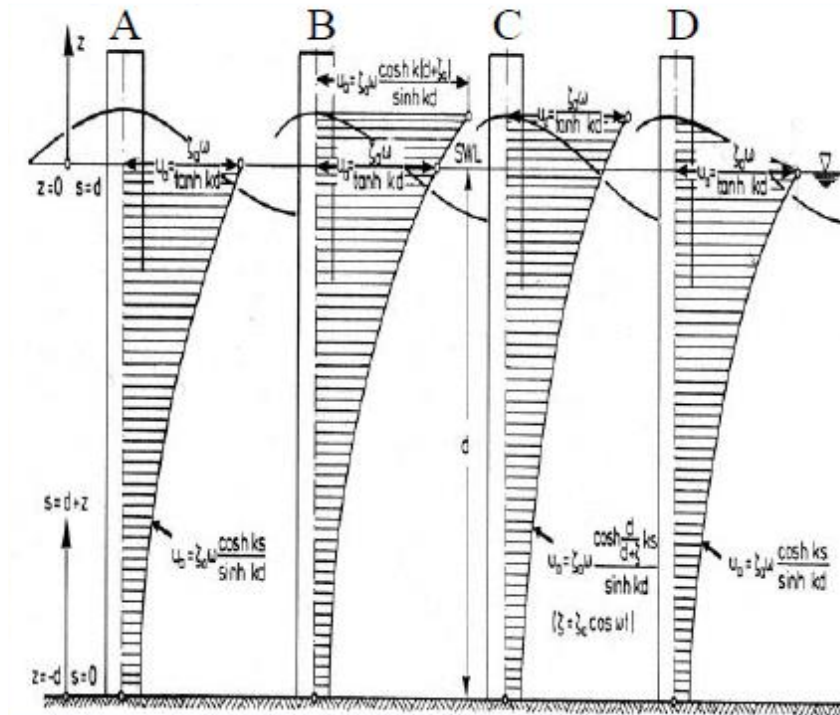


Figure 2.3: the comparison of vertical distribution of horizontal water particle velocity for (A) Airy which is limited to MWL, (B) Extrapolation of linear wave theory, (C) Stretching of linear wave theory, and (D) Modified linear wave theory "Chakrabarti"

Table 2.1: The linear theory different relationship (Bhattachargee, S., 1990)

RELATIVE DEPTH	SHALLOW WATER $\frac{d}{L} < \frac{1}{25}$	TRANSITIONAL WATER $\frac{1}{25} < \frac{d}{L} < \frac{1}{2}$	DEEP WATER $\frac{d}{L} > \frac{1}{2}$
1. Wave profile	Same As $\rightarrow$		Same As $\leftarrow$
2. Wave celerity	$C = \frac{L}{T} = \sqrt{gd}$	$\eta = \frac{H}{2} \cos \left[ \frac{2\pi x}{L} - \frac{2\pi t}{T} \right] = \frac{H}{2} \cos \theta$	$C = C_0 = \frac{L}{T} = \frac{gT}{2\pi}$
3. Wavelength	$L = T \sqrt{gd} = CT$	$C = \frac{L}{T} = \frac{gT}{2\pi} \tanh \left( \frac{2\pi d}{L} \right)$	$L = L_0 = \frac{gT^2}{2\pi} = C_0 T$
4. Group velocity	$C_g = C = \sqrt{gd}$	$L = \frac{gT^2}{2\pi} \tanh \left( \frac{2\pi d}{L} \right)$	$C_g = \frac{1}{2} C = \frac{gT}{4\pi}$
5. Water Particle Velocity		$C_g = nC = \frac{1}{2} \left[ 1 + \frac{4\pi d/L}{\sinh(4\pi d/L)} \right] C$	
(a) Horizontal	$u = \frac{H}{2} \sqrt{\frac{g}{d}} \cos \theta$	$u = \frac{H}{2} \frac{gT}{L} \frac{\cosh [2\pi(z+d)/L]}{\cosh(2\pi d/L)} \cos \theta$	$u = \frac{\pi H}{T} e^{\frac{2\pi z}{L}} \cos \theta$
(b) Vertical	$w = \frac{H\pi}{T} \left( 1 + \frac{z}{d} \right) \sin \theta$	$w = \frac{H}{2} \frac{gT}{L} \frac{\sinh [2\pi(z+d)/L]}{\cosh(2\pi d/L)} \sin \theta$	$w = \frac{\pi H}{T} e^{\frac{2\pi z}{L}} \sin \theta$
6. Water Particle Accelerations			
(a) Horizontal	$a_x = \frac{H\pi}{T} \sqrt{\frac{g}{d}} \sin \theta$	$a_x = \frac{g\pi H}{L} \frac{\cosh [2\pi(z+d)/L]}{\cosh(2\pi d/L)} \sin \theta$	$a_x = 2H \left( \frac{\pi}{T} \right)^2 e^{\frac{2\pi z}{L}} \sin \theta$
(b) Vertical	$a_z = -2H \left( \frac{\pi}{T} \right)^2 \left( 1 + \frac{z}{d} \right) \cos \theta$	$a_z = -\frac{g\pi H}{L} \frac{\sinh [2\pi(z+d)/L]}{\cosh(2\pi d/L)} \cos \theta$	$a_z = -2H \left( \frac{\pi}{T} \right)^2 e^{\frac{2\pi z}{L}} \cos \theta$
7. Water Particle Displacements			
(a) Horizontal	$\xi = \frac{HT}{4\pi} \sqrt{\frac{g}{d}} \sin \theta$	$\xi = -\frac{H}{2} \frac{\cosh [2\pi(z+d)/L]}{\sinh(2\pi d/L)} \sin \theta$	$\xi = -\frac{H}{2} e^{\frac{2\pi z}{L}} \sin \theta$
(b) Vertical	$\zeta = \frac{H}{2} \left( 1 + \frac{z}{d} \right) \cos \theta$	$\zeta = \frac{H}{2} \frac{\sinh [2\pi(z+d)/L]}{\sinh(2\pi d/L)} \cos \theta$	$\zeta = \frac{H}{2} e^{\frac{2\pi z}{L}} \cos \theta$
8. Subsurface Pressure	$p = \rho g (\eta - z)$	$p = \rho g \eta \frac{\cosh [2\pi(z+d)/L]}{\cosh(2\pi d/L)} - \rho g z$	$p = \rho g \eta e^{\frac{2\pi z}{L}} - \rho g z$

## 2.4 Wave Force

There are basically two different approaches for evaluating wave loads on fixed and floating structures:

- 1) **Empirical formulae**, relying heavily on experimental observation, physical insight and dimensional analysis. Examples include the Morison equation (by Morison et.al, 1950) and formulae for wave slamming, vortex shedding, etc.
- 2) **Theoretical methods**, which solve the boundary value problem describing flow around the structure. These methods are usually based on the classical theory of potential flow. The wave diffraction method or potential theory (by Hogben and Standing, 1975) falls into this category. It is sometimes necessary to add empirical terms representing non-ideal fluid effects, such as viscous drag.

The selection of the appropriate method of calculating wave loads is permanently governed by the size of the structure as, compared to the length of the incident wave the Morison equation technique is generally considered tube valid when the diameter of a structural member ( $D$ ), is small as compared to the length of the wave ( $\lambda$ ), the method assumes that the kinematics of the undisturbed flow are not altered due to the presence of the structure and is generally considered to be valid when  $D/\lambda$  is less than 0.2 as the size of a structure, or any of its components, becomes large compared to the wave length (i.e.  $D/\lambda$  greater than 0.2), the velocity and acceleration of the flow can not be considered constant over a distance equal to cylinder diameter in this case the presence of the structure begins to alter the incident flow field and the waves generally undergo scattering (or diffraction). Thus rendering the Morison equation invalid, therefore making it necessary to employ diffraction theory in order to determine the wave forces and the total force is determined by integrating the pressure evaluated from the superposition of the undisturbed pressure field and the pressure resulting from the disturbance of the flow field.

### 2.4.1 Wave Force Regimes

Wave forces on structures are computed by a variety of methods. The choice of a particular method depends on the dimension of the structure relative to the characteristic dimensions of the wave.

The parameters used to define these regimes for force computation purposes are cylinder diameter,  $D$ , peak to trough wave height,  $H$ , and the wave length,  $\lambda$ .

For  $D/\lambda > 1$ : Condition approximates pure reflection of the waves by the structure:

For  $D/\lambda > 0.2$ ; Diffraction forces need to be considered.

For  $D/\lambda \leq 0.2$ : Morison equation is valid in this region.

For  $0.5 \leq D/H \leq 1$ : Inertia forces can be used to represent, the total force on the structure.

For example, the large diameter structures like the columns supporting the decks of gravity type structures.

For  $0.1 \leq D/H \leq 0.5$ : both inertia and drag force need to be considered.

For  $D/H = 0.2$ : Drag and inertia forces are comparable.

For  $D/H \leq 0.1$ : Drag forces can be used to represent the total force. An example being Small diameter members like conductor tubes etc. Where, viscous effects provide the primary force contributions.

It is also worth noting at this point that the ratio  $D/H$  can be related to  $D/\lambda$ , based on the limiting heights of breaking waves. Waves become unstable and break when  $H/\lambda \geq 1/7$ . Thus for stable waves,  $D/H \geq D/\lambda$  in a strict sense, the concept of orbital width should be used. Instead of the wave height for identifying the force regimes the orbital width is defined as

$$W = 2 \left\| \frac{H \cosh kd}{2 \sinh kd} \right\| \cos(kx - \omega t) = \frac{H}{\tanh kd} \quad (2.33)$$

Note that in deep water  $\tanh(kd) \rightarrow 1$ , whereby  $W = H$  in the above Eqn. (2.33).

A very important assumption of Morison equation is that the waves are unaffected by the presence of the structure. This is justified only in case of relatively small diameter members. As indicated by the preceding relations, for members of larger diameters the diffraction and reflection effects become increasingly important, and Morison equation has to be replaced by diffraction theory that accounts for this (Chakrabarti, 1987).

### 2.4.2 Morison Equation

A very convenient empirical method for predicting the hydrodynamic forces on slender structural members has been proposed by Morison et. al, 1950, the formulation is based on experimental studies of wave forces on a pile and is a heuristic approximation of the measured forces by the assumption that the kinematics of the undisturbed flow in the region near the structure do not change in the incident wave direction. This empirical model is most appropriate for slender members, and accounts for the viscous as well as the inertia forces in an unsteady flow. Originally formulated for predicting forces on a rigid pile, the model is extensively used for evaluating wave and current forces on various submerged structural elements of offshore platforms, according to this model the total force on the structure can be considered to be the algebraic sum of a drag force and an inertia force Figure (2.4).

The drag force represents the contributions from viscous effects to the total force and attempts to incorporate the boundary layer and flow separation effects caused primarily by flow separation downstream from the cylinder. It depends on the fluid velocity in a quadratic manner, and linearly on the projected surface area. The drag force per unit length of a cylinder is defined as

$$dF_d = \frac{1}{2} \rho C_d D |U| U \quad (2.34)$$

and

$$U = u + \left( \frac{d+z}{d} U_c \right) \quad (2.35)$$

where,  $\rho$  is the fluid density,  $D$  is the diameter (or some characteristic dimension).  $U$ , is the undisturbed fluid velocity  $u$ , and current velocity  $U_c$  if exist, and  $C_d$  is the drag coefficient which is determined from experiments which the value of it ranges between 0.5 to 2.0 depending on the flow situation and surface roughness and commonly used value for it is 1.0, the term  $U/|U|$  is written in this form to ensure that the drag force component is in the same direction as the velocity.

In the ocean, wave and current loading naturally occur simultaneously; current direction need not coincide with wave direction and may vary with depth. The speed may

also change with depth as shown in Eqn. (2.35), to present a realistic description a profile which may vary in both magnitude and direction with depth considered and also the current velocity always takes about 10% wind velocity at a height of 10 m above the water surface.

The inertia force represents the contributions due to fluid acceleration and is present even under ideal fluid assumptions, and it is the force exerted by fluid while it accelerates and decelerates as the fluid passes the structure and it is also the force required to hold a rigid structure in a uniformly accelerated flow. The inertia force per unit length is expressed as

$$dF_i = \rho C_m A_s \frac{du}{dt} \quad (2.36)$$

Where  $A_s$  is the cross-sectional area, the coefficient,  $C_m$  is the inertia coefficient associated with the geometrical shape of the structure, and usually derived from experiments and can be theoretically obtained only in some special cases which the value of it ranges between 0.6 to 2.0 depending on the geometry of the member and commonly used value for it is 2.0.

According to this model the total force on the structure is the vectorial sum of these two forces. Thus, the total hydrodynamic force per unit length on a slender structural member subjected to an unsteady flow of a real fluid around it is given by

$$dF = \rho C_m A_s \frac{du}{dt} + \frac{1}{2} \rho C_d D |U|U \quad (2.37)$$

Other underlying assumption in formulating the Morison equation is:

- 1) The equation is for unbroken surface waves.
- 2) The equation is for a single vertical cylindrical object such as a pile which extends from the bottom upward above the wave crest.
- 3) The diameter of the pile is small compared to the wave height, wave length and water depth.
- 4) Coefficient  $C_m$  and  $C_d$  must be obtained experimentally.
- 5) In force calculation,  $u$  is taken as horizontal wave particle velocity and the convective acceleration terms are often ignored, i. e., it is assumed that

$$\frac{dU}{dt} = \frac{\delta u}{\delta t} \quad (2.38)$$

The values of the velocity and acceleration in this Eqn. (2.38) have to be known before the force can be evaluated. For computing forces due to waves or currents the velocity and acceleration in the flow field in the absence of the structural member is usually substituted. The true values of this kinematics in the presence of the solid body can be solved for only by considering the relatively complex fluid-Structure interaction problem. This simplification implies that the structural member does not affect the flow field significantly. This assumption is reasonably valid only for slender structural members, and hence the restriction of this model to small diameter members. For structural members of relatively larger dimension the diffraction and reflection effects play an increasingly important role. An assessment of the situations under which the different components play important roles are discussed in more detail in a following section.

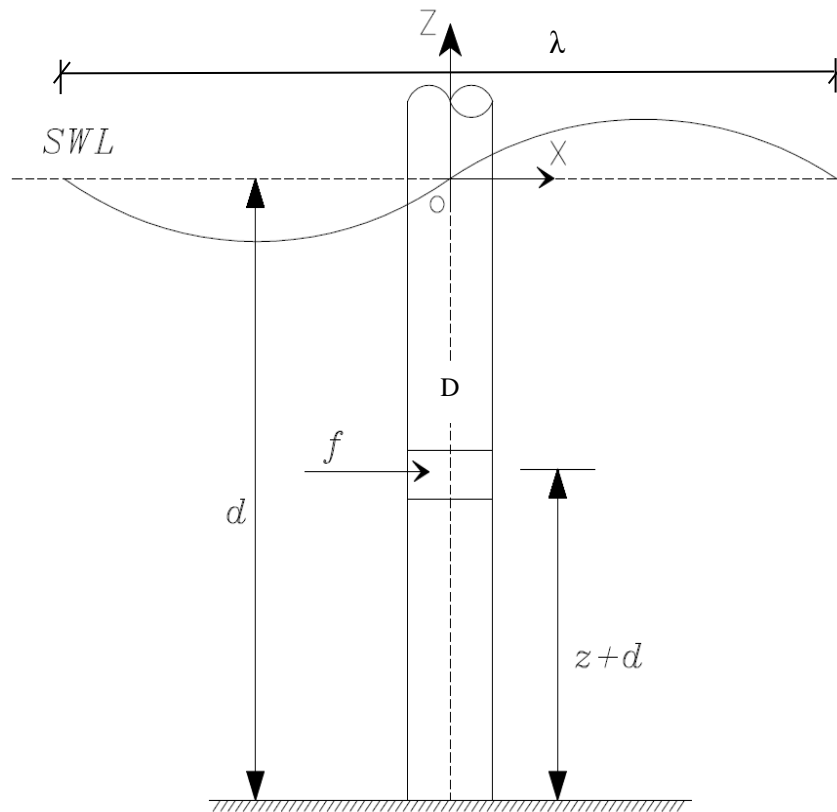


Figure 2.4: Wave force on a vertical cylinder

### 2.4.3 Modified Morison Equation

Morison equation was derived for rigid piles, and due consideration is required when analyzing the force on moving structures, especially if the structure is very flexible Figure (2.5). In a more sophisticated formulation the forces are considered to depend not on the absolute velocity and acceleration of the water particles, but on their relative magnitudes with respect to the structure of interest. The added mass effect and the Froude Krylov force are direct consequences of this force. It depends on the fluid acceleration and the cross-sectional area of the member. That is,

$$dF = \left[ \rho C_m A_s \left( \frac{du}{dt} - \frac{dx^{\bullet}}{dt} \right) \right] + 0.5 \rho C_d D \left| U - \frac{dx}{dt} \right| \left( U - \frac{dx}{dt} \right) - (C_m - 1) \rho A_s \frac{dx^{\bullet}}{dt} \quad (2.39)$$

Where  $x$  represent the displacement of the moving structure and the dots represent derivatives with respect to time. From Eqn. (2.39) it is noticed that the first term results from the fluid motion only and the second term is the added mass due to the movement of the cylinder in the water where the term  $(C_m - 1)$  is generally represented by  $C_a$  which is called the added mass coefficient. The applicability of the model for rigid piles to the case of a moving structure is an empirical extension of this model. The same coefficients are used but in conjunction with the relative motions. Systematic experimental values of the coefficients to cover the general case of a moving structure are not available, and the above model is accepted by engineering community as a logical extension of the theory.

The drag force term in Morison Eqn., can be simplified into a linear form using the assumption of (Penzien, 1976, Patel, 1989) because of the complicated of the absolute value integration as:

$$dF_d = \frac{1}{2} C_d \rho D_c [U - U_x] U - U_x |dz \approx \frac{1}{2} C_d \rho D_c (|U|U) - (2|U|U_x) dz \quad (2.40)$$

Where  $|U| = \hat{U}$  is time independent and for cylindrical section and equal to

$$|U| = \hat{U} \approx \frac{4e^{kz} \omega H}{3\pi} \quad (2.41)$$



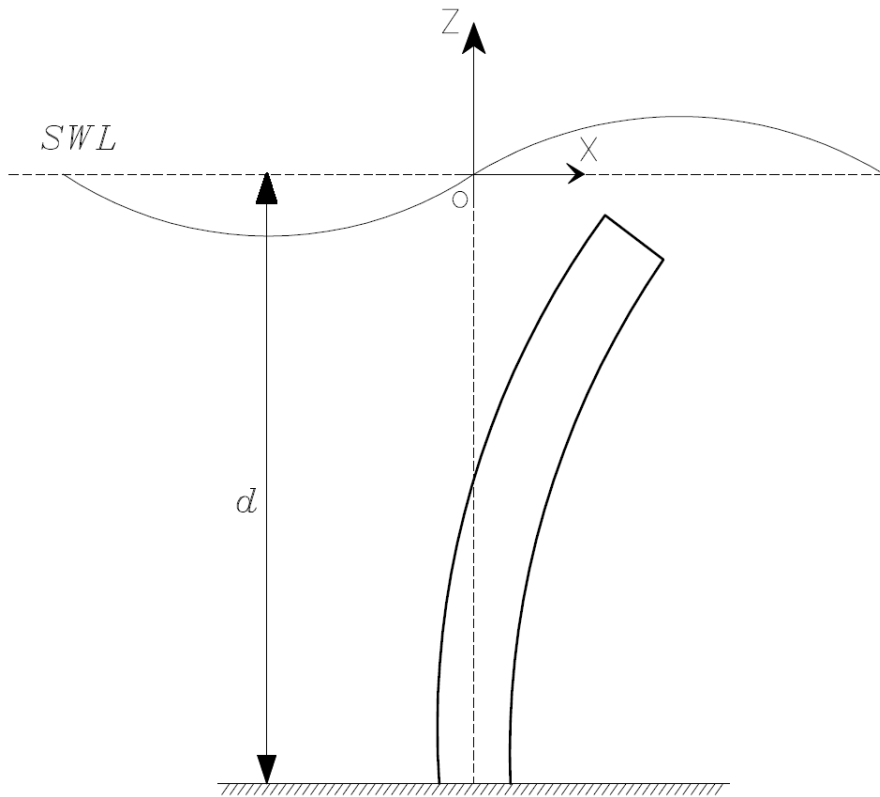


Figure 2.5: a flexible cylinder

#### 2.4.4 Modified Morison Equation for Inclined Cylinder

If the cylinder is located between coordinates  $(X_1, Y_1, Z_1)$  and  $(X_2, Y_2, Z_2)$  relative to principal platform axis, then direction cosines can be defined as follows (Figure 2.6)

$$\cos \alpha = \frac{X_2 - X_1}{L}, \cos \beta = \frac{Y_2 - Y_1}{L}, \cos \gamma = \frac{Z_2 - Z_1}{L} \quad (2.42)$$

The components of the normal velocity and acceleration vectors for a segment of submerged portion of an arbitrarily inclined cylinder can be expressed in terms of the direction cosines (Patel, 1989) as

$$u_x = (u - \dot{x}_1) \sin^2 \alpha - (w - \dot{x}_3) \cos \alpha \cos \gamma \quad (2.43)$$

$$u_y = (u - \dot{x}_2) \sin^2 \beta - (w - \dot{x}_3) \cos \beta \cos \gamma \quad (2.44)$$

$$u_z = (w - \dot{x}_3) \sin^2 \gamma - (u - \dot{x}_1) \cos \alpha \cos \gamma \quad (2.45)$$

$$\dot{u}_x = \dot{u} \sin^2 \alpha - \dot{w} \cos \alpha \cos \gamma \quad (2.46)$$

$$\dot{u}_y = \dot{u} \sin^2 \beta - \dot{w} \cos \beta \cos \gamma \quad (2.47)$$

$$\dot{u}_z = \dot{w} \sin^2 \gamma - \dot{u} \cos \alpha \cos \gamma \quad (2.48)$$

where,  $u$ ,  $w$  and  $\dot{u}$ ,  $\dot{w}$  are the horizontal and vertical water particle velocities and accelerations respectively.

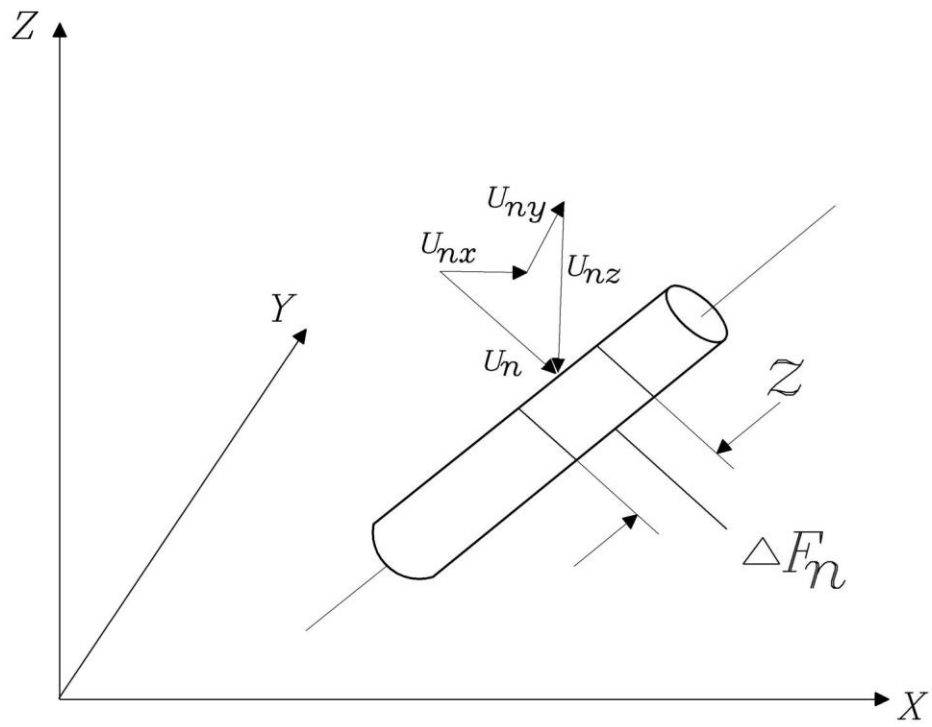


Figure 2.6: Sketch of wave loading on an inclined cylinder

## Chapter 3

### TLP DYNAMIC ANALYSIS

#### 3.1 Introduction

TLPs have very long period of vibration associated with motions in the horizontal plane, and resonant responses in these degrees of freedom are associated with second-order nonlinear wave forces as well as wind load. The periods of vibration associated with displacements in the vertical direction are much shorter than typical wave frequencies, and resonant responses in these degrees of freedom could be excited by nonlinear wave forces. For example, the heave, pitch and roll natural periods are of the order of 3 seconds, and the surge, sway and yaw are of order of 50 second or more. Typical wave spectral peak are between 6 to 15 seconds. Thus, both groups of motion responses fall outside the wave spectral period range, the former group at the lower end, and the latter group on the upper end of the energy spectra plotted against wave period. Consequently, direct resonances, a situation where damping effects control the response are unlikely to occur. (Figure 3.1)

For compliant structures, the inertia forces are predominant when they are dynamically excited. For such a situation, one has to perform rigorous dynamic analysis, and there exist two possibilities. One can do the linear analysis which is cheap and easy, but the major limitation to this is that one should be confident about the system being linear or nearly linear, such that the nonlinear effects, if present, are negligible. In order to incorporate the nonlinear phenomena, a nonlinear analysis has to be performed. Nonlinear effects can not be easily included in frequency domain analysis but best handled in the time domain analysis using Newmark's beta step-by-step numerical integration technique. In this chapter both analytical solutions for rectangular TLP and triangular TLP models will be carried out.

### 3.1.1 Structural Idealization and Assumptions

The equation of motion of both of rectangular and triangular TLP model under a regular wave is given as:

$$[M]\{\ddot{x}\} + [C]\{\dot{x}\} + [K]\{x\} = \{F_o(t)\} \quad (3.1)$$

Where

$\{x\}$  Is the structural displacement vector,

$\{\dot{x}\}$  Is the structural velocity vector,

$\{\ddot{x}\}$  Is the structural acceleration vector,

$[M]$  Is the structure mass matrix,

$[C]$  Is the structure damping matrix,

$[K]$  Is the structure stiffness matrix, and

$\{F_o(t)\}$  Is the hydrodynamic force vector

The mathematical model derived in this thesis based on that the platform and the tethers are treated as a single system and the analysis is carried out for the six degrees of freedom under different environmental loads where wave forces are estimated at the instantaneous equilibrium position of the platform by Morison's equation using Airy's linear wave theory, The effects of wave diffraction effects have been neglected and sheltering for wave forces have also been neglected and wave force coefficients,  $C_d$  and  $C_m$ , are the same for the pontoons and the columns and are independent of frequencies as well as constant over the water depth.

The following assumptions were made in the analysis:

1. Initial pre-tension in all tethers is equal and remains unaltered over time. It is quite large in comparison to the changes that occur during the life time of the TLP. However, the total pre-tension changes with the motion of the TLP.
2. Change in pre-tension is calculated at each time step, and writing the equation of equilibrium at that time step modifies the elements of the stiffness matrix.
3. The platform has been considered symmetrical along the surge axis. Directionality of wave approach to the structure has been ignored in the analysis and only a uni-directional wave train is considered.
4. The damping matrix has been assumed to be mass and stiffness proportional, based on the initial values.

5. The force on tethers (gravity, inertia, drag, hydrostatic and hydrodynamic forces) has been neglected because of its small area and also the tether curvature is not significant in motion, only the axial forces acting on tethers have been considered.
6. Hydrodynamic forces on connecting members and mooring legs have been neglected.
7. The wave, current and structure motions are assumed to occur in the same plane and in the same direction, the interaction of wave and current has been ignored.
8. Integration of hydrodynamic inertia and drag forces are carried out up to the actual level of submergence as suggested by Chakrabarti, 1971, when variable submergence is considered.

### 3.1.2 Mathematical Model of TLP

#### 3.1.2.1 Mass Matrix, $[M]$

The motion of a platform is described by the platform-fixed coordinate system (Figure 3.2).

Global structure mass matrix  $[M]$  can be written in the following form

$$[M] = \begin{pmatrix} M & 0 & 0 & 0 & r_3M & -r_2M \\ 0 & M & 0 & -r_3M & 0 & r_1M \\ 0 & 0 & M & r_2M & -r_1M & 0 \\ 0 & -r_3M & r_2M & J_{11} & -J_{12} & -J_{13} \\ r_3M & 0 & -r_1M & -J_{12} & J_{22} & -J_{23} \\ -r_2M & r_1M & 0 & -J_{13} & -J_{23} & J_{33} \end{pmatrix} \quad (3.2)$$

Where;

$M$  is the mass of the body,

$r_i$  is the location of the mass center with respect to the platform-fixed coordinate system and equal zero if the fixed coordinate is the mass center so  $r_1 = r_2 = r_3 = 0$

$$j_{ii} \text{ Is moments of inertia} = \int (r_j^2 + r_k^2) dm \quad , \quad (3.2.1)$$

$$j_{ij} \text{ Is products of inertia} = \int (r_i r_j) dm \quad , \quad (3.2.2)$$

And  $J_{ij}$  is equal to zero if the fixed coordinates is the mass center

The added mass,  $M_a$ , is due to the water surrounding the structural members and arising from the modified Morison equation has been considered up to the mean sea level (MSL) only when we calculate the damping and the natural time period. The fluctuating component of added mass due to the variable submergence of the structure in water is considered in the force vector depending upon whether the sea surface elevation is above (or) below the MSL that is when the coupling effect take into account but when we discuss the uncoupling effect we add the total added mass in the force vector. the added mass will be

$$[M_a] = \begin{pmatrix} M_{a11} & 0 & M_{a13} & 0 & M_{a15} & M_{a16} \\ 0 & M_{a22} & M_{a23} & M_{a24} & 0 & M_{a26} \\ M_{a31} & M_{a32} & M_{a33} & M_{a34} & M_{a35} & 0 \\ 0 & M_{a42} & M_{a43} & M_{a44} & 0 & 0 \\ M_{a51} & 0 & M_{a53} & 0 & M_{a55} & 0 \\ M_{a61} & M_{a62} & 0 & 0 & 0 & M_{a66} \end{pmatrix} \quad (3.4)$$

Where, the one-half of the symmetrical added mass matrix coefficients are

$$M_a(1,1) = \int_L (\rho C_a A \sin^2 \alpha) dL, \quad (3.4.1)$$

$$M_a(2,2) = \int_L (\rho C_a A \sin^2 \beta) dL, \quad (3.4.2)$$

$$M_a(1,3) = M_a(3,1) = \int_L -(\rho C_a A \cos \alpha \cos \gamma) dL, \quad (3.4.3)$$

$$M_a(3,2) = M_a(2,3) = \int_L -(\rho C_a A \cos \beta \cos \gamma) dL, \quad (3.4.4)$$

$$M_a(1,5) = M_a(5,1) = M_a(1,1)\bar{Z} - M_a(1,3)\bar{X}, \quad (3.4.5)$$

$$M_a(2,4) = M_a(2,2)\bar{Z} - M_a(1,3)\bar{Y}, \quad (3.4.6)$$

$$M_a(3,3) = \int_L (\rho C_a A \sin^2 \gamma) dL, \quad (3.4.7)$$

$$M_a(3,5) = M_a(5,3) = M_a(1,3)\bar{Z} - M_a(3,3)\bar{X}, \quad (3.4.8)$$

$$M_a(3,4) = M_a(4,3) = M_a(2,3)\bar{Z} - M_a(3,3)\bar{Y}, \quad (3.4.9)$$

$$M_a(5,5) = M_a(1,1)\bar{X}_m^2 - 2M_a(1,3)(ZX)_m + M_a(3,3)\bar{Z}_m^2, \text{ and} \quad (3.4.10)$$

$$M_a(4,4) = M_a(2,2)\overline{Y_m^2} - 2M_a(2,3)(ZY)_m + M_a(3,3)\overline{Z_m^2} \quad (3.4.11)$$

$$M_a(6,6) = M_a(2,2)\overline{Y_m^2} + M_a(1,1)\overline{X_m^2} \quad (3.4.12)$$

$$M_a(1,6) = M_a(6,1) = -M_a(1,1)\overline{Y} \quad (3.4.13)$$

$$M_a(2,6) = M_a(6,2) = -M_a(2,2)\overline{X} \quad (3.4.14)$$

Where,

$$A = \frac{\pi D^2}{4} \quad (3.4.15)$$

$$\overline{X} = \frac{X_1 + X_2}{2}, \quad (3.4.16)$$

$$\overline{Y} = \frac{Y_1 + Y_2}{2}, \quad (3.4.17)$$

$$\overline{Z} = \frac{Z_1 + Z_2}{2}, \quad (3.4.18)$$

$$\overline{X_m^2} = \frac{X_1^2 + X_1X_2 + X_2^2}{3}, \quad (3.4.19)$$

$$\overline{Y_m^2} = \frac{Y_1^2 + Y_1Y_2 + Y_2^2}{3} \quad (3.4.20)$$

$$\overline{Z_m^2} = \frac{Z_1^2 + Z_1Z_2 + Z_2^2}{3}, \quad (3.4.21)$$

$$(ZX)_m = \frac{2Z_1X_1 + 2Z_2X_2 + Z_1X_2 + Z_2X_1}{6}, \text{ and} \quad (3.4.22)$$

$$(ZY)_m = \frac{2Z_1Y_1 + 2Z_2Y_2 + Z_1Y_2 + Z_2Y_1}{6} \quad (3.4.23)$$

Where, every term of these matrices will be determined in the later section according to the specific type of TLP.



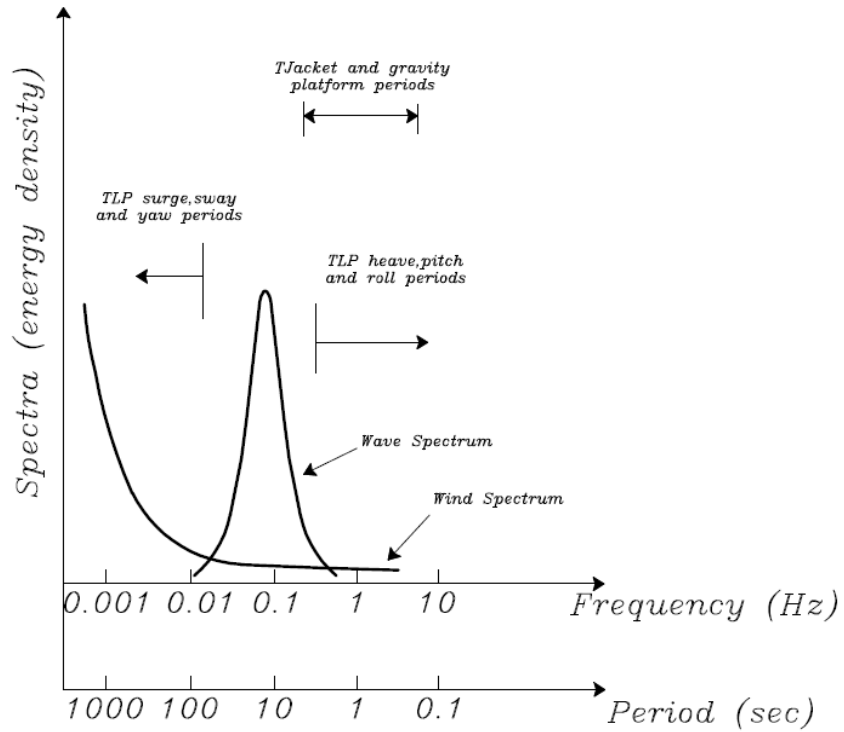


Figure 3.1: Wind and wave spectra relative to the fixed and TLP structures (Kareem, 1987)

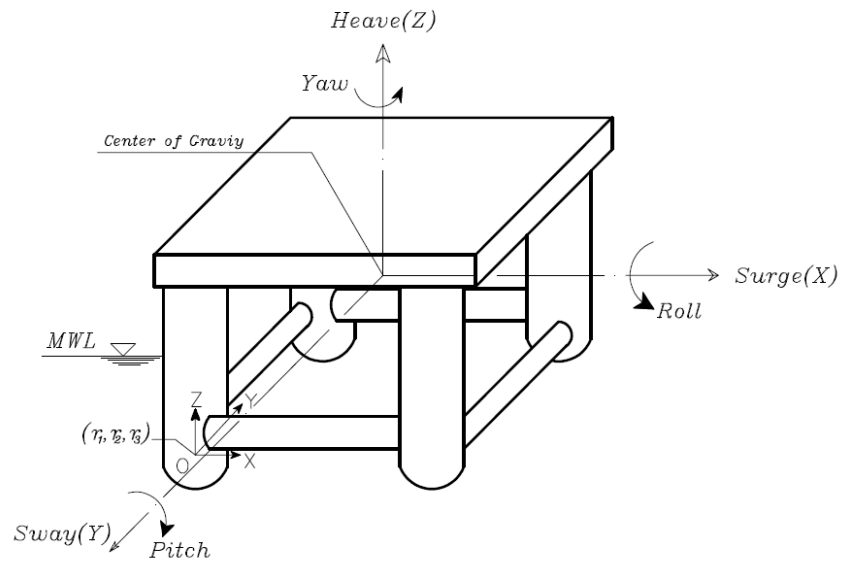


Figure 3.2: The global and local coordinate system of TLP

### 3.1.2.2 Structural Stiffness Matrix

A TLP is basically a floating structure held to the sea floor through pretensioned cables. The pretension in the cables is a result of the excess buoyancy of the platform. The stiffness of the platform is derived from a combination of hydrostatic restoring forces and restoring forces due to the cables. Restoring force for motions in the horizontal plane (surge, sway, and yaw) are the horizontal component of the pretension in the cables (Figure 3.2), while restoring forces for motions in the vertical plane arise primarily from the elastic properties of the cables, with a relatively small contribution due to hydrostatic forces.

The coefficients,  $K_{ij}$ , of the stiffness matrix of the rectangle TLP are derived as the reaction in the degree of freedom  $i$  due to unit displacement in the degree of freedom  $j$ , keeping all other degrees of freedom restrained. The coefficients of the stiffness matrix have nonlinear terms. Furthermore, the tether tension changes due to the motion of the TLP in different degrees of freedom make the stiffness matrix response-dependent.

### 3.1.2.3 Structural Damping $[C]$

The damping matrix  $[C]$  is equal to

$$[C] = [c_s] + [B] + [c_H] + [c_w] \quad (3.5)$$

Where,

$[c_s]$  Is the structure damping mass matrix is assumed to be mass and restoring force proportional,

$[B]$  Is the radiation damping matrix and is neglected,

$[c_H]$  Is the hydrodynamic drag damping and is included in the force vector, and

$[c_w]$  Is the aerodynamic damping and is neglected in this thesis since wind effect is not taken into account.

So the damping matrix is only equal to structural damping matrix. It can be written in the following form (Chopra, 1995):

$$c = m \left( \sum_{n=1}^{n=6} \frac{2\zeta_n \omega_n}{M_n} \phi_n \phi_n^T \right) m \quad (3.6)$$

Where;  $\{\phi_n\}$  and  $\omega_n$  are the mode shapes and structure's natural frequencies,  $\zeta_n$  is the structural damping ratio,  $C$  is the damping matrix,  $m$  is the total structure mass matrix and  $M_n$  is the corresponding element of the  $\{\phi_n\}^T [m] \{\phi_n\}$

This matrix is calculated based on the initial values of  $[K]$  and  $[M]$  depending on the type of the platform.

### 3.1.2.4 Hydrodynamic Force Vector, $\{F(t)\}$

Water particle kinematics is evaluated using Airy's linear wave theory. This description assumes the wave form whose wave height,  $H$ , is small in comparison to its wave length,  $L$ , and water depth,  $d$ . Knowing the water particle kinematics, the hydrodynamic force vector is calculated in each degree of freedom. Only a uni-directional wave train is considered in the surge direction. The force vector  $F(t)$  is given as:

$$F(t) = \{F_{11} \quad F_{21} \quad F_{31} \quad F_{41} \quad F_{51} \quad F_{61}\}^T \quad (3.7)$$

The hydrodynamic force attracted by the members in the surge, sway and heave degrees of freedom are computed and designated as  $F_{11}$ ,  $F_{21}$  and  $F_{31}$ , respectively. The moment of these forces about the x, y and z axes are designated as  $F_{41}$ ,  $F_{51}$  and  $F_{61}$ , respectively taking anticlockwise moments negative.

Since the wave is unidirectional, there would be no force in the sway degree-of-freedom  $F_{21}$  and hence there will be no moment in the roll degree of-freedom  $F_{41}$ . Because of the vertical water particle velocity and acceleration, the heave degree-of-freedom would experience wave force  $F_{31}$ . The force in the surge direction  $F_{11}$  on the vertical members will cause moment in the pitch degree-of-freedom  $F_{51}$ . However, forces in the surge degree-of-freedom are symmetrical about the x- axis (due to the symmetry of the platform to the approaching wave) and there will be no net moment caused in the yaw degree-of-freedom  $F_{61}$ .

So due to a uni-directional wave train in the surge direction the values of  $F_{21}=F_{41}=F_{61}=0$  but  $F_{11}$ ,  $F_{31}$ ,  $F_{51}$  have values that depend on type of TLP.

## 3.2 Development of a Rectangle TLP model

### 3.2.1 Draft Evaluation

At the original equilibrium position (Figure 3.3), summation of forces in the vertical direction gives:

$$W + T_i = F_B \quad (3.8)$$

So;

$$W + (4T_o) = F_B \quad (3.9)$$

And,

$$F_B = 0.25 \rho \pi g (4D_c^2 D_r + 2D_p^2 s_a + 2D_p^2 s_b) \quad (3.10)$$

From Eq. (3.11), we get:

$$D_r = \frac{[\{(W + T) / (0.25 \rho \pi g)\} - (2D_p^2 s_a) - (2D_p^2 s_b)]}{4D_c^2} \quad (3.11)$$

Where,  $F_B$  is the total buoyancy force,  $W$  is the total weight of the platform in air,  $T_i$  is the total instantaneous tension in the Tethers,  $T_o$  is the initial pre-tension in the tether,  $\rho$  is the mass density of sea water,  $D_c$  is the diameter of TLP columns,  $D_p$  is the diameter of pontoon,  $s_a$ ,  $s_b$  is the length of the pontoon between The inner edges of the columns in the x, y direction respectively, and  $D_r$  is the draft.

### 3.2.2 Stiffness Matrix of the Rectangle TLP Configuration

As shown in section (3.1.2.2) the coefficients of the stiffness matrix  $[K]$  of a rectangle TLP are:

$$[K] = \begin{pmatrix} K_{11} & 0 & 0 & 0 & K_{15} & 0 \\ 0 & K_{22} & 0 & K_{24} & 0 & 0 \\ K_{31} & K_{32} & K_{33} & K_{34} & K_{35} & K_{36} \\ 0 & K_{42} & 0 & K_{44} & 0 & 0 \\ K_{51} & 0 & 0 & 0 & K_{55} & 0 \\ 0 & 0 & 0 & 0 & 0 & K_{66} \end{pmatrix} \quad (3.12)$$

And can be determined as

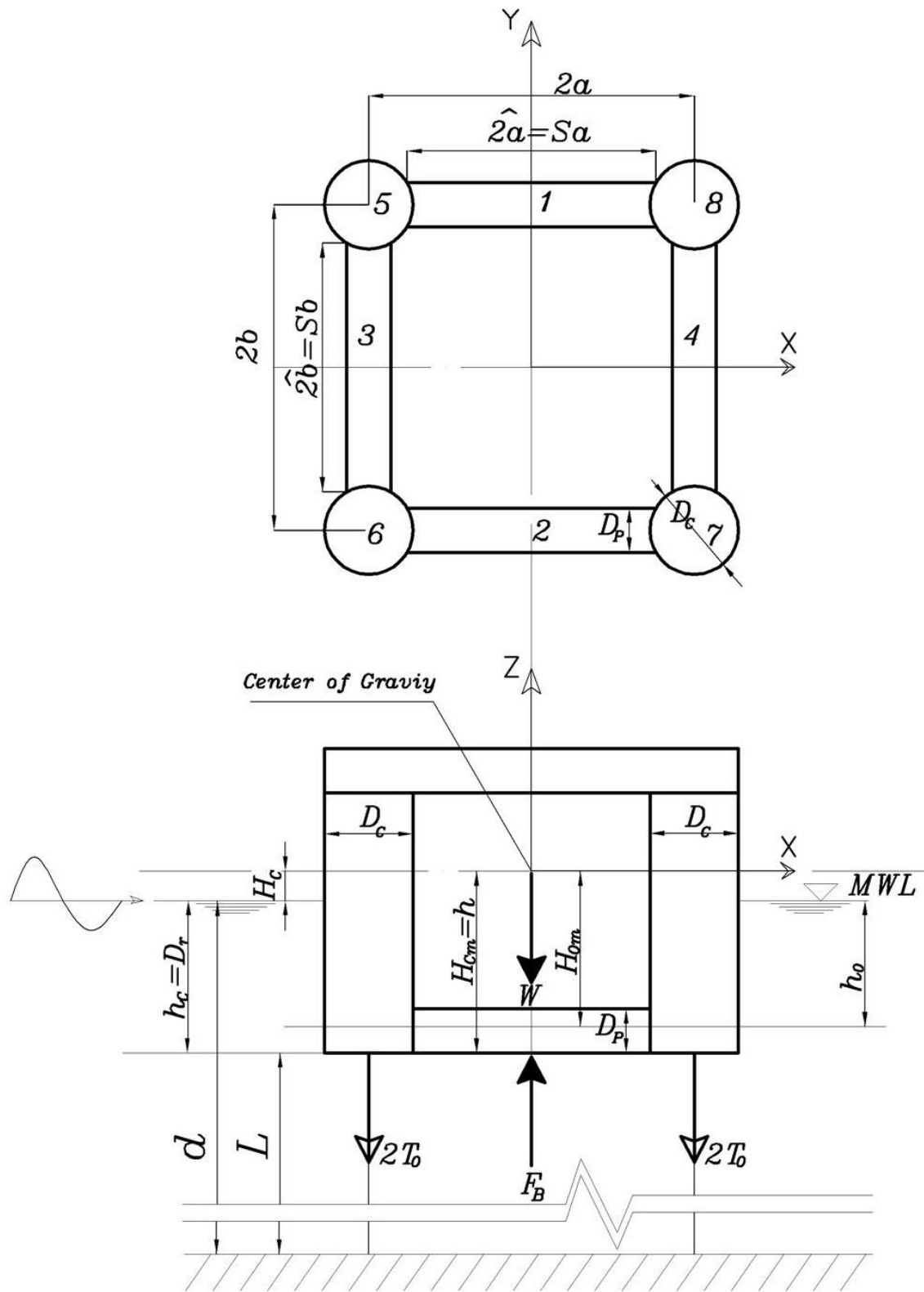


Figure 3.3: The rectangular TLP (plan and elevation).

### 3.2.2.1 Surge (1) Direction (Figure 3.4)

The coefficients of the first column of the restoring force matrix are found by giving a unity x displacement in the x-direction (surge):

The increase in the initial pretension in each leg is given by:

$$E = \frac{\text{Stress}}{\text{Strain}} = \frac{\Delta T_1}{A} \bigg/ \frac{\Delta L}{L} \quad (3.13)$$

$$\text{Where; } \Delta T_1 = \frac{E \times A \times \Delta L}{L} \quad (3.14)$$

$$\Delta L = \sqrt{x_1^2 + L^2} - L \quad (3.15)$$

Where,  $A$  is the cross-sectional area of the tether,  $E$  is Young's Modulus of the tether,  $\Delta T_1$  is the increase in the initial pre-tension due to the arbitrary displacement given in the surge degree of freedom,  $L$  is the length of the tether, and  $x_1$  is the arbitrary displacement in the surge degree of freedom.

Equilibrium of forces in the surge direction gives

$$\sum F_x = 4(T_o + \Delta T_1) \sin \delta_x = K_{11} x_1 \quad (3.16)$$

Where,  $\delta_x$  is the angle between the initial and the displaced position of the tether for unit displacement given in the surge direction.

$$\sin \delta_x = \frac{x_1}{\sqrt{x_1^2 + L^2}} \quad , \quad \cos \delta_x = \frac{L}{\sqrt{x_1^2 + L^2}} \quad (3.17)$$

Substitute (3.17) into (3.16)

$$4(T_o + \Delta T_1) \frac{x_1}{\sqrt{x_1^2 + L^2}} = K_{11} x_1 \quad (3.18)$$

$$\Rightarrow K_{11} = \frac{4(T_o + \Delta T_1)}{\sqrt{x_1^2 + L^2}} \quad (3.19)$$

Through summation of the vertical forces, we get:

$$\sum F_y = K_{31} x_1 = 4(T_o + \Delta T_1) \cos \delta_x + W - F_B \quad (3.20)$$

$$\Rightarrow K_{31} = \frac{[4T_o (\cos \delta_x - 1) + 4\Delta T_1 \cos \delta_x]}{x_1} \quad (3.21)$$

Summation of moments about the x-axis gives:

$$\sum Mx = 0 = K_{41} x_1 \Rightarrow K_{41} = 0 \quad (3.22)$$

Summation of moments about the y-axis gives:

$$\sum My = -\sum F_x h = -K_{11} h x_1 = K_{51} x_1 \quad (3.23)$$

Where, h is the distance between the center of mass and the bottom of the platform (Figure 3.5).

$$\Rightarrow K_{51} = (-K_{11} h) \quad (3.24)$$

The negative sign occurs due to the counterclockwise moment

Summation of moments about the z-axis gives:

$$\sum Mz = 0 = K_{61} x_1 \Rightarrow K_{61} = 0 \quad (3.25)$$

These coefficients agree well with other researchers as Jain, 1997, and Ali, 1996.

### 3.2.2.2 Sway (2) Direction (Figure 3.5)

The coefficients of the second column of the restoring force matrix are found in a similar manner by giving a unity y displacement in the y-direction (sway):

$$K_{12} = 0, K_{52} = 0 \text{ and } K_{62} = 0 \quad (3.26)$$

$$K_{22} = \frac{4(T_o + \Delta T_2)}{\sqrt{x_2^2 + L^2}} \quad (3.27)$$

$$K_{32} = \frac{[4(T_o [\cos \delta_y - 1])] + [4\Delta T_2 \cos \delta_y]}{x_2} \quad (3.28)$$

$$K_{42} = -h K_{22} \quad (3.29)$$

The negative sign occurs due to the counter clockwise moment.

Where  $\Delta T_2$  is the increase in tension due to sway and  $\delta_y$  is the angle of inclination of the cables with respect to the vertical when under sway movement

$$\text{Where; } \Delta T_2 = \frac{E \times A \times \Delta L}{L} \quad (3.30)$$

$$\Delta L = \sqrt{x_2^2 + L^2} - L \quad (3.31)$$

$$\sin \delta_y = \frac{x_1}{\sqrt{x_2^2 + L^2}}, \quad \cos \delta_y = \frac{L}{\sqrt{x_2^2 + L^2}} \quad (3.32)$$

These coefficients also agree with these presented by Jain1997, Ali, 1996.

### 3.2.2.3 Heave (3) Direction:

The third column is derived by giving the structure an arbitrary displacement in the z direction (heave). The sum of the forces in the all direction yield:

$$\begin{aligned} \sum F_x = \sum F_y = \sum M_x = \sum M_y = \sum M_z = 0 \\ \Rightarrow K_{13} = K_{23} = K_{43} = K_{53} = K_{63} = 0 \end{aligned} \quad (3.33)$$

The sum of the forces in the vertical direction yields

$$\begin{aligned} \sum F_z = 4(T_o + \Delta T_3) + W - (F_b + \Delta F_b) \\ \Rightarrow 4T_o + 4\Delta T_3 - 4T_o - \Delta F_b = K_{33} x_3 \end{aligned} \quad (3.34)$$

Where,  $x_3$  is the displacement in the heave direction,

$$E = \frac{\Delta TL}{Ax_3} \Rightarrow \Delta T_3 = \frac{EA}{L} x_3 = \gamma \times x_3 \quad (3.35)$$

$$F_{b1} = \left[ \frac{4\pi D_c^2}{4} Dr + \frac{2\pi D_p^2}{4} s_a + \frac{2\pi D_p^2}{4} s_b \right] \rho g \quad (3.36)$$

$$F_{b2} = 4 \left[ \frac{\pi D_c^2}{4} (Dr + x_3) + \frac{2\pi D_p^2}{4} s_a + \frac{2\pi D_p^2}{4} s_b \right] \rho g \quad (3.37)$$

By subtracting Eqn. 3.38 from Eqn. 3.37, we obtain

$$\Delta F_b = 4 \frac{\pi D_c^2}{4} pgx_3 \quad (3.38)$$

From Eqn. (3.38) and Eqn. (3.34)

$$\Rightarrow K_{33} = 4\gamma + \Delta F_b \quad (3.39)$$

These also coefficients also agree with Jain1997, and Ali, 1996.



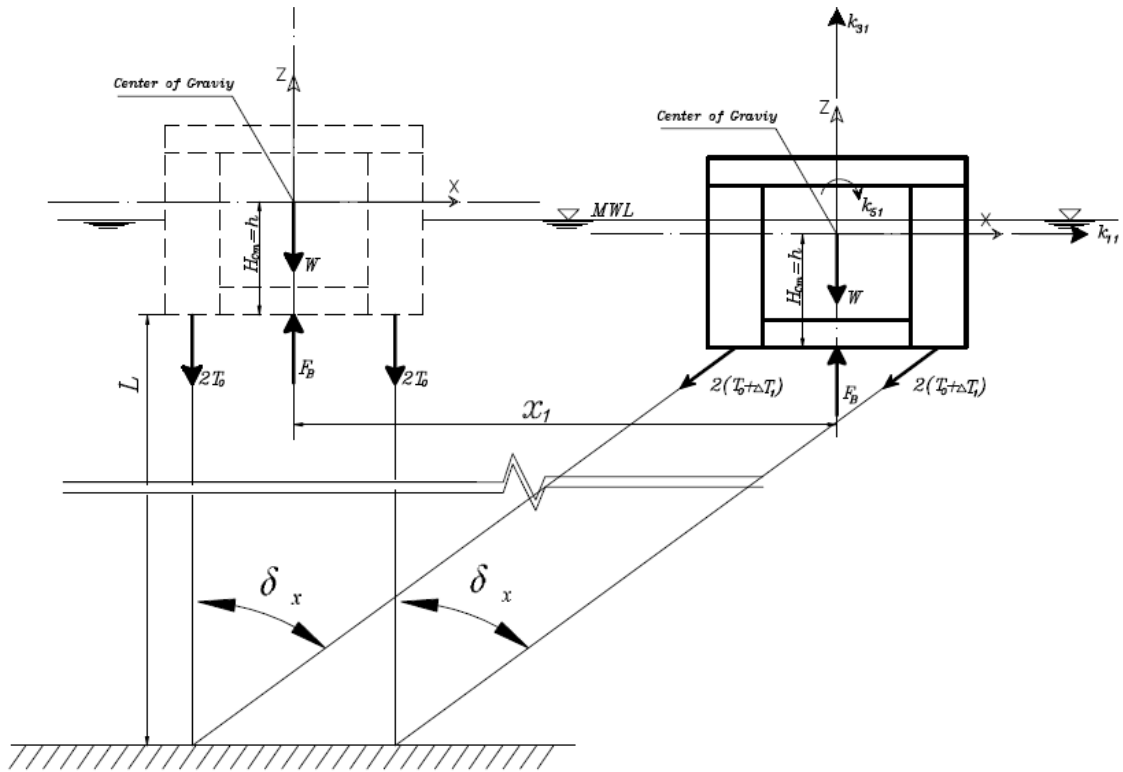


Figure 3.4: The Surge displacement in a rectangular TLP.

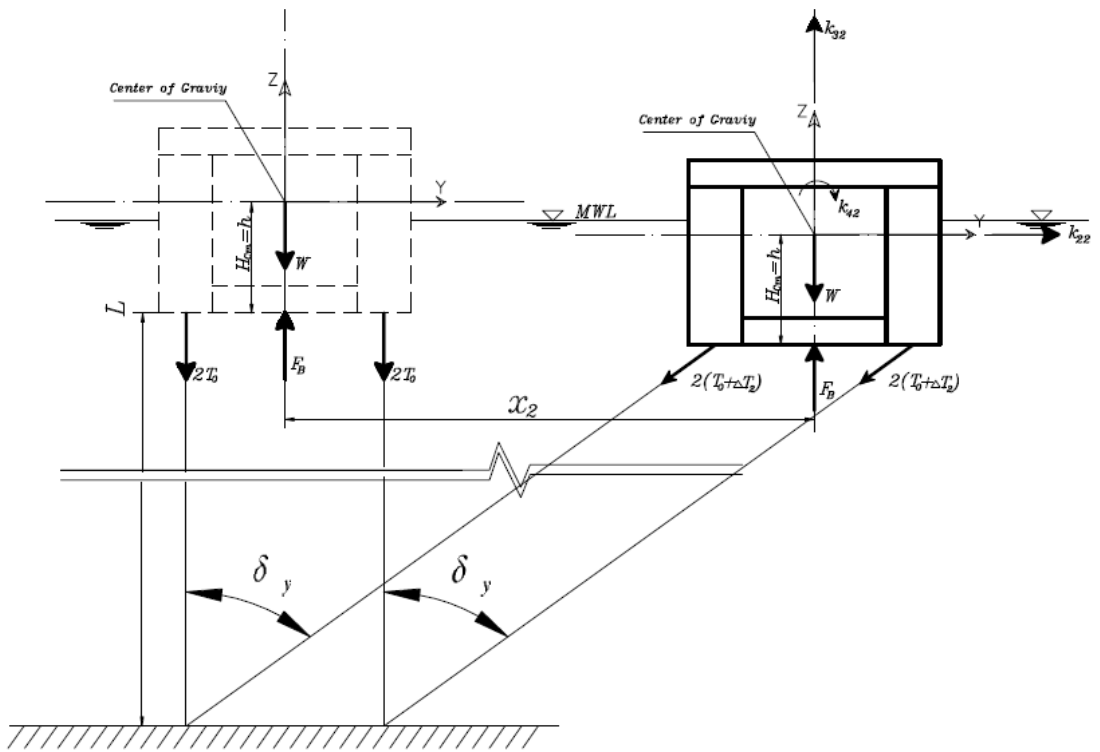


Figure 3.5: The Sway displacement in a rectangular TLP.

### 3.2.2.4 Roll (4) Direction (Figure 3.6)

The coefficients of the fourth column of the restoring force matrix are found by giving the structure in arbitrary rotation  $x_4$  about the x-axis. Summation of the moments of the resulting forces about the x-axis give:

$$K_{14} = K_{54} = K_{64} = 0 \quad (3.40)$$

The change in the initial pretension in each leg is obtained by examining the geometry of Figure 3.6 as following:

$$h_{o4} = H - H \cos x_4, e_{o4} = H \sin x_4, e_{o14} = \frac{h_{o4}}{\tan x_4}, e_{o24} = e_{o4} - e_{o14}$$

$$L_{CG14} = \sqrt{(e_{o14}^2 + h_{o4}^2)} + b, L_{CG24} = 2b - L_{CG14}, L_{14} = L_{CG14} \times \cos x_4$$

$$L_{24} = L_{CG24} \times \cos x_4, e_{14} = L_{14} - b + e_{o24}, e_{24} = -L_{24} + b + e_{o24}$$

$$h_{14} = L_{14} \times \tan x_4, h_{24} = L_{24} \times \tan \theta_4, L_{T14} = \sqrt{(L + h_{14})^2 + e_{14}^2}$$

$$L_{T24} = \sqrt{(L - h_{24})^2 + e_{24}^2}$$

$$\Rightarrow \Delta T_{24} = \frac{AE}{L} \times (L_{T24} - L) \quad (3.41)$$

$$\Rightarrow \Delta T_{14} = \frac{AE}{L} \times (L_{T14} - L) \quad (3.42)$$

$$\Rightarrow \Delta T_4 = 2\Delta T_{14} + 2\Delta T_{24} \quad (3.43)$$

$$\theta_{14} = \tan^{-1}\left(\frac{e_{14}}{L}\right), \theta_{24} = \tan^{-1}\left(\frac{e_{24}}{L}\right) \quad (3.44)$$

By taking summation of forces in y-axis we find

$$\sum y = -[2(T_o + \Delta T_{14}) \sin \theta_{14} + 2(T_o + \Delta T_{24}) \sin \theta_{24}] = K_{24} x_4 \quad (3.45)$$

$$\Rightarrow K_{24} = \frac{-[2(T_o + \Delta T_{14}) \sin \theta_{14} + 2(T_o + \Delta T_{24}) \sin \theta_{24}]}{x_4} \quad (3.46)$$

By taking summation of forces in z-direction we find

$$\sum Z = K_{34} \times x_4 = [2(T_o + \Delta T_{14}) \cos \theta_{14} + 2(T_o + \Delta T_{24}) \cos \theta_{24} - 4T_o] \quad (3.47)$$

$$\Rightarrow K_{34} = [2(T_o + \Delta T_{14}) \cos \theta_{14} + 2(T_o + \Delta T_{24}) \cos \theta_{24} - 4T_o] / x_4 \quad (3.48)$$

By taking summation of moment about x axis we find

$$\sum M_x = K_{44} \times x_4 = \begin{bmatrix} 2(T_o + \Delta T_{14}) \cos \theta_{14} (b + e_{14}) \\ -2(T_o + \Delta T_{24}) \cos \theta_{24} (b - e_{24}) \\ + F_B \times e_{o4} + 2(T_o + \Delta T_{24}) \sin \theta_{24} (H - h_{24}) \\ + 2(T_o + \Delta T_{14}) \sin \theta_{14} \times (H - h_{14}) \end{bmatrix} \quad (3.49)$$

$$\Rightarrow K_{44} = \left[ \begin{array}{l} 2(T_o + \Delta T_{14}) \cos \theta_{14} (b + e_{14}) - 2(T_o + \Delta T_{24}) \cos \theta_{24} (b - e_{24}) \\ + F_B \times e_{o4} + 2(T_o + \Delta T_{24}) \sin \theta_{24} (H - h_{24}) \\ + 2(T_o + \Delta T_{14}) \sin \theta_{14} \times (H - h_{14}) \end{array} \right] / x_4 \quad (3.50)$$

Most researchers assumed that the tether remains vertical so  $\theta_{24} = \theta_{14} = 0$  (angle of inclination is vary small) and also assumed that distance  $e_{14} = e_{24}$ ,  $h_{14} = h_{24}$

$$\text{From that } \Delta T_{14} = -\Delta T_{24} = \frac{EA}{L} x_4, \Delta T = 0$$

$$\text{This leads to } \Rightarrow K_{24} = K_{34} = 0 \quad (3.51)$$

$$\Rightarrow K_{44} = [2(\Delta T_{14} b) + 2(\Delta T_{24} b) + F_B e_{o4}] / x_4 \quad (3.52)$$

### 3.2.2.5 Pitch (5) Direction (Figure 3.7)

The coefficients of the fifth column of the restoring force matrix are found by giving the structure an arbitrary rotation  $x_5$  about the y-axis. Summation of the moments of the resulting forces about the y-axis gives:

$$K_{25} = K_{45} = K_{65} = 0 \quad (3.53)$$

The change in the initial pretension in each leg is obtained by examining the geometry of Figure 3.7 as following:

$$h_{o5} = H - H \cos x_5, e_{o5} = H \sin x_5, e_{o15} = \frac{h_{o5}}{\tan x_5}, e_{o25} = e_{o5} - e_{o15}$$

$$L_{CG15} = \sqrt{(e_{o15}^2 + h_{o5}^2)} + a, L_{CG25} = 2a - L_{CG15}, L_{15} = L_{CG15} \times \cos x_5$$

$$L_{25} = L_{CG25} \times \cos x_5, e_{15} = L_{15} - a + e_{o25}, e_{25} = -L_{25} + a + e_{o25}$$

$$h_{15} = L_{15} \times \tan x_5, h_{25} = L_{25} \times \tan x_5, L_{T15} = \sqrt{(L + h_{15}) + e_{15}^2}$$

$$L_{T25} = \sqrt{(L - h_{25}) + e_{25}^2}$$

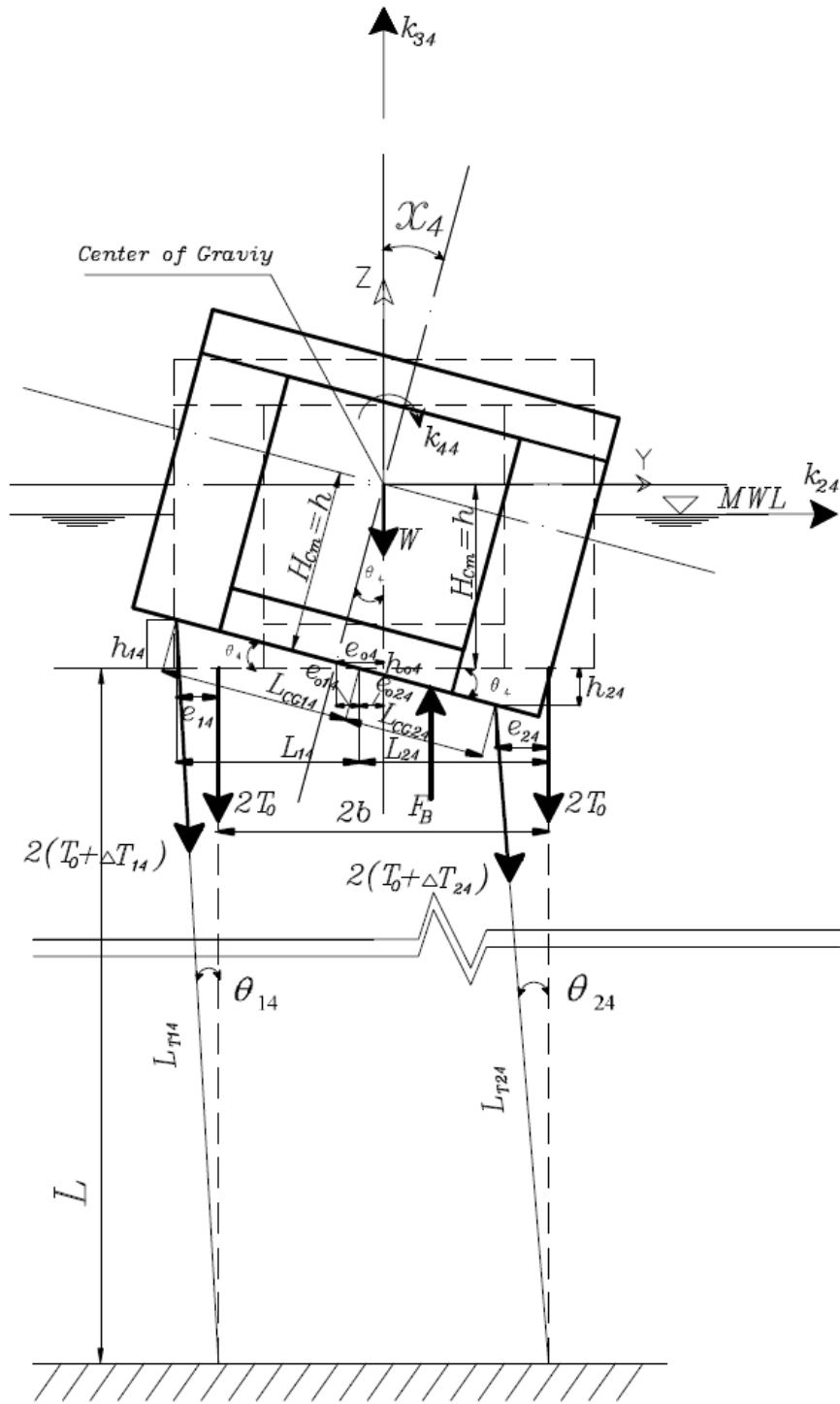


Figure 3.6: The Roll displacement in a rectangular TLP.

$$\Rightarrow \Delta T_{25} = \frac{AE}{L} \times (L_{T25} - L) \quad (3.54)$$

$$\Rightarrow \Delta T_{15} = \frac{AE}{L} \times (L_{T15} - L) \quad (3.55)$$

$$\Rightarrow \Delta T_5 = 2\Delta T_{15} + 2\Delta T_{25} \quad (3.56)$$

$$\theta_{15} = \tan^{-1}\left(\frac{e_{15}}{L}\right), \theta_{25} = \tan^{-1}\left(\frac{e_{25}}{L}\right) \quad (3.57)$$

By taking summation of forces in x-direction

$$\sum x = -[2(T_o + \Delta T_{15}) \sin \theta_{15} + 2(T_o + \Delta T_{25}) \sin \theta_{25}] = K_{15} x_5 \quad (3.58)$$

$$\Rightarrow K_{15} = \frac{-[2(T_o + \Delta T_{15}) \sin \theta_{15} + 2(T_o + \Delta T_{25}) \sin \theta_{25}]}{x_5} \quad (3.59)$$

By taking summation of forces in z-direction we find

$$\sum Z = K_{35} \times x_5 = [2(T_o + \Delta T_{15}) \cos \theta_{15} + 2(T_o + \Delta T_{25}) \cos \theta_{25} - 4T_o] \quad (3.60)$$

$$\Rightarrow K_{35} = [2(T_o + \Delta T_{15}) \cos \theta_{15} + 2(T_o + \Delta T_{25}) \cos \theta_{25} - 4T_o] / x_5 \quad (3.61)$$

y taking summation of moment about y-axis we find

$$\sum M_y = k_{55} \times x_5 = \left[ \begin{array}{l} 2(T_o + \Delta T_{15}) \cos \theta_{15} (a + e_{15}) \\ - 2(T_o + \Delta T_{25}) \cos \theta_{25} (a - e_{25}) \\ + F_B \times e_{o5} + 2(T_o + \Delta T_{25}) \sin \theta_{25} (H - h_{25}) \\ + 2(T_o + \Delta T_{15}) \sin \theta_{15} \times (H - h_{15}) \end{array} \right] \quad (3.62)$$

$$\Rightarrow K_{55} = \left[ \begin{array}{l} 2(T_o + \Delta T_{15}) \cos \theta_{15} (a + e_{15}) \\ - 2(T_o + \Delta T_{25}) \cos \theta_{25} (a - e_{25}) \\ + F_B \times e_{o5} + 2(T_o + \Delta T_{25}) \sin \theta_{25} (H - h_{25}) \\ + 2(T_o + \Delta T_{15}) \sin \theta_{15} \times (H - h_{15}) \end{array} \right] / x_5 \quad (3.63)$$

Most researchers assumed that the tether remains vertical so  $\theta_{25} = \theta_{15} = 0$  (angle of inclination is vary small) and also assumed that distance  $e_{15} = e_{25}$ ,  $h_{15} = h_{25}$

From that  $\Delta T_{15} = -\Delta T_{25} = \frac{EA}{L} x_5$ ,  $\Delta T = 0$

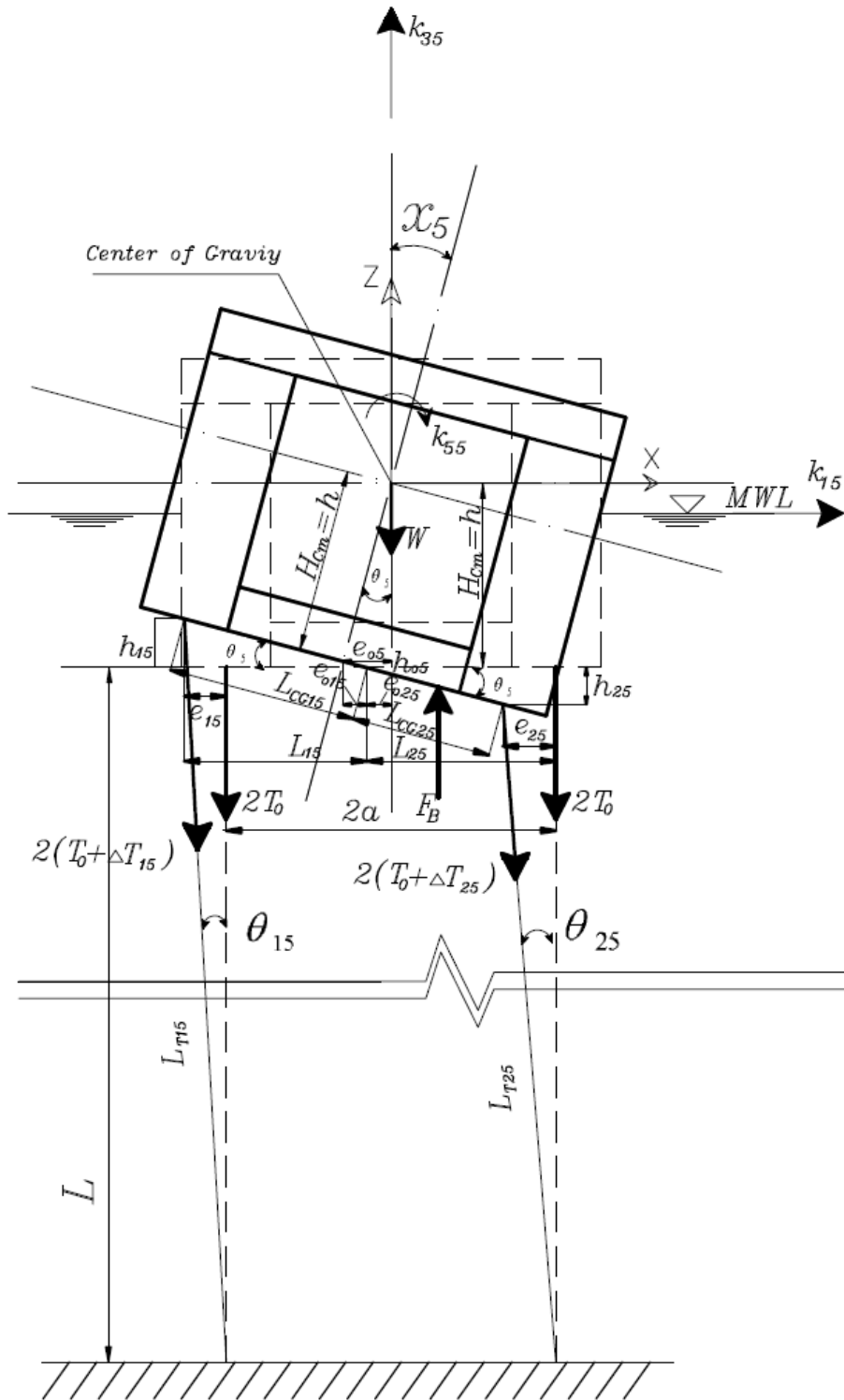


Figure 3.7: The Pitch displacement in a rectangular TLP.

$$\text{This leads to } \Rightarrow K_{15} = K_{35} = 0 \quad (3.64)$$

$$\Rightarrow K_{44} = [2(\Delta T_{15}a) + 2(\Delta T_{25}a) + F_B e_{05}] / x_5 \quad (3.65)$$

### 3.2.2.6 Yaw (6) Direction (Figure 3.8)

By giving an arbitrary rotation  $x_6$  in the yaw degree of freedom, the sixth column of the restoring force matrix can be obtained. The summation of the moment about the z-axis gives:

$$K_{16} = K_{26} = K_{46} = K_{56} = 0 \quad (3.66)$$

$$L_l = \sqrt{L^2 + x_6^2 (a^2 + b^2)} \quad (3.67)$$

$$\sin \delta_6 = \frac{\phi_6 \sqrt{a^2 + b^2}}{L_l}, \cos \delta_6 = \frac{L}{L_l} \quad (3.68)$$

The change in the initial pre-tension in each leg is given by:

$$\Delta T_6 = \frac{AE}{L} (L_l - L) \quad (3.69)$$

By taking summation of moment about z-axis we find

$$\sum M_z = 4(T_o + \Delta T_6)(a^2 + b^2) \frac{x_6}{L_l} = K_{66} \times x_6 \quad (3.70)$$

$$\Rightarrow K_{66} = 4(T_o + \Delta T_6) \frac{(a^2 + b^2)}{L_l} \quad (3.71)$$

Finally, through summation of forces in the vertical direction one obtains:

$$\sum F_z = W - F_B + 4(T_o + \Delta T_6) \cos \delta_6 = K_{36} x_6 \quad (3.72)$$

$$\Rightarrow K_{36} x_6 = -4T_o + 4T_o \frac{L}{L_l} + 4\Delta T_6 \frac{L}{L_l} \quad (3.73)$$

$$\Rightarrow K_{36} = [4T_o (\frac{L}{L_l} - 1) + 4\Delta T_6 (\frac{L}{L_l})] / x_6 \quad (3.74)$$

These coefficients also agree with Jain, 1997, and Ali, 1996.

The stiffness matrix shows:

- 1- The presence of off-diagonal terms, which reflects the coupling effect between the various degrees of freedom,
- 2- The coefficients depend on the change in the tension of the tethers, which is affecting by the buoyancy of the system. Hence, the matrix is response dependent.

Hence, the stiffness matrix  $[K]$  is not constant for all time instants, but the coefficients are continuously changing at each time step depending upon the response value at the previous step.

### 3.2.3 Mass Matrix, $[M]$

As shown in section (3.1.2.1)  $[M]$  is assumed to be lumped at each degree of freedom. Hence, it is diagonal in nature and is constant

$$[M] = \begin{pmatrix} M & 0 & 0 & 0 & 0 & 0 \\ 0 & M & 0 & 0 & 0 & 0 \\ 0 & 0 & M & 0 & 0 & 0 \\ 0 & 0 & 0 & Mr_x^2 & 0 & 0 \\ 0 & 0 & 0 & 0 & Mr_y^2 & 0 \\ 0 & 0 & 0 & 0 & 0 & Mr_z^2 \end{pmatrix} \quad (3.75)$$

Where;

$r_x$  Is the radius of gyration about the  $x$  -axis,

$r_y$  Is the radius of gyration about the  $y$  -axis,

$r_z$  Is the radius of gyration about the  $z$  -axis,

Using the added mass,  $M_a$  we obtain all terms of the mass matrix (refer to Eqn. 3.4). These terms can be obtained as follows



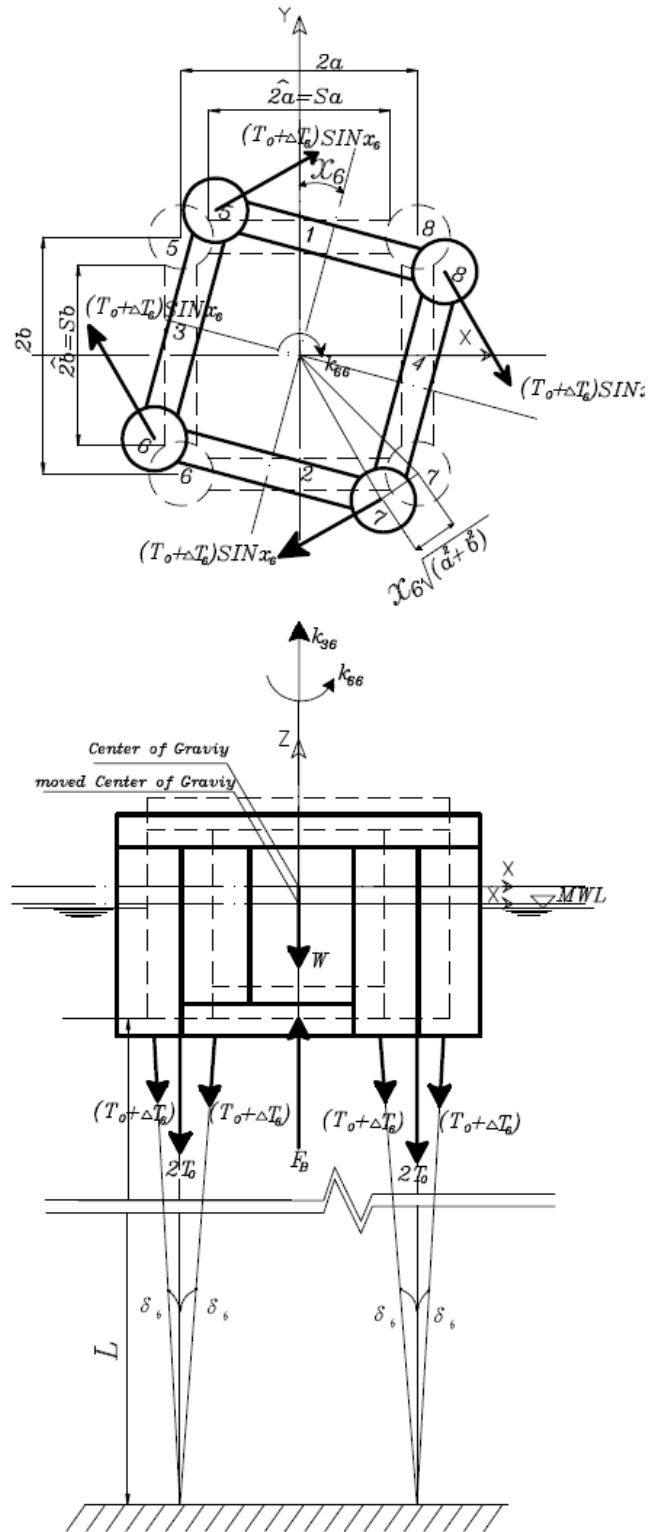


Figure 3.8: The Yaw displacement in a rectangular TLP.

### 3.2.3.1 Surge Direction

$$M_{a11} = C_a \rho \left[ \int_{-hc}^{\eta} \left[ \frac{4\pi D_c^2}{4} dz \right] + \left( \frac{2\pi D_p^2}{4} Sb \right) \right] \quad (3.76)$$

$$\Rightarrow M_{a11} = C_a \rho \left[ \left[ \frac{4\pi D_c^2}{4} (h_c + \eta) \right] + \left( \frac{2\pi D_p^2}{4} Sb \right) \right] \quad (3.77)$$

$$M_{a15} = M_{a51} = C_a \rho \left[ 4 \int_{-hc}^{\eta} \left[ \frac{\pi D_c^2}{4} (z - H_c) dz \right] + \left( \frac{2\pi D_p^2}{4} \times Sb \times -H_{om} \right) \right] \quad (3.78)$$

$$\Rightarrow M_{a51} = C_a \rho \left[ \left[ \frac{4\pi D_c^2}{4} \left( \frac{-h_c^2}{2} - H_c h_c + \frac{\eta^2}{2} - H_c \eta \right) \right] + \left( \frac{2\pi D_p^2}{4} \times Sb \times -H_{om} \right) \right] \quad (3.79)$$

### 3.2.3.2 Sway Direction

$$M_{a22} = C_a \rho \left[ 4 \int_{-hc}^{\eta} \left[ \frac{\pi D_c^2}{4} dz \right] + 2 \left( \frac{\pi D_p^2}{4} Sa \right) \right] \quad (3.80)$$

$$\Rightarrow M_{a22} = C_a \rho \left[ \left[ \frac{4\pi D_c^2}{4} (h_c + \eta) \right] + 2 \left( \frac{\pi D_p^2}{4} Sa \right) \right] \quad (3.81)$$

$$M_{a24} = M_{a42} = C_a \rho \left[ 4 \int_{-hc}^{\eta} \left[ \frac{\pi D_c^2}{4} (z - H_c) dz \right] + \left( \frac{2\pi D_p^2}{4} \times Sa \times -H_{om} \right) \right] \quad (3.82)$$

$$\Rightarrow M_{a42} = C_a \rho \left[ \left[ \frac{4\pi D_c^2}{4} \left( \frac{-h_c^2}{2} - H_c h_c + \frac{\eta^2}{2} - H_c \eta \right) \right] + \left( \frac{2\pi D_p^2}{4} \times Sa \times -H_{om} \right) \right] \quad (3.83)$$

### 3.2.3.3 Heave Direction

$$M_{a33} = C_a \rho \left[ \left( \frac{2\pi D_p^2}{4} Sa \right) + \left( \frac{2\pi D_p^2}{4} Sb \right) \right] \quad (3.84)$$

$$M_{a34} = M_{a43} = C_a \rho \left[ \left[ \frac{\pi D_p^2}{4} \times Sa \times -b \right] + \left[ \frac{\pi D_p^2}{4} \times Sa \times b \right] + 2 \int_{-\frac{sa}{2}}^{\frac{sa}{2}} \left[ \frac{\pi D_p^2}{4} y dy \right] \right] = 0 \quad (3.85)$$

$$M_{a35} = M_{a53} = C_a \rho \left[ \left[ \frac{\pi D_p^2}{4} \times Sb \times -a \right] + \left[ \frac{\pi D_p^2}{4} \times Sb \times a \right] + 2 \int_{-\frac{s_b}{2}}^{\frac{s_b}{2}} \frac{\pi D_p^2}{4} x dx \right] = 0 \quad (3.86)$$

$$M_{a23} = M_{a13} = 0 \quad (3.87)$$

### 3.2.3.4 Roll Direction

$$M_{a44} = C_a \rho \left[ 4 \int_{-hc}^{\eta} \left[ \frac{\pi D_c^2}{4} (z - H_c)^2 dz \right] + 2 \left( \frac{\pi D_p^2}{4} \times Sa \times H_{om}^2 \right) \right. \\ \left. + 2 \int_{-\frac{s_a}{2}}^{\frac{s_a}{2}} \frac{\pi D_p^2}{4} y^2 dy + \left( \frac{\pi D_p^2}{4} \times Sa \times b^2 \right) \right] \quad (3.88)$$

$$M_{a44} = C_a \rho \left[ 4 \frac{\pi D_c^2}{4} \left( H_c^2 h_c + h_c^2 H_c + \frac{h_c^3}{3} + H_c^2 \eta - \eta^2 H_c + \frac{\eta^3}{3} \right) \right. \\ \left. + 2 \left( \frac{\pi D_p^2}{4} \times Sa \times H_{om}^2 \right) + \left( 2 \frac{\pi D_p^2}{4} \frac{s_b^3}{12} \right) + \left( \frac{\pi D_p^2}{4} \times Sa \times b^2 \right) \right] \quad (3.89)$$

### 3.2.3.5 Pitch Direction

$$M_{a55} = C_a \rho \left[ 4 \int_{-hc}^{\eta} \left[ \frac{\pi D_c^2}{4} (z - H_c)^2 dz \right] + 2 \left( \frac{\pi D_p^2}{4} \times Sb \times H_{om}^2 \right) \right. \\ \left. + 2 \int_{-\frac{s_a}{2}}^{\frac{s_a}{2}} \frac{\pi D_p^2}{4} x^2 dy + \left( \frac{\pi D_p^2}{4} \times Sb \times a^2 \right) \right] \quad (3.90)$$

$$M_{a55} = C_a \rho \left[ 4 \frac{\pi D_c^2}{4} \left( H_c^2 h_c + h_c^2 H_c + \frac{h_c^3}{3} + H_c^2 \eta - \eta^2 H_c + \frac{\eta^3}{3} \right) \right. \\ \left. + 2 \left( \frac{\pi D_p^2}{4} \times Sb \times H_{om}^2 \right) + \left( 2 \frac{\pi D_p^2}{4} \frac{s_a^3}{12} \right) + \left( \frac{\pi D_p^2}{4} \times Sb \times a^2 \right) \right] \quad (3.91)$$

### 3.2.3.6 Yaw Direction

$$M_{a61} = M_{a16} = C_a \rho \left[ \begin{array}{c} 2 \int_{-hc}^{\eta} \left[ \frac{\pi D_c^2}{4} adz \right] + 2 \int_{-hc}^{\eta} \left[ \frac{\pi D_c^2}{4} (z - H_c)^2 - adz \right] + \\ 2 \int_{-\frac{s_b}{2}}^{\frac{s_b}{2}} \frac{\pi D_p^2}{4} y dy \end{array} \right] = 0 \quad (3.92)$$

$$M_{a62} = M_{a26} = C_a \rho \left[ \begin{array}{c} 2 \int_{-hc}^{\eta} \left[ \frac{\pi D_c^2}{4} b dz \right] + 2 \int_{-hc}^{\eta} \left[ \frac{\pi D_c^2}{4} (z - H_c)^2 - b dz \right] + \\ 2 \int_{-\frac{s_a}{2}}^{\frac{s_a}{2}} \frac{\pi D_p^2}{4} x dx \end{array} \right] = 0 \quad (3.93)$$

$$M_{a66} = C_a \rho \left[ \begin{array}{c} 4 \int_{-hc}^{\eta} \left[ \frac{\pi D_c^2}{4} b^2 dz \right] + 4 \int_{-hc}^{\eta} \left[ \frac{\pi D_c^2}{4} a^2 dz \right] + 2 \int_{-\frac{s_a}{2}}^{\frac{s_a}{2}} \frac{\pi D_p^2}{4} x^2 dx \\ + 2 \int_{-\frac{s_b}{2}}^{\frac{s_b}{2}} \frac{\pi D_p^2}{4} y^2 dx \end{array} \right] \quad (3.94)$$

$$M_{a66} = C_a \rho \left[ \begin{array}{c} \left( 4 \frac{\pi D_c^2}{4} b^2 (h_c + \eta) \right) + \left( 4 \frac{\pi D_c^2}{4} a^2 (h_c + \eta) \right) + 2 \left( \frac{\pi D_p^2}{4} \frac{Sb^3}{12} \right) \\ + 2 \left( \frac{\pi D_p^2}{4} \frac{Sa^3}{12} \right) \end{array} \right] \quad (3.95)$$

The presence of off diagonal terms in the mass matrix indicates a contribution in the added mass due to the hydrodynamic loading. The loading will be attracted only in the surge, heave and pitch degrees of freedom due to the unidirectional wave acting in the surge direction on a symmetric configuration of the platform about the  $x$  and  $z$  axes. Therefore, added mass matrix can be written as:

$$[M_a] = \begin{pmatrix} M_{a11} & 0 & 0 & 0 & M_{a15} & 0 \\ 0 & 0 & 0 & 0 & 0 & 0 \\ 0 & 0 & M_{a33} & 0 & M_{a35} & 0 \\ 0 & 0 & 0 & 0 & 0 & 0 \\ M_{a51} & 0 & M_{a53} & 0 & 0 & 0 \\ 0 & 0 & 0 & 0 & 0 & 0 \end{pmatrix} \quad (3.96)$$

### 3.2.4 Structural Damping

Applying Eqn. (3.6) in section (3.1.2.3) we get the mode shape as

$$V = \begin{matrix} \text{Heave} & \text{Sway} & \text{Roll} & \text{Surge} & \text{Pitch} & \text{Yaw} \\ \left( \begin{array}{cccccc} 0 & 0 & 0 & 1 & 1 & 0 \\ 0 & 1 & 1 & 0 & 0 & 0 \\ 1 & V_1 & V_3 & V_5 & V_7 & V_9 \\ 0 & V_2 & V_4 & 0 & 0 & 0 \\ 0 & 0 & 0 & V_6 & V_8 & 0 \\ 0 & 0 & 0 & 0 & 0 & 1 \end{array} \right) \end{matrix} \quad (3.97)$$

And the damping matrix will be

$$C = \begin{matrix} \left( \begin{array}{cccccc} C_1 & 0 & C_7 & 0 & C_{16} & 0 \\ 0 & C_4 & C_8 & C_{13} & 0 & 0 \\ C_2 & C_5 & C_9 & C_{14} & C_{17} & C_{19} \\ 0 & C_6 & C_{10} & C_{15} & 0 & 0 \\ C_3 & 0 & C_{11} & 0 & C_{18} & 0 \\ 0 & 0 & C_{12} & 0 & 0 & C_{20} \end{array} \right) \end{matrix} \quad (3.98)$$

It should be noticed that motion in direction z depends on motion in all directions, in agreement with Jain, 1997, and Ali, 1996. But motion in direction (4) depends on direction (2) and direction (3) motion contrary to Jain, 1997, and Ali, 1996, where they assumed that it is independent. Moreover motion in direction (5) depends on direction (1) and direction (3) motions contrary to Jain, 1997, and Ali, 1996, where they assumed that it is independent.

### 3.2.5 Hydrodynamic Force Vector, $\{F(t)\}$ on Rectangular TLP

As shown in section (3.1.2.4) the hydrodynamic force attracted by the members due to a uni-directional wave train in the surge direction  $\{F(t)\}$  is given by Eqn. (3.8) and the values of  $F_{21}=F_{41}=F_{61}=0$ . Expressions for  $F_{11}$ ,  $F_{31}$ , and  $F_{51}$  can be obtained as following:

### 3.2.5.1 Surge Force $F_{I1}$

The horizontal surge force on the TLP contributions to the surge force from horizontal forces on the hulls (pontoons) and vertical columns, Figure (3.3).

The inertia surge force on a single column located at distant  $x$  from the wave crest, is obtained by

$$F I_{ic} = \int_{z=-h_c}^{z=\eta} (.25 \times a_x \times dz) \times \rho \times \pi D_c^2 \times C_m dz \quad (3.99)$$

$$F I_{ic} = \int_{z=-h_c}^{z=\eta} .5 \times \omega^2 \times H \times e^{(zk)} \times \sin(kx - \omega t) \times \rho \times .25 \times \pi D_c^2 \times C_m \times dz \quad (3.100)$$

$$\begin{aligned} &= \rho \times \frac{\pi D_c^2}{4} \times C_m \times \omega^2 \times \frac{H}{2} \times \sin(kx - \omega t) \int (e^{zk}) dz \\ &= \rho \times \frac{\pi D_c^2}{4} \times C_m \times \omega^2 \times \frac{H}{2} \times \sin(kx - \omega t) \left[ \frac{e^{\eta k}}{k} - \frac{e^{-h_c k}}{k} \right] \\ &= \rho \times \frac{\pi D_c^2}{4} \times C_m \times g \times \frac{H}{2} \times \sin(kx - \omega t) [e^{\eta k} - e^{-h_c k}] \end{aligned} \quad (3.101)$$

so for columns at  $x=a$

$$F I_{ic7} + F I_{ic8} = 2\rho \times \frac{\pi D_c^2}{4} \times C_m \times g \times \frac{H}{2} \times \sin((ka) - \omega t) [e^{\eta k} - e^{-h_c k}] \quad (3.102)$$

and for columns at  $x=-a$

$$F I_{ic5} + F I_{ic6} = 2\rho \times \frac{\rho D_c^2}{4} \times C_m \times g \times \frac{H}{2} \times \sin((-ka) - \omega t) [e^{\eta k} - e^{-h_c k}] \quad (3.103)$$

Also the drag surge force on a single column located at distant  $x$  from the wave crest, is obtained by

$$F I_{cd} = \int_{-h_c}^{\eta} \frac{1}{2} C_d \rho D_c \times \frac{4}{3} \frac{\omega H}{\pi} \left[ \frac{\pi H}{T} e^{2kz} \cos(kx - \omega t) + \frac{(z+d)e^{kz} U_c}{d} \right. \\ \left. - 2e^{kz} U_x \right] dz \quad (3.104)$$

$$= \frac{2}{3} C_d \rho D_c \frac{\omega H}{\pi} \left[ \frac{\pi H}{T} \frac{e^{2kz}}{2k} \cos(kx - \omega t) + \frac{ze^{kz} U_c}{d \times k} - \frac{e^{kz} U_c}{d \times k^2} + \frac{e^{kz} U_c}{k} \right]_{z=-h_c}^{z=\eta} \quad (3.105)$$

$$F I_{cd} = \frac{2}{3} C_d \rho D_c \frac{\omega H}{\pi} \left[ \begin{array}{l} \frac{\pi H}{T} \frac{e^{2\eta k}}{2k} \cos(kx - \omega t) + \frac{ne^{\eta k} U_c}{d \times k} - \frac{e^{\eta k} U_c}{h_c \times k^2} + \frac{e^{\eta k} U_c}{k} \\ - \frac{2e^{\eta k}}{k} U_x - \frac{\pi H}{T} \frac{e^{-2h_c k}}{2k} \cos(kx - \omega t) + \frac{h_c e^{-h_c k} U_c}{d \times k} \\ + \frac{e^{-h_c k} U_c}{d \times k^2} - \frac{e^{-h_c k} U_c}{k} + \frac{2e^{-h_c k}}{k} U_x \end{array} \right] \quad (3.106)$$

$$\Rightarrow x = a \Rightarrow F I_{dc7} + F I_{dc8} \quad (3.107)$$

$$x = -a \Rightarrow F I_{dc5} + F I_{dc6} \quad (3.108)$$

Where  $U_x$  is the body velocity in surge direction, and  $U_c$  is the current velocity

So total surge force on columns equal

$$\Rightarrow F I_C = F I_{ic7} + F I_{ic8} + F I_{ic5} + F I_{ic6} + F I_{dc7} + F I_{dc8} + F I_{dc5} + F I_{dc6} \quad (3.109)$$

The inertia surge forces are experienced only by the hull aligned normal to the direction of wave propagation. Thus an inertia surge force varies only due to wave action on hull 3 and 4 and is obtained by:

$$F I_{ip} = \int_{-\hat{b}}^{\hat{b}} \rho \frac{\pi D_p^2}{4} C_m \frac{\omega^2}{2} H e^{-h_o k} \sin(kx - \omega t) dy \quad (3.110)$$

$$F I_{ip} = \rho \frac{\pi D_p^2}{4} C_m \frac{\omega^2}{2} H e^{-h_o k} \sin(kx - \omega t) S b \quad (3.111)$$

$$\Rightarrow x = a \rightarrow F I_{ip4} \quad (3.112)$$

$$x = -a \rightarrow F I_{ip3} \quad (3.113)$$

Also the drag surge forces are experienced only by the hull aligned normal to the direction of wave propagation. Thus drag surge forces varies only on hull 3 and 4 and is obtained by

$$F I_{dp} = \left[ \int_{-\hat{b}}^{\hat{b}} \frac{1}{2} C_d \rho D_p \left[ \left( \frac{\pi H}{T} \right) e^{-h_o k} \cos(kx - \omega t) + \frac{-h_o + d}{d} U_c - U_x \right] dy \right] \quad (3.114)$$

$$= \left[ \frac{1}{2} C_d \rho D_p \left[ \left( \frac{\pi H}{T} \right) e^{-h_o k} \cos(kx - \omega t) + \frac{-h_o + d}{d} U_c - U_x \right] \times \left| \frac{\pi H}{T} e^{-h_o k} \cos(kx - \omega t) + \frac{-h_o + d}{d} U_c - U_x \right| S b \right] \quad (3.115)$$

$$\Rightarrow x = a \rightarrow F1_{dp4} \quad (3.116)$$

$$x = -a \rightarrow F1_{dp3} \quad (3.117)$$

So total surge force on hulls equal

$$\Rightarrow F1_p = F1_{ip3} + F1_{ip4} + F1_{dp3} + F1_{dp4} \quad (3.118)$$

So the total surge force  $F_{11}$

$$\Rightarrow F_{11} = F1_p + F1_c \quad (3.119)$$

### 3.2.5.2 Heave Force $F_{31}$

The vertical wave force on TLP results from several factors:

- (1) The dynamic pressure at the bottom of the columns.
- (2) The forces on the hulls.
- (3) The change of the instantaneous waterline on the columns.

Effect of the dynamic pressure at the bottom of the columns can be obtained as:

$$pressure = \rho \left[ \frac{d\Phi}{dt} \right]_{z=-h_c} = \rho g \frac{H}{2} e^{-h_c k} \cos(kx - \omega t) \quad (3.120)$$

With further assumption that column diameter is small compared to the wave length, so that the dynamic pressure can be assumed to be constant across the bottom surface, the vertical columns force is

$$force = pressure \times area = \frac{\pi D_c^2}{4} \rho g \frac{H}{2} e^{-h_c k} \cos(kx - \omega t) \quad (3.121)$$

$$\Rightarrow x = -a \Rightarrow F3_{c5} + F3_{c6} \quad (3.122)$$

$$x = a \Rightarrow F3_{c7} + F3_{c8} \quad (3.123)$$

So total heave force on columns equal

$$\Rightarrow F3_c = F3_{c7} + F3_{c8} + F3_{c5} + F3_{c6} \quad (3.124)$$

The magnitude of vertical force, hulls 3 and 4, is constant along the hull length and the integration reduces to a simple multiplication. So the inertia force

$$F3_{ip} = - \int_{-\hat{b}}^{\hat{b}} \rho \frac{\pi D_p^2}{4} C_m \frac{\omega^2}{2} H e^{-h_o k} \cos(kx - \omega t) dy \quad (3.125)$$

$$F3_{ip} = - \rho \frac{\pi D_p^2}{4} C_m \frac{\omega^2}{2} H e^{-h_o k} \cos(kx - \omega t) S b \quad (3.126)$$



$$\Rightarrow x = -a \rightarrow F3_{ip3} \quad (3.127)$$

$$x = a \rightarrow F3_{ip4} \quad (3.128)$$

Also the drag force will be

$$F3_{dp} = \left[ \int_{-\hat{b}}^{\hat{b}} \frac{1}{2} C_d \rho D_p \left[ \left( \frac{\pi H}{T} \right) e^{-h_o k} \sin(kx - \omega t) + \frac{-h_o + d}{d} U_c - U_v \right] dy \right. \\ \left. \times \left| \frac{\pi H}{T} e^{-h_o k} \sin(kx - \omega t) + \frac{-h_o + d}{d} U_c - U_v \right| \right] \quad (3.129)$$

$$F3_{dp} = \left[ \frac{1}{2} C_d \rho D_p \left[ \left( \frac{\pi H}{T} \right) e^{-h_o k} \sin(kx - \omega t) + \frac{-h_o + d}{d} U_c - U_v \right] \right. \\ \left. \times \left| \frac{\pi H}{T} e^{-h_o k} \sin(kx - \omega t) + \frac{-h_o + d}{d} U_c - U_v \right| S b \right] \quad (3.130)$$

$$\Rightarrow x = -a \rightarrow F3_{dp3} \quad (3.131)$$

$$x = a \rightarrow F3_{dp4} \quad (3.132)$$

Where,  $U_v$  is the body velocity in heave direction and  $U_c$  is the current velocity

The magnitude of vertical force, hulls 1 and 2, is varied along the hull length and the integration reduces to a simple multiplication. So the inertia force

$$F3_{ip1} + F3_{ip2} = 2 \int_{-\hat{a}}^{\hat{a}} \rho \frac{\pi D_p^2}{4} C_m \frac{-\omega^2}{2} H e^{-h_o k} \cos(kx - \omega t) dx \quad (3.133)$$

$$= -2 \rho \frac{\pi D_p^2}{4} C_m \frac{g}{2} H e^{-h_o k} [\sin(k \hat{a} - \omega t) - \sin(k(-\hat{a}) - \omega t)] \quad (3.134)$$

Also the drag force will be

$$F3_{dp1} + F3_{dp2} = 2 \int_{-a}^a \frac{1}{2} C_d \rho D_p \times \frac{4}{3} \frac{\omega H}{\pi} \left[ \begin{array}{l} \frac{\pi H}{T} e^{-2kh_o} \sin(kx - \omega t) \\ + \frac{(-h_o + d) e^{-kh_o} U_c}{d} \\ - 2e^{-kh_o} U_v \end{array} \right] dx \quad (3.135)$$

$$= \frac{4}{3} C_d \rho D_p \frac{\omega H}{\pi} \left[ \begin{array}{l} \frac{-\pi H}{T \times k} e^{-2kh_o} \cos(kx - \omega t) + \frac{(d - h_o) e^{-kh_o} x U_c}{d} \\ - 2x e^{-kh_o} U_v \end{array} \right] \Bigg|_{x=-a}^{x=a} \quad (3.136)$$

So total heave force on hulls equal

$$\Rightarrow F_{3p} = F_{3ip3} + F_{3ip4} + F_{3ip1} + F_{3ip2} + F_{3dp3} + F_{3dp4} + F_{3dp1} + F_{3dp2} \quad (3.137)$$

Finally the total heave force  $F_{3I}$

$$\Rightarrow F_{3I} = F_{3p} + F_{3C} \quad (3.138)$$

### 3.2.5.3 Pitch response $F_{5I}$

The pitching behavior of a rectangle TLP is some what different from that of a free floating body like a ship or a semi submersible. In the latter case the restoring moment is provided by the action of emerged and immersed volumes around the water plane. In contrast for a TLP, the pitch restoring moment is provided primarily by changes in the tether tension due to elastic deformation. This effect outweighs, by far, the contributions due to changes in column submergence. In strict senses, the pitching access is one about which moment of all the forces (including elastic tether deformation) are zero. The tether deformation, in turn, depends on the location of the pitching axis. Thus, explicit solution for the location of the pitch access is not possible. Here, it would be assumed that the pitch access is at the level of the connection of the tethers to the columns (kirk and Etok, 1979).

The contribution to pitching moment comes from four sources:

- 1) The horizontal acceleration on all vertical columns.
- 2) The horizontal acceleration on hulls aligned normal to the direction of wave propagation.
- 3) The vertical acceleration of the wave particles on hulls 1, 2, 3 and 4.
- 4) The dynamic pressure variation on the bases on the four corner columns.

The horizontal acceleration on hulls 1 and 2 have no contribution to the pitch moment. However, the horizontal force on hulls 3 and 4 produces a pitch moment. This is obtained by multiplying the horizontal force with the lever, measured from the pitching axis. Thus, the pitching moment from hulls 3 and 4 can be obtained as following:

For the inertia force

$$MH_{ip} = \int_{-b}^b \rho \frac{\pi D_p^2}{4} C_m \frac{\omega^2}{2} H e^{-h_o k} \sin(kx - \omega t) (-H_{om}) dy \quad (3.139)$$

$$MH_{ip} = -\rho \frac{\pi D_p^2}{4} C_m \frac{\omega^2}{2} H e^{-h_o k} \sin(kx - \omega t) H_{om} S b \quad (3.140)$$

$$\Rightarrow x = -a \rightarrow MH_{ip3} \quad (3.141)$$

$$x = a \rightarrow MH_{ip4} \quad (3.142)$$

For the drag force

$$MH_{dp} = \left[ \int_{-b}^b \frac{1}{2} C_d \rho D_p \left[ \left( \frac{\pi H}{T} \right) e^{-h_o k} \cos(kx - \omega t) + \frac{(d - h_o)}{d} U_c - U_x \right] \right] dy \quad (3.143)$$

$$\times \left| \frac{\pi H}{T} e^{-h_o k} \cos(kx - \omega t) + \frac{(d - h_o)}{d} U_c - U_x \right| (-H_{om})$$

$$MH_{dp} = \left[ -\frac{1}{2} C_d \rho D_p \left[ \left( \frac{\pi H}{T} \right) e^{-h_o k} \cos(kx - \omega t) + \frac{(d - h_o)}{d} U_c - U_x \right] \right] \quad (3.144)$$

$$\times \left| \frac{\pi H}{T} e^{-h_o k} \cos(kx - \omega t) + \frac{(d - h_o)}{d} U_c - U_x \right| H_{om} S b$$

$$\Rightarrow x = -a \rightarrow MH_{dp3} \quad (3.145)$$

$$x = a \rightarrow MH_{dp4} \quad (3.146)$$

So total surge pitching moment on hull is

$$MH_p = (MH_{dp4} + MH_{dp3} + MH_{ip3} + MH_{ip4}) \quad (3.147)$$

The inertia surge pitching moment on a single column located at x from the wave crest, is obtained by

$$MH_{ic} = \int_{-h_c}^{\eta} (z - Hc) \rho \frac{\pi D_c^2}{4} C_m \frac{\omega^2 H}{2} \sin(kx - \omega t) e^{kz} dz \quad (3.148)$$

$$= \frac{\pi D_c^2}{4} C_m \frac{\omega^2 H}{2} \sin(kx - \omega t) \left[ \begin{array}{l} (\eta - Hc) \frac{e^{\eta k}}{k} - \frac{e^{\eta k}}{k^2} + \frac{e^{-h_c k}}{k^2} \\ - \frac{(-h_c - Hc) e^{-h_c k}}{k} \end{array} \right] \quad (3.149)$$

$$\Rightarrow x = -a \rightarrow MH_{ic5} + MH_{ic6} \quad (3.150)$$

$$x = a \rightarrow MH_{ic7} + MH_{ic8} \quad (3.151)$$

And the drag surge pitching moment is:

$$MH_{dc} = \left[ \int_{-h_c}^{\eta} \left[ \frac{2}{3} C_d \rho D_c \frac{\omega H}{\pi} \left[ \frac{\pi H}{T} e^{2kz} \cos(kx - \omega t) + \frac{z U_c e^{kz}}{h_c} - 2e^{kz} U_x \right] (Z - H_c) dz \right] \right] \quad (3.152)$$

$$= \left[ \frac{2}{3} C_d \rho D_c \frac{\omega H}{\pi} \left[ \frac{\pi H}{T} \cos(kx - \omega t) \left[ (z - H_c) \frac{e^{2kz}}{2k} - \frac{e^{2kz}}{4k^2} \right] + \left[ \frac{U_c}{d} \left( \frac{z e^{kz}}{k} (z - H_c) - \frac{e^{kz}}{k^2} (2z - H_c) + \frac{2e^{kz}}{k^3} \right) \right] \right] \right]_{z=\eta}^{z=-h_c} \quad (3.153)$$

$$= \left[ \frac{2}{3} C_d \rho D_c \frac{\omega H}{\pi} \left\{ \frac{\pi H}{T} \cos(kx - \omega t) \left[ \frac{(\eta - H_c) e^{2\eta k}}{2k} - \frac{e^{2\eta k}}{4k^2} + \frac{e^{-2h_c k}}{4k^2} - \frac{(-h_c - H_c) e^{-2h_c k}}{2k} \right] + \left[ \frac{U_c}{d} \left( \frac{\eta e^{\eta k}}{k} (\eta - H_c) - \frac{e^{\eta k}}{k^2} (2\eta - H_c) + \frac{e^{2\eta k}}{k^3} + \frac{e^{-h_c k}}{k^2} (-2h_c - H_c) \right) - \frac{h_c e^{-h_c k}}{k} (-h_c - H_c) - \frac{e^{2h_c k}}{k^3} + \frac{U_c e^{k\eta}}{k} (\eta - H_c) - \frac{U_c e^{k\eta}}{k^2} - \frac{U_c e^{-kh_c}}{k} (-h_c - H_c) + \frac{U_c e^{-kh_c}}{k^2} \right] - (2U_x \left[ (\eta - H_c) \frac{e^{\eta k}}{k} - \frac{e^{\eta k}}{k^2} + \frac{e^{-h_c k}}{k^2} - \frac{e^{-h_c k}}{k} (-h_c - H_c) \right]) \right\} \right] \quad (3.154)$$

$$\Rightarrow x = -a \rightarrow MH_{dc5} + MH_{dc6} \quad (3.155)$$

$$x = a \rightarrow MH_{dc7} + MH_{dc8} \quad (3.156)$$

So total horizontal pitching moment on columns will be

$$MH_c = \left( MH_{ic5} + MH_{ic6} + MH_{ic7} + MH_{ic8} + MH_{dc5} + MH_{dc6} + MH_{dc7} + MH_{dc8} \right) \quad (3.157)$$

So total surge moment on TLP will be

$$MH = MH_c + MH_p \quad (3.158)$$

To calculate the vertical pitching moment on hulls, first, consider hulls 1 and 2 aligned along the direction of wave propagation. The vertical pitching moment on these hulls is given as

$$MV_{ip1} + MV_{ip2} = \left[ 2 \frac{\pi}{4} \rho C_m D_p^2 \int_{-a}^a \frac{-H}{2} \omega^2 e^{-kh_o} \cos(kx - \omega t) x dx \right] \quad (3.159)$$

$$= \left[ 2 * \frac{\pi}{4} D_p^2 \rho C_m \frac{-H}{2} \omega^2 e^{-kh_o} \left[ \frac{x \sin(kx - \omega t)}{k} + \frac{\cos(kx - \omega t)}{k^2} \right] \right] \Bigg|_{x=-a}^x \Bigg|_{x=a} \quad (3.160)$$

And the vertical drag moment will be

$$MV_{dp1} + MV_{dp2} = 2 \int_{-a}^a \frac{1}{2} C_d \rho D_p \frac{4 - x\omega H}{3 \pi} \left[ \frac{\pi H}{T} e^{-2kh_o} \sin(kx - \omega t) + \frac{(d - h_o) e^{-kh_o} U_c - 2e^{-kh_o} U_v}{d} \right] dx \quad (3.161)$$

$$= \frac{4}{3} C_d \rho D_p \frac{\omega H}{\pi} \left[ \frac{\pi H}{T} e^{-2kh_o} \left[ \frac{-x \cos(kx - \omega t)}{k} + \frac{\sin(kx - \omega t)}{k^2} \right] + \frac{(d - h_o) x^2 e^{-kh_o} U_c - x^2 e^{-kh_o} U_v}{2d} \right] \Bigg|_{x=-a}^x \Bigg|_{x=a} \quad (3.162)$$

Next, consider the effect of the vertical acceleration on hulls 3 and 4. These hulls are parallel to the Crestline, and the force per unit of length is constant along the length of the hull. The pitch inertia vertical moment is obtained by multiplying the vertical force, derived for heave excitation, by the lever distance from the centerline so the force on these hulls will be:

$$MV_{ip} = -2 \int_{-\hat{b}}^{\hat{b}} \rho \frac{\pi D_p^2}{4} C_m \frac{\omega^2}{2} H e^{-h_o k} \cos(kx - \omega t) x dy \quad (3.163)$$

$$MV_{ip} = -2 \rho \frac{\pi D_p^2}{4} C_m \frac{\omega^2}{2} H e^{-h_o k} \cos(kx - \omega t) x S_b \quad (3.164)$$

$$\Rightarrow x = -a \rightarrow MV_{ip3} \quad (3.165)$$

$$x = a \rightarrow MV_{ip4} \quad (3.166)$$

Also the drag vertical pitching moment will be

$$MV_{dp} = \left[ \int_{-\hat{b}}^{\hat{b}} \frac{1}{2} C_d \rho D_p \left[ \left( \frac{\pi H}{T} \right) e^{-h_o k} \sin(kx - \omega t) + \frac{(d - h_o)}{d} U_c - U_v \right] \times \left| \frac{\pi H}{T} e^{-h_o k} \sin(kx - \omega t) + \frac{(d - h_o)}{d} U_c - U_v \right| x dy \right] \quad (3.167)$$

$$MV_{dp} = \left[ \frac{1}{2} C_d \rho D_p \left[ \left( \frac{\pi H}{T} \right) e^{-h_o k} \sin(kx - \omega t) + \frac{(d - h_o)}{d} U_c - U_v \right] \times \left| \frac{\pi H}{T} e^{-h_o k} \sin(kx - \omega t) + \frac{(d - h_o)}{d} U_c - U_v \right| x S_b \right] \quad (3.168)$$

$$\Rightarrow x = -a \rightarrow MV_{dp3} \quad (3.169)$$

$$x = a \rightarrow MV_{dp4} \quad (3.170)$$

So total heave pitching moment on hull will be

$$MV_p = \left( \begin{array}{l} MV_{ip1} + MV_{ip2} + MV_{ip3} + MV_{ip4} + MV_{dp1} + MV_{dp2} + MV_{dp3} \\ + MV_{dp4} \end{array} \right) \quad (3.171)$$

For calculating the vertical pitch moment on columns, the exposed base of the corner columns i.e. all columns of the TLP experience a hydrostatic pressure which has no contribution to the pitch moment, when the integration is taken to the still waterline. However, there is dynamic pressure variation due to the passage of the waves whose net contribution is non zero. The associated pitching moment arising from this is given by

$$MV_c = \frac{\pi D_c^2}{4} \rho g \frac{H}{2} x e^{-h_c k} \cos(kx - \omega t) \quad (3.172)$$

$$\Rightarrow x = -a \rightarrow MV_{c5} + MV_{c6} \quad (3.173)$$

$$x = a \rightarrow MV_{c7} + MV_{c8} \quad (3.174)$$

So total heave pitching moment on columns will be

$$MV_c = (MV_{c5} + MV_{c6} + MV_{c7} + MV_{c8}) \quad (3.175)$$

So total heave pitching moment on TLP will be

$$MV = (MV_p + MV_c) \quad (3.176)$$

So total pitching moment on TLP will be

$$F_{51} = (MV + MH) \quad (3.177)$$

### 3.3 Development of a Triangular TLP Model

The same development for the rectangle model will be carried out, except that we have only three tethers instead of four. At the original equilibrium position (Figure 3.9).

#### 3.3.1 Draft Evaluation

Summation of forces in the vertical direction given by Eqn. (3.8) and Eqn. (3.9) applies with the exception that we have three tethers instead of four.

But

$$F_B = \frac{3}{4} \rho \pi g (D_c^2 D_r + D_p^2 S) \quad (3.178)$$

From Eq. (3.168), we get:

$$D_r = \left[ I \{ (W + T_t) / (\frac{3}{4} \rho \pi g) - (D_p^2 S) \} / D_c^2 \right] \quad (3.179)$$

#### 3.3.2 Stiffness Matrix of the Triangular TLP Configuration

As shown in section (3.1.2.2) the coefficients of the stiffness matrix [K] of a rectangle TLP are:

$$[K] = \begin{pmatrix} K_{11} & 0 & 0 & 0 & K_{15} & 0 \\ 0 & K_{22} & 0 & K_{24} & 0 & 0 \\ K_{31} & K_{32} & K_{33} & K_{34} & K_{35} & K_{36} \\ 0 & K_{42} & 0 & K_{44} & 0 & 0 \\ K_{51} & 0 & 0 & 0 & K_{55} & 0 \\ 0 & 0 & 0 & 0 & 0 & K_{66} \end{pmatrix} \quad (3.180)$$

And can be determined as following

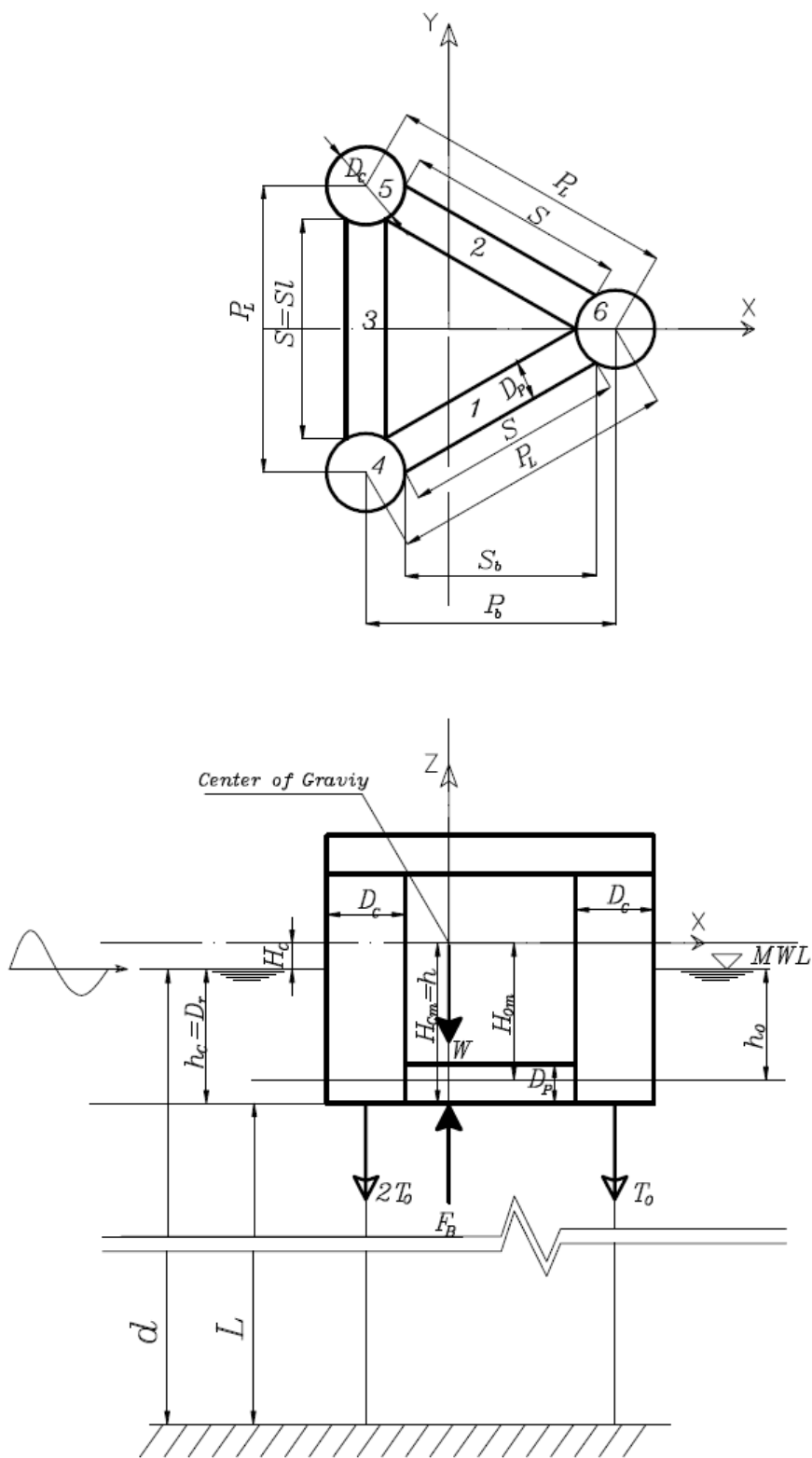


Figure 3.9: The triangular TLP (plan and elevation)



### 3.3.2.1 Surge (1) direction (Figure 3.10)

By giving an arbitrary displacement  $x_1$  in the surge direction, the increase in the initial pretension in each leg is calculated as rectangular TLP as following:

Equilibrium of forces in the surge direction gives

$$\sum Fx = 3(T_o + \Delta T_1) \sin \delta_x = K_{11} x_1 \quad (3.181)$$

From Eqn. (3.13), Eqn. (3.14), Eqn. (3.15) and Eqn. (3.17)

$$3(T_o + \Delta T_1) \frac{x_1}{\sqrt{x_1^2 + L^2}} = K_{11} x_1 \quad (3.182)$$

$$\Rightarrow K_{11} = \frac{3(T_o + \Delta T_1)}{\sqrt{x_1^2 + L^2}} \quad (3.183)$$

Through summation of the vertical forces, we get:

$$\sum Fy = K_{31} x_1 = +3(T_o + \Delta T_1) \cos \delta_x + W - F_B \quad (3.184)$$

$$\Rightarrow K_{31} = + \frac{[3T_o (\cos \delta_x - 1) + 3\Delta T_1 \cos \delta_x]}{x_1} \quad (3.185)$$

Summation of moments about the x-axis gives:

$$\sum Mx = 0 = K_{41} x_1 \Rightarrow K_{41} = 0 \quad (3.186)$$

Summation of moments about the y-axis gives:

$$\sum My = -\sum F_x h = -K_{11} h x_1 = K_{51} x_1 \quad (3.187)$$

$$\Rightarrow K_{51} = (-K_{11} h) \quad (3.188)$$

The negative sign occurs due to the counter clockwise moment

Summation of moments about the z-axis gives:

$$\sum Mz = 0 = K_{61} x_1 \Rightarrow K_{61} = 0 \quad (3.189)$$

Also these coefficients agree well with other researchers (Ex. Jain, 2002).

### 3.3.2.2 Sway (2) Direction (Figure 3.11)

The coefficients of the second column of the restoring force matrix are found in a similar manner by giving  $x_2$  displacement in the y-direction (sway)

$$K_{12} = 0 \quad (3.190)$$

$$K_{22} = \frac{3(T_o + \Delta T_2)}{\sqrt{x_2^2 + L^2}} \quad (3.191)$$

$$K_{32} = \frac{[3(T_o [\cos \delta y - 1])] + [3\Delta T_2 \cos \delta y]}{x_2} \quad (3.192)$$

$$K_{42} = -h K_{22} \quad (3.193)$$

The negative sign occurs due to the counterclockwise moment

$$K_{52} = 0 \quad (3.194)$$

$$K_{62} = 0 \quad (3.195)$$

And also Eqn. (3.30), Eqn. (3.31) and Eqn. (3.32) can be applied.

Also these coefficients agree with these presented by Jain, 2002.

### 3.3.2.3 Heave (3) Direction:

The third column is derived by giving the structure an arbitrary displacement z in the z direction (heave). The sum of the forces in the all direction yields:

$$\sum F_x = \sum F_y = \sum M_x = \sum M_y = \sum M_z = 0 \quad (3.196)$$

$$\text{So; } K_{13} = K_{23} = K_{43} = K_{53} = K_{63} = 0 \quad (3.197)$$

The summation of the forces in the vertical direction yields

$$\begin{aligned} \sum F_z &= 3(T_o + \Delta T_3) + W - (F_B + \Delta F_b) \\ &= 3T_o + 3\Delta T_3 - 3T_o - \Delta F_b = K_{33} x_3 \end{aligned} \quad (3.198)$$

Where  $x_3$  is the displacement in the heave direction,

$$F_{b1} = 3 \left[ \frac{\pi D_c^2}{4} Dr + \frac{\pi D_p^2}{4} s \right] \rho g \quad (3.199)$$

$$F_{b2} = 3 \left[ \frac{\pi D_c^2}{4} (Dr + x_3) + \frac{\pi D_p^2}{4} s \right] \rho g \quad (3.200)$$

By subtracting Eqn. (3.200) from Eqn. (3.199) we get

$$\Delta F_b = 3 \frac{\pi D_c^2}{4} \rho g x_3 \quad (3.201)$$

From Eqn. (3.201) and Eqn. (3.198) we get

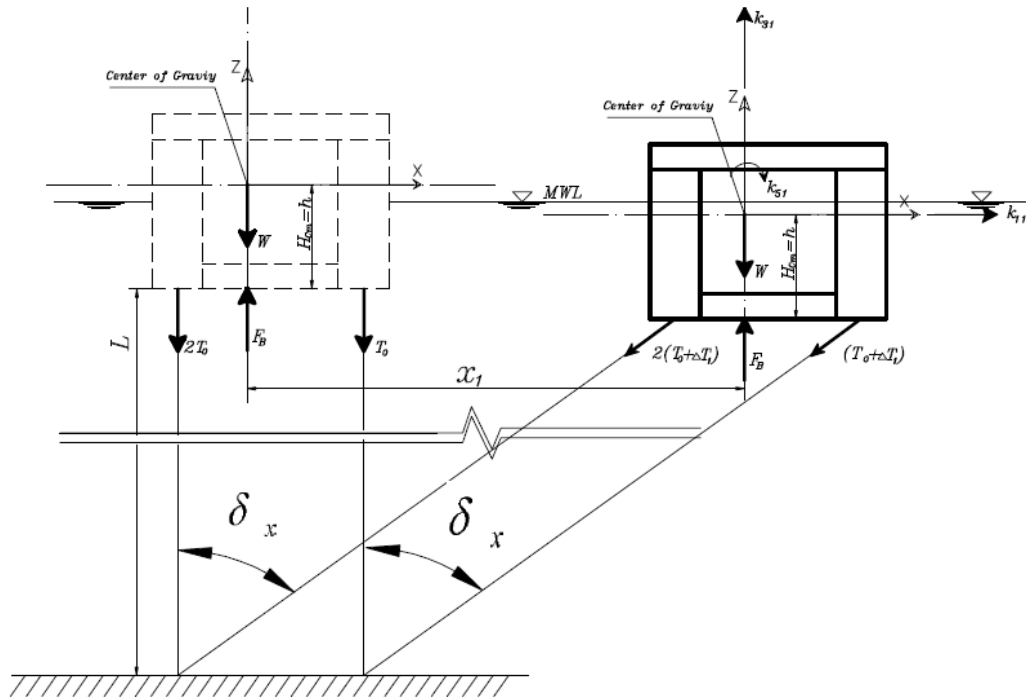


Figure 3.10: The Surge displacement in a triangular TLP.

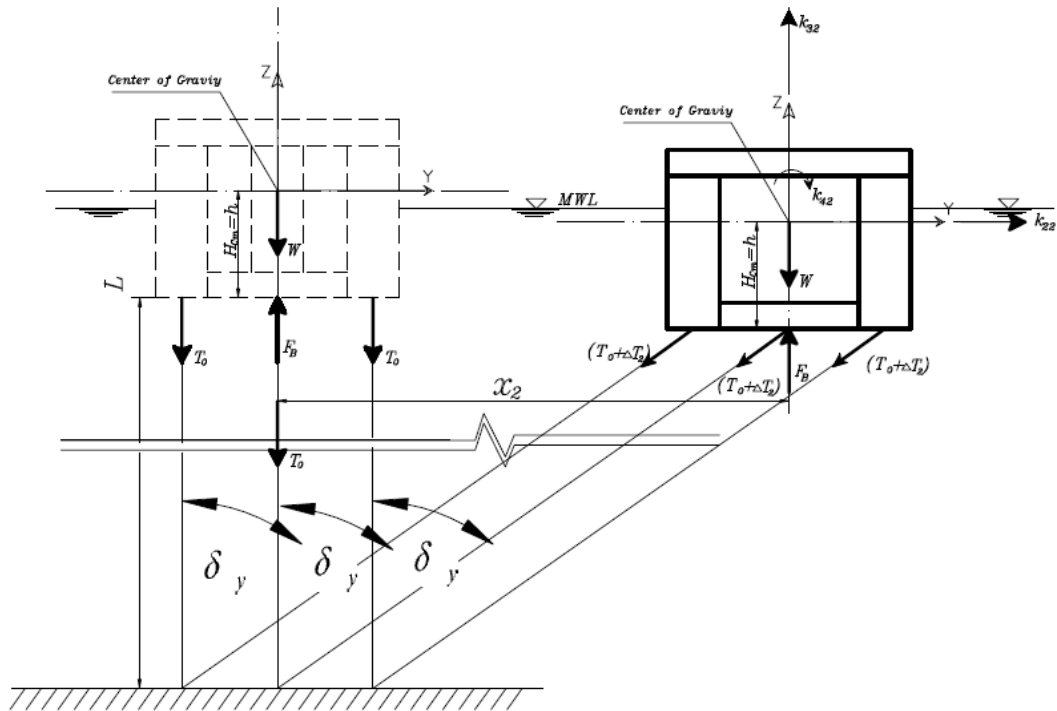


Figure 3.11: The Sway displacement in a triangular TLP.

$$\Rightarrow K_{33} = 3\gamma + \Delta F_b \quad (3.202)$$

Where,  $\gamma$  is given by Eqn. (3.35).

These coefficients also agree with those of Jain, 2002.

### 3.3.2.4 Roll (4) Direction (Figure 3.12):

The coefficients of the fourth column of the restoring force matrix are found by giving the structure an arbitrary rotation  $x_4$  about the x-axis. Summation of the moments of the resulting forces about the x-axis gives:

$$K_{14} = K_{54} = K_{64} = 0 \quad (3.203)$$

The change in the initial pretension in each leg is obtained by examining the geometry of Figure 3.12. So,

$$h_{o4} = H - H \cos x_4, e_{o4} = H \sin x_4, e_{o14} = \frac{h_{o4}}{\tan x_4}, e_{o24} = e_{o4} - e_{o14}$$

$$L_{CG14} = \sqrt{(e_{o14}^2 + h_{o4}^2)} + \frac{PL}{2}, L_{CG24} = PL - L_{CG14}, L_{14} = L_{CG14} \times \cos x_4 \quad (3.204)$$

$$L_{24} = L_{CG24} \times \cos x_4, e_{14} = L_{14} - \frac{PL}{2} + e_{o24}, e_{24} = -L_{24} + \frac{PL}{2} + e_{o24}$$

$$h_{14} = L_{14} \times \tan x_4, h_{24} = L_{24} \times \tan x_4, L_{T14} = \sqrt{(L + h_{14})^2 + e_{14}^2}$$

$$L_{T24} = \sqrt{(L - h_{24})^2 + e_{24}^2}, L_{T04} = \sqrt{(L + h_{o4})^2 + e_{o4}^2}$$

$$\Rightarrow \Delta T_{24} = \frac{AE}{L} \times (L_{T24} - L) \quad (3.205)$$

$$\Rightarrow \Delta T_{14} = \frac{AE}{L} \times (L_{T14} - L) \quad (3.206)$$

$$\Rightarrow \Delta T_{04} = \frac{AE}{L} \times (L_{T04} - L) \quad (3.207)$$

$$\Rightarrow \Delta T_4 = \Delta T_{14} + \Delta T_{24} + \Delta T_{04} \quad (3.208)$$

$$\theta_{14} = \tan^{-1}\left(\frac{e_{14}}{L}\right), \theta_{24} = \tan^{-1}\left(\frac{e_{24}}{L}\right), \theta_{04} = \tan^{-1}\left(\frac{e_{04}}{L}\right) \quad (3.209)$$

By taking summation of force in sway direction we get

$$\Sigma y = K_{24} \times x_4 = - \left[ \begin{aligned} &((T_o + \Delta T_{14}) \sin \theta_{14} + (T_o + \Delta T_{04}) \sin \theta_{04}) \\ &+ (T_o + \Delta T_{24}) \sin \theta_{24} \end{aligned} \right] \quad (3.210)$$

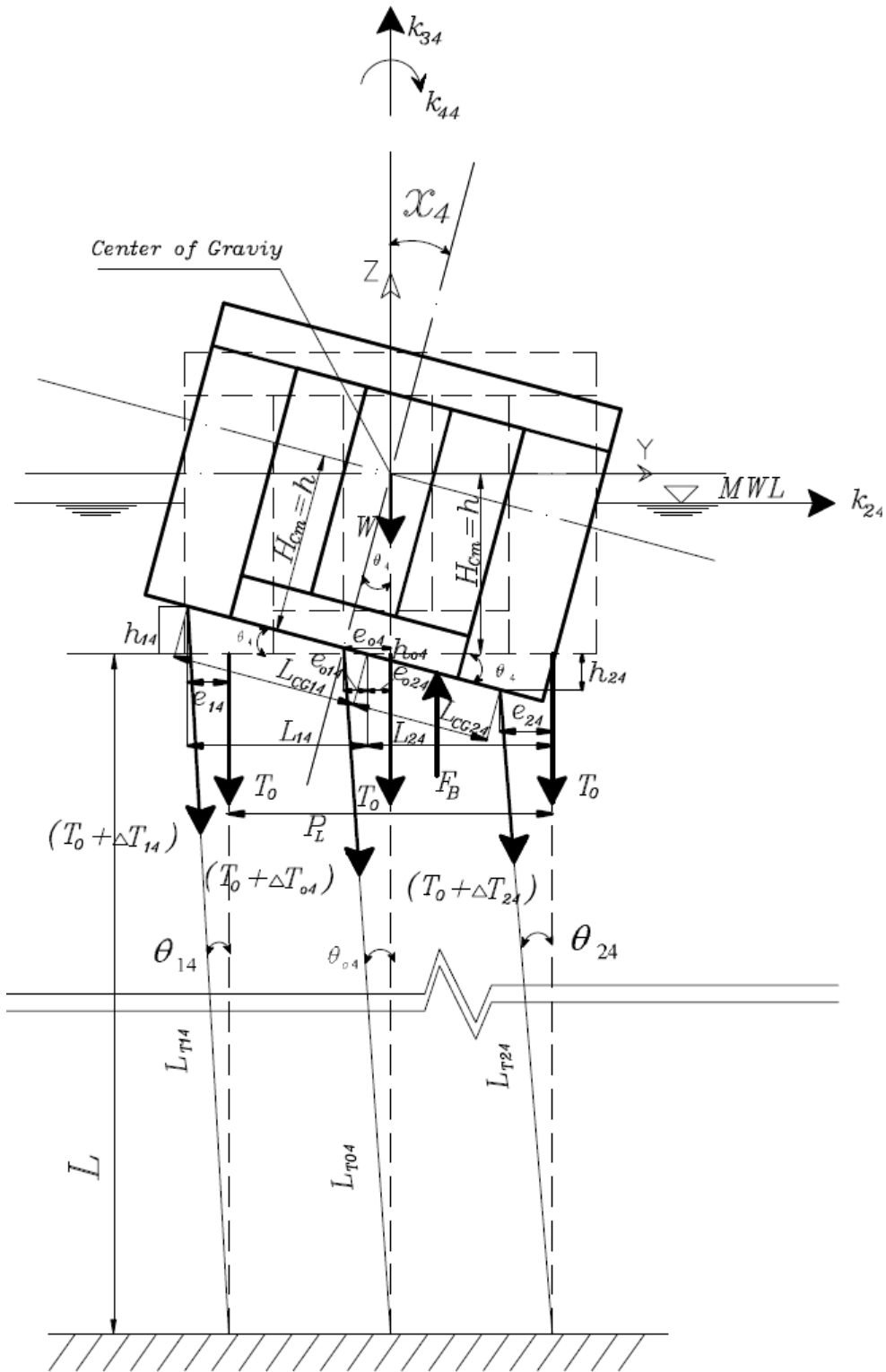


Figure 3.12: The Roll displacement in a triangular TLP.

$$\Rightarrow K_{24} = -\frac{[(T_o + \Delta T_{14}) \sin \theta_{14} + (T_o + \Delta T_{04}) \sin \theta_{04} + (T_o + \Delta T_{24}) \sin \theta_{24}]}{x_4} \quad (3.211)$$

By taking summation of force in heave direction we get

$$\Sigma Z = K_{34} \times x_4 = \left[ \begin{array}{l} ((T_o + \Delta T_{14}) \cos \theta_{14} + (T_o + \Delta T_{04}) \cos \theta_{04}) \\ + (T_o + \Delta T_{24}) \cos \theta_{24} - 3T_o \end{array} \right] \quad (3.212)$$

$$\Rightarrow K_{34} = \left[ \begin{array}{l} ((T_o + \Delta T_{14}) \cos \theta_{14} + (T_o + \Delta T_{04}) \cos \theta_{04}) \\ + (T_o + \Delta T_{24}) \cos \theta_{24} - 3T_o \end{array} \right] / x_4 \quad (3.213)$$

By taking summation of moment in roll direction we get

$$\Sigma M_x = K_{44} \times x_4 = \left[ \begin{array}{l} ((T_o + \Delta T_{14}) \cos \theta_{14} (\frac{PL}{2} + e_{14}) + (T_o + \Delta T_{04}) \cos \theta_{04} \times e_{04}) \\ - (T_o + \Delta T_{24}) \cos \theta_{24} (\frac{PL}{2} - e_{24}) + F_B \times e_{04} \\ + (T_o + \Delta T_{14}) \sin \theta_{14} (H - h_{14}) \\ + (T_o + \Delta T_{04}) \sin \theta_{04} \times (H - h_{04}) \\ + (T_o + \Delta T_{24}) \sin \theta_{24} (H - h_{24}) \end{array} \right] \quad (3.214)$$

$$\Rightarrow K_{44} = \left[ \begin{array}{l} ((T_o + \Delta T_{14}) \cos \theta_{14} (\frac{PL}{2} + e_{14}) + (T_o + \Delta T_{04}) \cos \theta_{04} \times e_{04}) \\ - (T_o + \Delta T_{24}) \cos \theta_{24} (\frac{PL}{2} - e_{24}) + F_B \times e_{04} \\ + (T_o + \Delta T_{14}) \sin \theta_{14} (H - h_{14}) \\ + (T_o + \Delta T_{04}) \sin \theta_{04} \times (H - h_{04}) \\ + (T_o + \Delta T_{24}) \sin \theta_{24} (H - h_{24}) \end{array} \right] / x_4 \quad (3.215)$$

Most researchers assumed that the tether remains vertical so  $\theta_{24} = \theta_{14} = \theta_{04} = 0$  (angle of inclination is vary small) and also assumed that distance  $e_{14} = e_{24} = e_{04}$ ,  $h_{14} = h_{24}$

From that  $\Delta T_{14} = -\Delta T_{24} = \frac{EA}{L} \frac{PL}{2} x_4 \cos(x_4)$ ,  $\Delta T = T_{04}$

This leads to  $\Rightarrow K_{24} = 0$  (3.216)

$$\Rightarrow K_{44} = [T_o + \Delta T_{o4} + F_B] e_{o4} \quad (3.217)$$

$$\Rightarrow K_{44} = \frac{EA}{L} \frac{PL}{2} \cos(x_4) \quad (3.218)$$

### 3.3.2.5 Pitch (5) Direction (Figure 3.13)

The coefficients of the fifth column of the restoring force matrix are found by giving the structure an arbitrary rotation  $x_5$  about the y-axis. Summation of the moments of the resulting forces about the y-axis gives:

$$K_{25} = K_{45} = K_{65} = 0 \quad (3.219)$$

The change in the initial pretension in each leg is obtained by examining the geometry of Figure 3.13. So,

$$h_{o5} = H - H \cos x_5, e_{o5} = H \sin x_5, e_{o15} = \frac{h_{o5}}{\tan x_5}, e_{o25} = e_{o5} - e_{o15}$$

$$L_{CG15} = \sqrt{(e_{o5}^2 + h_{o5}^2)} + \frac{Pb}{3}, L_{CG25} = Pb - L_{CG15}, L_{15} = L_{CG15} \times \cos x_5$$

$$L_{25} = L_{CG25} \times \cos x_5, e_{15} = L_{15} - \frac{Pb}{3} + e_{o25}, e_{25} = -L_{25} + \frac{2Pb}{3} + e_{o25}$$

$$h_{15} = L_{15} \times \tan x_5, h_{25} = L_{25} \times \tan x_5, L_{T15} = \sqrt{(L + h_{15})^2 + e_{15}^2}$$

$$L_{T25} = \sqrt{(L - h_{25})^2 + e_{25}^2}$$

$$\Rightarrow \Delta T_{25} = \frac{AE}{L} \times (L_{T25} - L) \quad (3.220)$$

$$\Rightarrow \Delta T_{15} = \frac{AE}{L} \times (L_{T15} - L) \quad (3.221)$$

$$\Rightarrow \Delta T_5 = 2\Delta T_{15} + \Delta T_{25} \quad (3.222)$$

$$\theta_{15} = \tan^{-1}\left(\frac{e_{15}}{L}\right), \theta_{25} = \tan^{-1}\left(\frac{e_{25}}{L}\right) \quad (3.223)$$

By taking summation of force in surge direction we get

$$\sum x = K_{15} \times x_5 = -[2(T_o + \Delta T_{15}) \sin \theta_{15} + (T_o + \Delta T_{25}) \sin \theta_{25}] \quad (3.224)$$

$$\Rightarrow K_{15} = -\frac{[2(T_o + \Delta T_{15}) \sin \theta_{15} + (T_o + \Delta T_{25}) \sin \theta_{25}]}{x_5} \quad (3.225)$$

By taking summation of force in heave direction we get

$$\sum Z = K_{35} \times x_5 = [2(T_o + \Delta T_{15}) \cos \theta_{15} + (T_o + \Delta T_{25}) \cos \theta_{25} - 3T_o] \quad (3.226)$$

$$\Rightarrow K_{35} = [2(T + \Delta T_{15}) \cos \theta_{15} + (T + \Delta T_{25}) \cos \theta_{25} - 3T_o ] / x_5 \quad (3.227)$$

By taking summation of moment in pitch direction we get

$$\sum M_y = K_{55} \times x_5 = \begin{bmatrix} 2(T_o + \Delta T_{15}) \cos \theta_{15} (\frac{Pb}{3} + e_{15}) \\ -(T_o + \Delta T_{25}) \cos \theta_{25} (\frac{2Pb}{3} - e_{25}) \\ + F_B \times e_{o5} + (T_o + \Delta T_{25}) \sin \theta_{25} (H - h_{25}) \\ + (T_o + \Delta T_{15}) \sin \theta_{15} \times (H - h_{15}) \end{bmatrix} \quad (3.228)$$

$$\Rightarrow K_{55} = \begin{bmatrix} 2(T_o + \Delta T_{15}) \cos \theta_{15} (\frac{Pb}{3} + e_{15}) \\ -(T_o + \Delta T_{25}) \cos \theta_{25} (\frac{2Pb}{3} - e_{25}) \\ + F_B \times e_{o5} + (T_o + \Delta T_{25}) \sin \theta_{25} (H - h_{25}) \\ + (T_o + \Delta T_{15}) \sin \theta_{15} \times (H - h_{15}) \end{bmatrix} / x_5 \quad (3.229)$$

Most researchers assumed that the tether remains vertical so  $\theta_{25} = \theta_{15} = \theta_{o5} = 0$  (angle of inclination is vary small) and also assumed that distance  $e_{15} = e_{25}$ ,  $h_{15} = h_{25}$

$$\text{From that } 2\Delta T_{15} = -\Delta T_{25} = \frac{EA Pb}{L} \frac{Pb}{3} x_5 \cos(x_5), \Delta T = 0$$

$$\text{This leads to } \Rightarrow K_{15} = K_{35} = 0 \quad (3.230)$$

$$\Rightarrow K_{55} = F_B \frac{H \sin(x_5)}{x_5} \quad (3.231)$$

### 3.3.2.6. Yaw (6) Direction (Figure 3.14)

By giving an arbitrary rotation  $x_6$  in the yaw degree of freedom, we get the sixth column of the restoring force matrix.

$$\sin \delta_6 = \frac{\phi_6 \sqrt{2a^2}}{L_1}, \cos \delta_6 = \frac{L}{L_1} \quad (3.232)$$

$$a^2 = (\frac{P_l}{2})^2 + (\frac{P_b}{3})^2 \quad (3.233)$$

$$L_1 = \sqrt{L^2 + x_6^2 (2a^2)} \quad (3.234)$$



The change in the initial pretension, in each leg, is given by Eqn. (3.66).

By taking summation of force in surge direction we get

$$\sum Fx = (T_o + \Delta T_6) [-\cos(30 - x_6) + \cos(30 + x_6) - \sin(x_6)] = K_{16} x_6 \quad (3.235)$$

$$\Rightarrow K_{16} = 0 \quad (3.236)$$

By taking summation of force in sway direction we get

$$\sum Fy = (T_o + \Delta T_6) [-\sin(30 - x_6) - \sin(30 + x_6) + \cos(x_6)] = K_{16} x_6 \quad (3.237)$$

$$\Rightarrow K_{26} = 0 \quad (3.238)$$

By taking summation of forces in the heave direction one obtains:

$$\sum Fz = W - FB + 3(T_o + \Delta T_6) \cos \delta_6 \quad (3.239)$$

$$\Rightarrow K_{36} x_6 = -3T_o + 3T_o \frac{L}{L_1} + 3\Delta T_6 \frac{L}{L_1}$$

$$\Rightarrow K_{36} = [3T_o (\frac{L}{L_1} - 1) + 3\Delta T_6 (\frac{L}{L_1})] / x_6 \quad (3.240)$$

By taking summation of moment in the roll direction one obtains:

$$\sum Mx = K_{46} \times x_6 = 0 \quad (3.241)$$

$$\Rightarrow K_{46} = 0 \quad (3.242)$$

By taking summation of moment in the pitch direction one obtains:

$$\sum My = K_{56} \times x_6 = 0 \quad (3.243)$$

$$\Rightarrow K_{56} = 0 \quad (3.244)$$

By taking summation of moment in the yaw direction one obtains:

$$\sum Mz = 3(T_o + \Delta T_6) (2a^2) \frac{x_6}{L_1} = K_{66} \times x_6 \quad (3.245)$$

$$\Rightarrow K_{66} = 3(T_o + \Delta T_6) \frac{(2a^2)}{L_1} \quad (3.246)$$

These coefficients are agreement with Jain, 2002.

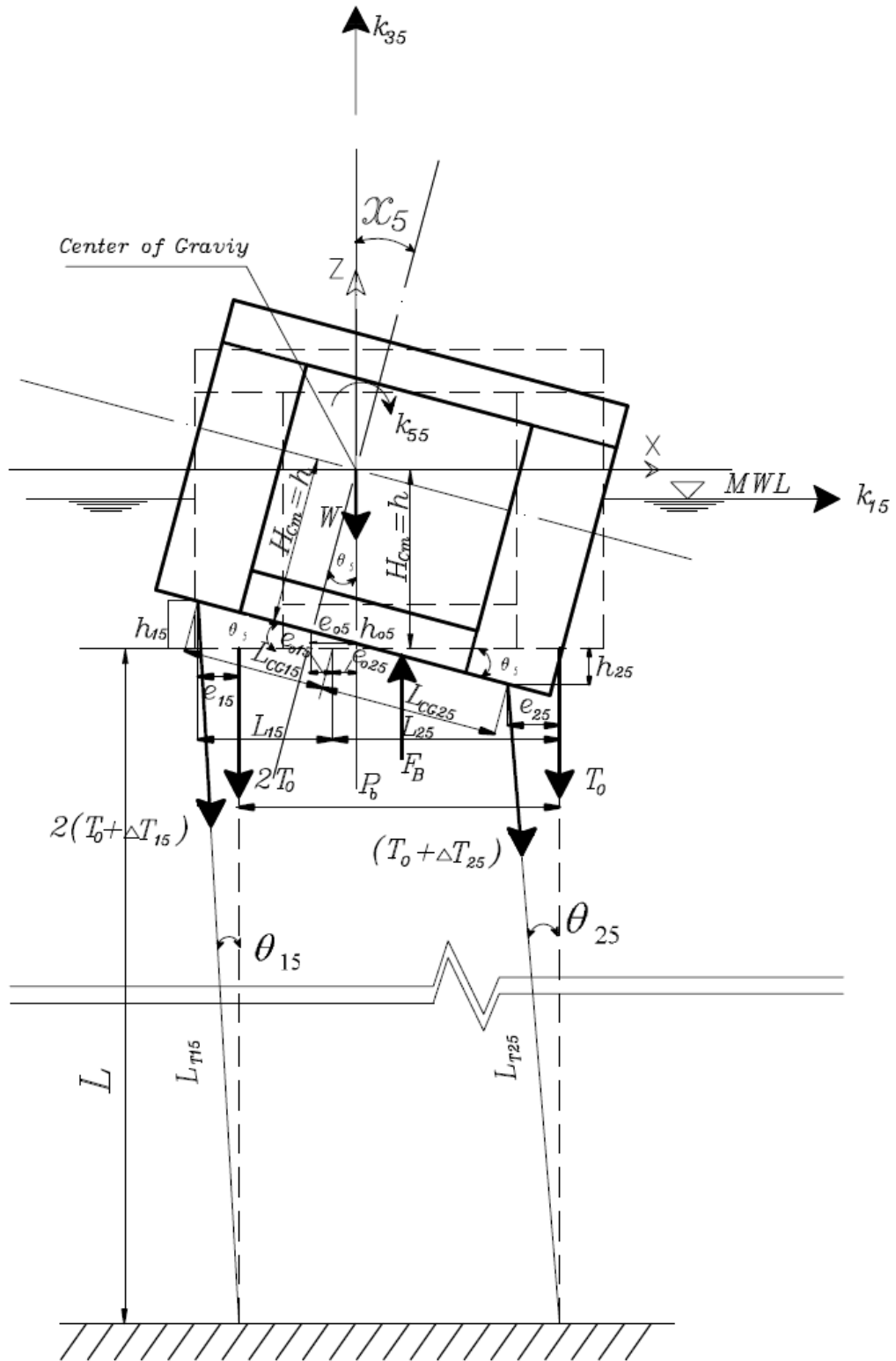


Figure 3.13: The Pitch displacement in a triangular TLP.

The stiffness matrix shows:

- 1- The presence of off-diagonal terms, which reflects the coupling effect between the various degrees of freedom;
- 2- The coefficients depend on the change in the tension of the tethers, which is affected by the buoyancy of the system. Hence, the matrix is response dependent.

Hence, the  $[K]$  is not constant for all time instants, but the coefficients are replaced by new values computed at each time step depending upon the response values at the previous time step.

### 3.3.3 Mass Matrix, $[M]$

As shown in section (3.1.2.1)  $[M]$  is assumed to be lumped at each degree of freedom. Hence, it is diagonal in nature and is constant and given by Eqn. (3.75).

Now we deduce every coefficient on Eqn. (3.4).

#### 3.3.3.1 Surge Direction

$$M_{a11} = C_a \rho \left[ \int_{-hc}^{\eta} \left[ \frac{3\pi D_c^2}{4} dz \right] + \left( \frac{\pi D_p^2}{4} S \right) + \left( \frac{2\pi D_p^2}{4} S \sin^2 \alpha \right) \right] \quad (3.247)$$

$$\Rightarrow M_{a11} = C_a \rho \left[ \left[ \frac{\pi D_c^2}{4} (h_c + \eta) \right] + \left( \frac{\pi D_p^2}{4} S \right) + \left( \frac{2\pi D_p^2}{4} S \sin^2 \alpha \right) \right] \quad (3.248)$$

#### 3.3.3.2 Sway Direction

$$M_{a22} = C_a \rho \left[ \int_{-hc}^{\eta} \left[ \frac{3\pi D_c^2}{4} dz \right] + \left( \frac{2\pi D_p^2}{4} S \sin^2 \beta \right) \right] \quad (3.249)$$

$$\Rightarrow M_{a22} = C_a \rho \left[ \left[ \frac{\pi D_c^2}{4} (h_c + \eta) \right] + \left( \frac{2\pi D_p^2}{4} S \sin^2 \beta \right) \right] \quad (3.250)$$

#### 3.3.3.3 Heave Direction

$$M_{a33} = 3C_a \rho \left[ \left( \frac{\pi D_p^2}{4} S \right) \right] \quad (3.251)$$

$$M_{a31} = M_{a13} = M_{a32} = M_{a23} = 0 \quad (3.252)$$

### 3.3.3.4 Roll Direction

$$M_{a42} = M_{a24} = C_a \rho \left[ \int_{-hc}^{\eta} \left[ \frac{3\pi D_c^2}{4} (z - H_c) dz \right] + \left( \frac{2\pi D_p^2}{4} \times S \times -H_{om} \times \sin^2 \beta \right) \right] \quad (3.253)$$

$$\Rightarrow M_{a42} = M_{a24} = C_a \rho \left[ \left[ \frac{3\pi D_c^2}{4} \left( \frac{-h_c^2}{2} - H_c h_c + \frac{\eta^2}{2} - H_c \eta \right) \right] + \left( \frac{2\pi D_p^2}{4} \times S \times -H_{om} \times \sin^2 \beta \right) \right] \quad (3.254)$$

$$M_{a43} = M_{a34} = C_a \rho \frac{\pi D_p^2}{4} \left[ \int_{-\frac{s}{2}}^{\frac{s}{2}} y dy + \int_0^{\frac{s}{2}} \frac{y dy}{\cos \beta} + \int_{-\frac{s}{2}}^0 y \frac{dy}{\cos \beta} \right] = 0 \quad (3.255)$$

$$M_{a44} = C_a \rho \left[ \int_{-hc}^{\eta} \left[ \frac{3\pi D_c^2}{4} (z - H_c)^2 dz \right] + \left( \frac{\pi D_p^2}{4} \times S \times \sin^2 \beta \times H_{om}^2 \right) + \left( \frac{\pi D_p^2}{4} \times S \times \sin^2 \beta \times H_{om}^2 \right) + \frac{\pi D_p^2}{4} \left[ \int_{-\frac{s}{2}}^{\frac{s}{2}} y^2 dy + \int_0^{\frac{s}{2}} \frac{y^2 dy}{\cos \beta} + \int_{-\frac{s}{2}}^0 y^2 \frac{dy}{\cos \beta} \right] \right] \quad (3.256)$$

$$\Rightarrow M_{a44} = C_a \rho \left[ 3 \frac{\pi D_c^2}{4} \left( H_c^2 h_c + h_c^2 H_c + \frac{h_c^3}{3} + H_c^2 \eta - \eta^2 H_c + \frac{\eta^3}{3} \right) + 2 \left( \frac{\pi D_p^2}{4} S \times H_{om}^2 \times \sin^2 \beta \right) + \left( \frac{\pi D_p^2}{4} \frac{s^3}{12} \right) + \left( \frac{\pi D_p^2}{4 \cos \beta} \frac{s^3}{12} \right) \right] \quad (3.257)$$

### 3.3.3.5 Pitch Direction

$$M_{a51} = M_{a15} = C_a \rho \left[ \int_{-hc}^{\eta} \left[ \frac{\pi D_c^2}{4} (z - H_c) dz \right] + \left( \frac{\pi D_p^2}{4} \times S \times -H_{om} \right) + \left( \frac{2\pi D_p^2}{4} \times S \times -H_{om} \times \sin^2 \alpha \right) \right] \quad (3.258)$$

$$\Rightarrow M_{a51} = M_{a15} = C_a \rho \left[ \begin{array}{l} \left[ \frac{\pi D_c^2}{4} \left( \frac{-h_c^2}{2} - H_c h_c + \frac{\eta^2}{2} - H_c \eta \right) \right] \\ + \left( \frac{\pi D_p^2}{4} \times S \times -H_{om} \right) \\ + \left( \frac{2\pi D_p^2}{4} \times S \times -H_{om} \times \sin^2 \alpha \right) \end{array} \right] \quad (3.259)$$

$$M_{a53} = M_{a35} = C_a \rho \left[ \begin{array}{l} \left[ \frac{\pi D_p^2}{4} \times S \times \frac{-p_b}{3} \right] + 2 \int_{\frac{-s_b}{3}}^{\frac{2s_b}{3}} \frac{\pi D_p^2}{4} \frac{xdx}{\cos \alpha} \end{array} \right] \quad (3.260)$$

$$= C_a \rho \left[ \begin{array}{l} \left[ \frac{\pi D_p^2}{4} \times S \times \frac{-p_b}{3} \right] + 2 \frac{\pi D_p^2}{4} \frac{x^2}{2 \cos \alpha} \left[ \frac{2s_b}{3} \right] \\ \left[ \frac{-s_b}{3} \right] \end{array} \right]$$

$$= C_a \rho \left( \begin{array}{l} \left[ \frac{\pi D_p^2}{4} \times S \times \frac{-p_b}{3} \right] + 2 \frac{\pi D_p^3}{4} \left[ \frac{4S_b^2}{9} - \frac{S_b^2}{9} \right] \\ \left[ \frac{2 * \cos \alpha} \right] \end{array} \right)$$

$$= C_a \rho \frac{\pi D_p^2}{4} \left[ \left( S \frac{-p_b}{3} \right) + 2 \frac{S_b^2}{6 \cos \alpha} \right]$$

$$\Rightarrow M_{a53} = M_{a35} = C_a \rho \frac{\pi D_p^2}{4} \left[ \frac{-Sp_b}{3} + \frac{S_b^2}{3 \cos \alpha} \right] \quad (3.261)$$

$$M_{a55} = C_a \rho \left[ \begin{array}{l} \int_{-hc}^{\eta} \left[ \frac{3\pi D_c^2}{4} (z - H_c)^2 dz \right] + \left( \frac{\pi D_p^2}{4} \times S \times \sin^2 \alpha \times H_{om}^2 \right) \\ + \left( \frac{\pi D_p^2}{4} \times S \times \left( \frac{-pb}{3} \right)^2 \right) + \left( \frac{\pi D_p^2}{4} \times S \times \sin^2 \alpha \times H_{om}^2 \right) \\ + \left( \frac{2\pi D_p^2}{4} \int_{\frac{-s_b}{3}}^{\frac{2s_b}{3}} \frac{x^2 dy}{\cos \alpha} \right) \end{array} \right] \quad (3.262)$$

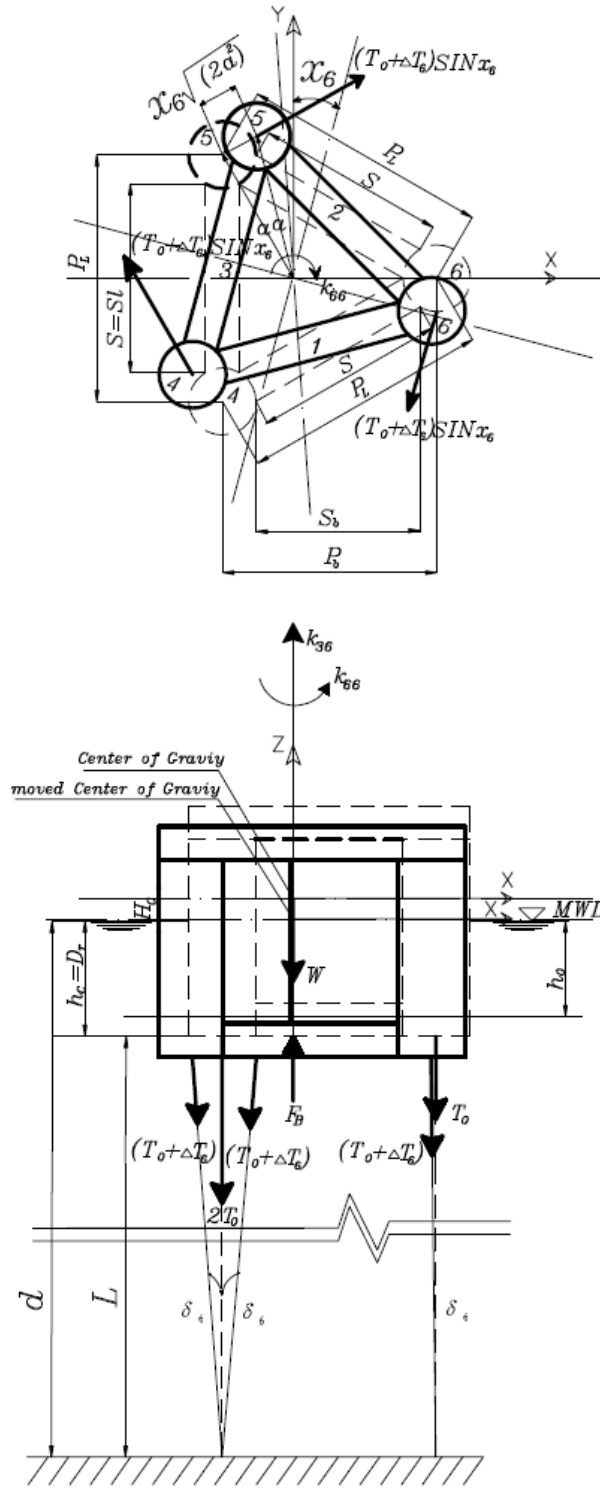


Figure 3.14: The Yaw displacement in a triangular TLP.

$$\Rightarrow M_{a55} = C_a \rho \left[ \begin{aligned} & 3 \frac{\pi D_c^2}{4} \left( H_c^2 h_c + h_c^2 H_c + \frac{h_c^3}{3} + H_c^2 \eta - \eta^2 H_c + \frac{\eta^3}{3} \right) \\ & + \left( \frac{\pi D_p^2}{4} \times S \times H_{om}^2 \right) + 2 \left( \frac{\pi D_p^2}{4} \times S \times H_{om}^2 \times \sin^2 \alpha \right) \\ & + \left( \frac{\pi D_p^2}{4} \frac{S \times pb^2}{9} \right) + \left( \frac{2\pi D_p^2}{4 \cos \beta} \frac{s_b^3}{9} \right) \end{aligned} \right] \quad (3.263)$$

### 3.3.3.5 Yaw Direction

$$M_{a61} = M_{a16} = C_a \rho \left[ \begin{aligned} & \int_{-hc}^{\eta} \left[ \frac{\pi D_c^2}{4} \frac{pb}{2} dz \right] \\ & + \int_{-hc}^{\eta} \left[ \frac{\pi D_c^2}{4} \frac{-pb}{2} dz \right] + 2 \int_{-\frac{sb}{2}}^{\frac{sb}{2}} \frac{\pi D_p^2}{4} \frac{y}{\cos \alpha} dy \end{aligned} \right] = 0 \quad (3.264)$$

$$M_{a62} = M_{a26} = C_a \rho \left[ \begin{aligned} & 2 \int_{-hc}^{\eta} \left[ \frac{\pi D_c^2}{4} \frac{-pb}{3} dz \right] + \\ & \int_{-hc}^{\eta} \left[ \frac{\pi D_c^2}{4} \frac{2pb}{3} dz \right] + 2 \int_{-\frac{sb}{3}}^{\frac{2sb}{3}} \frac{\pi D_p^2}{4} \frac{x \sin^2 \beta dx}{\cos \alpha} \end{aligned} \right] \\ \Rightarrow M_{a62} = C_a \rho \left[ 2 \int_{-\frac{sb}{3}}^{\frac{2sb}{3}} \frac{\pi D_p^2}{4} \left[ \frac{sb^2}{6} \right] \frac{x \sin^2 \beta}{\cos \alpha} \right] \quad (3.265)$$

$$M_{a66} = C_a \rho \left[ \begin{aligned} & 2 \int_{-hc}^{\eta} \left[ \frac{\pi D_c^2}{4} \left( \frac{-pb}{3} \right)^2 dz \right] + \int_{-hc}^{\eta} \left[ \frac{\pi D_c^2}{4} \left( \frac{2pb}{3} \right)^2 dz \right] \\ & + 2 \int_{-hc}^{\eta} \left[ \frac{\pi D_c^2}{4} \left( \frac{pl}{2} \right)^2 dz \right] + \int_{-\frac{sa}{2}}^{\frac{sa}{2}} \frac{\pi D_p^2}{4} y^2 dy \\ & + \int_{-\frac{s}{2}}^0 \frac{\pi D_p^2}{4} y^2 dy \frac{\sin^2 \alpha}{\cos \alpha} + 2 \int_{-\frac{s}{2}}^0 \frac{\pi D_p^2}{4} y^2 dy \frac{\sin^2 \alpha}{\cos \alpha} \\ & + 2 \int_0^{\frac{s}{2}} \frac{\pi D_p^2}{4} y^2 dy \frac{\sin^2 \alpha}{\cos \alpha} + 2 \int_{-\frac{pb}{3}}^{\frac{2pb}{3}} \frac{\pi D_p^2}{4} x^2 dx \frac{\sin^2 \beta}{\cos \alpha} \end{aligned} \right] \quad (3.266)$$

$$\Rightarrow M_{a66} = C_a \rho \left[ \begin{aligned} & \left( 2 \frac{\pi D_c^2}{4} (h_c + \eta) \left( \frac{-pb}{3} \right)^2 \right) + \left( \frac{\pi D_c^2}{4} \left( \frac{2pb}{3} \right)^2 (h_c + \eta) \right) \\ & + \left( 2 \frac{\pi D_c^2}{4} \left( \frac{pl}{2} \right)^2 (h_c + \eta) \right) \\ & + \frac{\pi D_p^2}{4} \frac{s^3}{12} + \frac{\pi D_p^2}{4} \frac{s^3 \sin^2 \alpha}{12 \cos \alpha} + \frac{2\pi D_p^2}{4} \frac{pb^3 \sin^2 \beta}{9 \cos \alpha} \end{aligned} \right] \quad (3.267)$$

The presence of off diagonal terms in the mass matrix indicates a contribution in the added mass due to the hydrodynamic loading. The loading will be attracted only in the surge, heave and pitch degrees of freedom due to the unidirectional wave acting in the surge direction on a symmetric configuration of the platform about the  $x$  and  $z$  axes. So added mass matrix will be as Eqn. (3.96) in section (3.2.3).

### 3.3.4 Structural Damping

Applying Eqn. (3.7) in section (3.1.2.3) we get the mode shape as

	Surge	Heave	Pitch	Roll	Sway	Yaw
$V =$	$1$	$V_3$	$1$	$V_7$	$V_{12}$	$V_{17}$
	$0$	$0$	$0$	$1$	$1$	$V_{18}$
	$V_1$	$1$	$V_5$	$V_8$	$V_{13}$	$V_{19}$
	$0$	$0$	$0$	$V_9$	$V_{14}$	$V_{20}$
	$V_2$	$V_4$	$V_6$	$V_{10}$	$V_{15}$	$V_{21}$
	$0$	$0$	$0$	$V_{11}$	$V_{16}$	$1$

(3.268)

And the damping matrix will be

$$C = \begin{pmatrix} C_1 & C_7 & C_{13} & C_{19} & C_{25} & C_{31} \\ C_2 & C_8 & C_{14} & C_{20} & C_{26} & C_{32} \\ C_3 & C_9 & C_{15} & C_{21} & C_{27} & C_{33} \\ C_4 & C_{10} & C_{16} & C_{22} & C_{28} & C_{34} \\ C_5 & C_{11} & C_{17} & C_{23} & C_{29} & C_{35} \\ C_6 & C_{12} & C_{18} & C_{24} & C_{30} & C_{36} \end{pmatrix} \quad (3.269)$$

It should be noticed that motions in all directions depend in each other contrary to Jain, 2002.



### 3.3.5 Hydrodynamic Force Vector, $\{F(t)\}$ on Triangular TLP

As shown in section (3.1.2.4) the hydrodynamic force attracted by the members due to a uni-directional wave train in the surge direction  $\{F(t)\}$  is given by Eqn. (3.8) and The values of  $F_{21}=F_{41}=F_{61}=0$ . Terms  $F_{11}$ ,  $F_{31}$  and  $F_{51}$  have values which can be obtained as following

#### 3.3.5.1 Surge Force $F_{11}$

The horizontal surge force on the triangular TLP results from contributions from horizontal forces on the hulls (pontoons) and vertical columns, Figure (3.8).

The inertia surge force on a single column located at distant  $x$  from the wave crest, is obtained by Eqn. (3.101) so,

$$\text{For columns at } x = \frac{-Pb}{3}$$

$$F_{1_{ci5}} + F_{1_{ci4}} = 2\rho \times \frac{\pi D_c^2}{4} \times C_m \times g \times \frac{H}{2} \times \sin\left(k \times \frac{-Pb}{3} - \omega t\right) \left[ e^{\eta_{xk}} - e^{-h_c k} \right] \quad (3.270)$$

$$\text{For columns at } x = \frac{2 \times Pb}{3}$$

$$F_{1_{ci6}} = \rho \times \frac{\rho D_c^2}{4} \times C_m \times g \times \frac{H}{2} \times \sin\left(k \times \frac{2Pb}{3} - \omega t\right) \left[ e^{\eta_{xk}} - e^{-h_c k} \right] \quad (3.271)$$

Also the drag surge force on a single column located at  $x$  from the wave crest is obtained by Eqn. (3.106).

$$\Rightarrow x = \frac{-Pb}{3} \rightarrow F_{1_{dc4}} + F_{1_{dc5}} \quad (3.272)$$

$$x = \frac{2Pb}{3} \rightarrow FF_{1_{dc6}} \quad (3.273)$$

So the total surge force on columns will be

$$\Rightarrow F_{1_C} = F_{1_{ic4}} + F_{1_{ic5}} + F_{1_{ic6}} + F_{1_{dc4}} + F_{1_{dc5}} + F_{1_{dc6}} \quad (3.274)$$

The inertia surge forces are experienced only by the hull aligned normal to the direction of wave propagation. Thus an inertia surge force varies only due wave action on hull 1 and 2 and is obtained by

$$F I_{ip3} = \int \frac{S_L}{2} \rho \frac{\pi D_P^2}{4} C_m \frac{\omega^2}{2} H e^{-h_o k} \sin(kx - \omega t) dy \quad (3.275)$$

$$\Rightarrow F I_{ip3} = \rho \frac{\pi D_P^2}{4} C_m \frac{\omega^2}{2} H e^{-h_o k} \sin(k(-Pb/3) - \omega t) S_L \quad (3.276)$$

$$F I_{ip1} + F I_{ip2} = 2 \int \frac{2S_b}{3} \rho \frac{\pi D_P^2}{4} C_m \frac{\omega^2}{2} H e^{-h_o k} \sin(kx - \omega t) \frac{\sin^2 \alpha}{\cos \alpha} dx \quad (3.277)$$

$$= 2 \rho \frac{\pi D_P^2}{4} C_m \frac{g}{2} H e^{-h_o k} [-\cos(k(2s_b/3) - \omega t) + \cos(k(-s_b/3) - \omega t)] \frac{\sin^2 \alpha}{\cos \alpha} \quad (3.278)$$

Also the drag surge forces are experienced only by the hull aligned normal to the direction of wave propagation. Thus drag surge force varies only on hull 1 and 2 and is obtained by

$$F I_{dp3} = \left[ \int \frac{S_L}{2} \frac{1}{2} C_d \rho D_P \left[ \left( \frac{\pi H}{T} \right) e^{-h_o k} \cos(kx - \omega t) + \frac{(d - h_o) e^{-kh_o} U_c - U_x}{d} \right] \right. \\ \left. \times \left| \frac{\pi H}{T} e^{-h_o k} \cos(kx - \omega t) - \frac{(d - h_o) e^{-kh_o} U_c}{d} U_x \right| dy \right] \quad (3.279)$$

$$\Rightarrow F I_{dp3} = \left[ \frac{1}{2} C_d \rho D_P \left[ \left( \frac{\pi H}{T} \right) e^{-h_o k} \cos(k \times (-Pb/3) - \omega t) + \frac{(d - h_o) e^{-kh_o} U_c - U_x}{d} \right] \right. \\ \left. \times \left| \frac{\pi H}{T} e^{-h_o k} \cos(k \times (-Pb/3) - \omega t) + \frac{(d - h_o) e^{-kh_o} U_c}{d} - U_x \right| S_L \right] \quad (3.280)$$

$$F I_{dp1} + F I_{dp2} = 2 \int \frac{2S_b}{3} \frac{1}{2} C_d \rho D_P \times \frac{4}{3} \frac{\omega H}{\pi} \left[ \frac{\pi H}{T} e^{-2kh_o} \cos(kx - \omega t) + \frac{(d - h_o) e^{-kh_o} U_c}{d} - 2e^{-kh_o} U_x \right] \frac{\sin^2 \alpha}{\cos \alpha} dx \quad (3.281)$$

$$= \left[ \frac{4}{3} C_d \rho D_p \frac{\omega H}{\pi} \left[ \frac{-\pi H e^{-2kh_o}}{T k} \sin(kx - \omega t) + \frac{(d - h_o) x e^{-kh_o} U_c}{d} - 2x e^{-kh_o} U_x \right] \right]_{x = \frac{-sb}{3}}^{x = \frac{2sb}{3}} \frac{\sin^2 \alpha}{\cos \alpha} \quad (3.282)$$

So total surge force on hulls equal

$$\Rightarrow F1_p = F1_{ip1} + F1_{ip2} + F1_{ip3} + F1_{dp1} + F1_{dp2} + F1_{dp3} \quad (3.283)$$

Finally the total surge force  $F_{11}$

$$\Rightarrow F_{11} = F1_p + F1_c \quad (3.284)$$

### 3.3.5.2 Heave Force $F_{31}$ :-

The vertical wave force on TLP results from several effects:

- (1) The dynamic pressure at the bottom of the columns.
- (2) The forces on the hulls.
- (3) The change of the instantaneous waterline on the columns.

Effect of the dynamic pressure at the bottom of the columns can be obtained as Eqn. (3.120).

With further assumption that the columns diameter is small compared to the wave length, so that the dynamic pressure can be assumed to remain constant across the bottom surface. The vertical columns force can be obtained from Eqn. (3.121).

$$\Rightarrow x = \frac{-Pb}{3} \Rightarrow F3_{c4} + F3_{c5} \quad (3.285)$$

$$x = \frac{2Pb}{3} \Rightarrow F3_{c6} \quad (3.286)$$

So total heave force on columns equal

$$\Rightarrow F3_C = F1_{c4} + F1_{c5} + F1_{c6} \quad (3.287)$$

The magnitude of vertical force, hull 3, is constant along the hull length and the integration reduces to a simple multiplication. So, the inertia force is

$$F_{3_{ip3}} = \int_{\frac{-S_L}{2}}^{\frac{S_L}{2}} \rho \frac{\pi D_P^2}{4} C_m \frac{-\omega^2}{2} H e^{-h_o k} \cos(kx - \omega t) dy \quad (3.288)$$

$$\Rightarrow F_{3_{ip3}} = -\rho \frac{\pi D_P^2}{4} C_m \frac{\omega^2}{2} H e^{-h_o k} \cos(k(-Pb/3) - \omega t) S_L \quad (3.289)$$

The magnitude of vertical force, hulls 1 and 2, is varied along the hull length and the integration reduces to a simple multiplication so the inertia force

$$F_{3_{ip1}} + F_{3_{ip2}} = 2 \int_{\frac{-S_b}{3}}^{\frac{2S_b}{3}} \rho \frac{\pi D_P^2}{4} C_m \frac{-\omega^2}{2} H e^{-h_o k} \cos(kx - \omega t) \frac{\sin^2 \alpha}{\cos \alpha} dx \quad (3.290)$$

$$= -2\rho \frac{\pi D_P^2}{4} C_m \frac{g}{2} H e^{-h_o k} [\sin(k(2S_b/3) - \omega t) - \sin(k(-S_b/3) - \omega t)] \frac{\sin^2 \alpha}{\cos \alpha} \quad (3.291)$$

Also the drag vertical force on hull 3 will be

$$F_{3_{dp3}} = \left[ \int_{\frac{-S_L}{2}}^{\frac{S_L}{2}} \frac{1}{2} C_d \rho D_p \left[ \left( \frac{\pi H}{T} \right) e^{-h_o k} \sin(kx - \omega t) + \frac{(d - h_o) e^{-kh_o} U_c - U_v}{d} \right] \right] \times \left[ \frac{\pi H}{T} e^{-h_o k} \sin(kx - \omega t) + \frac{(d - h_o) e^{-kh_o} U_c - U_v}{d} \right] dy \quad (3.292)$$

$$\Rightarrow F_{3_{dp3}} = \left[ \frac{1}{2} C_d \rho D_p \left[ \left( \frac{\pi H}{T} \right) e^{-h_o k} \sin(k \times (-Pb/3) - \omega t) + \frac{(d - h_o) e^{-kh_o} U_c - U_v}{d} \right] \right] \times \left[ \frac{\pi H}{T} e^{-h_o k} \sin(k \times (-Pb/3) - \omega t) + \frac{(d - h_o) e^{-kh_o} U_c - U_v}{d} \right] S_L \quad (3.293)$$

Also the drag vertical force on hulls 1 and 2 will be

$$F3_{dp1} + F3_{dp2} = 2 \int_{-\frac{sb}{3}}^{\frac{2sb}{3}} \frac{1}{2} C_d \rho D_p \frac{4}{3} \frac{\omega H}{\pi} \left[ \frac{\frac{\pi H}{T} e^{-2kh_o} \sin(kx - \omega t)}{+ \frac{(d - h_o) e^{-kh_o} U_c - 2e^{-kh_o} U_v}{d}} \right] \frac{\sin^2 \alpha}{\cos \alpha} dx \quad (3.294)$$

$$= \left[ \frac{4}{3} C_d \rho D_p \frac{\omega H}{\pi} \left[ \frac{-\frac{\pi H}{T} e^{-2kh_o} \frac{\cos(kx - \omega t)}{k}}{+ \frac{(d - h_o) x e^{-kh_o} U_c - 2x e^{-kh_o} U_v}{d}} \right] \right]_{x=-\frac{sb}{3}}^{x=\frac{2sb}{3}} \frac{\sin^2 \alpha}{\cos \alpha} \quad (3.295)$$

So total heave force on hulls equal

$$\Rightarrow F3_p = F3_{ip1} + F3_{ip2} + F3_{ip3} + F3_{dp1} + F3_{dp2} + F3_{dp3} \quad (3.296)$$

So the total heave force  $F_{31}$

$$\Rightarrow F_{31} = F3_p + F3_c \quad (3.297)$$

### 3.3.5.3 Pitch Response $F_{51}$

The pitching behavior of a triangular TLP is some what different from that of a free floating body like a ship or a semi submersible. In the latter case the restoring moment is provided by the action of emerged and immersed volumes around the water plane. In contrast for a TLP, the pitch restoring moment is provided primarily by changes in the tether tension due to elastic deformation. This effect outweighs, by far, the contributions due to changes in column submergence. In strict senses, the pitching access is one about which moment of all the forces (including elastic tether deformation) are zero. The tether deformation, in turn, depends on the location of the pitching axis. Thus, explicit solution for the location of the pitch access is not possible. Here, it would be assumed that the pitch access is at the level of the connection of the tethers to the columns (kirk and Etok, 1979). The contribution to pitching moment come from four sources:

- 1) The horizontal acceleration on all vertical columns.
- 2) The horizontal acceleration on hulls aligned normal to the direction of wave propagation.
- 3) The vertical acceleration of the wave particles on hulls 1, 2 and 3.
- 4) The dynamic pressure variation on the bases on the three corner columns.

The horizontal force on hulls 3 produces a pitch moment. This is obtained by multiplying the horizontal force with the lever, measured from the pitching axis as:

For inertia force

$$MH_{ip3} = \int_{-\frac{S_L}{2}}^{\frac{S_L}{2}} \rho \frac{\pi D_P^2}{4} C_m \frac{\omega^2}{2} H e^{-h_o k} \sin(kx - \omega t) (-H_{om}) dy \quad (3.298)$$

$$\Rightarrow MH_{ip3} = -\rho \frac{\pi D_P^2}{4} C_m \frac{\omega^2}{2} H e^{-h_o k} \sin(k(-Pb/3) - \omega t) H_{om} S_L \quad (3.299)$$

$$MH_{ip1} + MH_{ip2} = 2 \int_{-\frac{S_b}{3}}^{\frac{2S_b}{3}} \rho \frac{\pi D_P^2}{4} C_m \frac{\omega^2}{2} H e^{-h_o k} \sin(kx - \omega t) (-H_{om}) dx \quad (3.300)$$

$$= \left[ -2\rho \frac{\pi D_P^2}{4} C_m \frac{g}{2} H e^{-h_o k} [-\cos(k(2s_b/3) - \omega t) + \cos(k(-s_b/3) - \omega t)] H_{om} \right] \quad (3.301)$$

Also for drag force

$$MH_{dp3} = \left[ \int_{-\frac{S_L}{2}}^{\frac{S_L}{2}} \frac{1}{2} C_d \rho D_p \left[ \left( \frac{\pi H}{T} \right) e^{-h_o k} \cos(kx - \omega t) + \frac{(d - h_o) e^{-kh_o} U_c}{d} - U_x \right] \right. \quad (3.302)$$

$$\left. \times \left[ \frac{\pi H}{T} e^{-h_o k} \cos(kx - \omega t) + \frac{(d - h_o) e^{-kh_o} U_c}{d} - U_x \right] (-H_{om}) dy \right]$$

$$MH_{dp3} = \left[ -\frac{1}{2} C_d \rho D_p \left[ \left( \frac{\pi H}{T} \right) e^{-h_o k} \cos(k \times (-Pb/3) - \omega t) + \frac{(d - h_o) e^{-kh_o} U_c}{d} - U_x \right] \right. \quad (3.303)$$

$$\left. \times \left[ \frac{\pi H}{T} e^{-h_o k} \cos(k \times (-Pb/3) - \omega t) + \frac{(d - h_o) e^{-kh_o} U_c}{d} - U_x \right] H_{om} S_L \right]$$

$$MH_{dp1} + MH_{dp2} = 2 \int_{-\frac{S_b}{3}}^{\frac{2S_b}{3}} \frac{1}{2} C_d \rho D_p \frac{4}{3} \frac{\omega H}{\pi} \left[ \frac{\pi H}{T} e^{-2kh_o} \cos(kx - \omega t) + \frac{(d - h_o) e^{-kh_o} U_c}{d} - 2e^{-kh_o} U_x \right] \times -H_{om} dx \quad (3.304)$$

$$= \left[ \frac{4}{3} C_d \rho D_p \frac{\omega H}{\pi} (-H_{om}) \left[ \frac{\pi H e^{-2kh_o}}{T k} \sin(kx - \omega t) + \frac{(d - h_o) x e^{-kh_o} U_c}{d} - 2x e^{-kh_o} U_x \right] \right] \Bigg|_{\frac{-sb}{3}}^{\frac{2sb}{3}} \quad (3.305)$$

So total surge pitching moment on hull is

$$MH_p = (MH_{dp1} + MH_{dp2} + MH_{dp3} + MH_{ip1} + MH_{ip2} + MH_{ip3}) \quad (3.306)$$

The inertia surge pitching moment on a single column located at x from the wave crest, is obtained by Eqn. (3.149) so,

$$\Rightarrow x = -\frac{Pb}{3} \rightarrow MH_{ic4} + MH_{ic5} \quad (3.307)$$

$$x = \frac{2Pb}{3} \rightarrow MH_{ic6} \quad (3.308)$$

Also for drag force pitching moment on columns can obtain from Eqn. (3.154) so,

$$\Rightarrow x = -\frac{Pb}{3} \rightarrow MH_{dc4} + MH_{dc5} \quad (3.309)$$

$$x = \frac{2Pb}{3} \rightarrow MH_{dc6}$$

So total horizontal pitching moment on columns will be

$$MH_c = (MH_{ic4} + MH_{ic5} + MH_{ic6} + MH_{dc4} + MH_{dc5} + MH_{dc6}) \quad (3.310)$$

So total surge moment on TLP will be

$$MH = MH_c + MH_p \quad (3.311)$$

For calculating vertical pitch moment on hulls first, consider hulls 1 and 2 aligned along the direction of wave propagation. The pitching moment on these hulls is given as

$$MV_{ip1} + MV_{ip2} = \left[ 2 \frac{\pi}{4} \rho C_m D_p^2 \int_{\frac{-sb}{3}}^{\frac{2sb}{3}} \frac{H}{2} \omega^2 e^{-kh_o} \cos(kx - \omega t) \times -x dx \right] \frac{\sin^2 \alpha}{\cos \alpha} \quad (3.312)$$

$$= \left[ 2 \frac{\pi}{4} D_p^2 \rho C_m \frac{-H}{2} \omega^2 e^{-kh_o} \left[ \frac{x \sin(kx - \omega t)}{k} + \frac{\cos(kx - \omega t)}{k^2} \right] \right] \Bigg|_{x=\frac{-sb}{3}}^{x=\frac{2sb}{3}} \frac{\sin^2 \alpha}{\cos \alpha} \quad (3.313)$$

$$= \left[ \begin{array}{c} 2 \frac{\pi}{4} D_p^2 \rho C_m \frac{-H}{2} \omega^2 e^{-kh_o} \left[ \begin{array}{c} + \frac{\frac{2sb}{3} \sin((k \frac{2sb}{3}) - \omega t)}{k} \\ + \frac{\cos((k \frac{2sb}{3}) - \omega t)}{k^2} \end{array} \right] \\ - \left( \frac{\frac{-sb}{3} \sin((k \frac{-sb}{3}) - \omega t)}{k} - \frac{\cos((k \frac{-sb}{3}) - \omega t)}{k^2} \right) \end{array} \right] \frac{\sin^2 \alpha}{\cos \alpha} \quad (3.314)$$

Next, consider the effect of the vertical acceleration on hull 3. This hull is parallel to the Crestline, and the force per unit of length is constant along the length of the hull. The pitch moment is obtained by multiplying the vertical force, derived for heave excitation, by the lever distance from the centerline so the inertia moment on these hulls will be:

$$MV_{ip1} = \int_{\frac{-SL}{2}}^{\frac{SL}{2}} \rho \frac{\pi D_p^2}{4} C_m \frac{-\omega^2}{2} H e^{-h_o k} \cos(kx - \omega t) x dy \quad (3.315)$$

$$\Rightarrow MV_{ip1} = -\rho \frac{\pi D_p^2}{4} C_m \frac{\omega^2}{2} H e^{-h_o k} \cos(k(-Pb/3) - \omega t) \frac{-pb}{3} S_L \quad (3.316)$$

Also for drag vertical pitch moment on hulls

$$MV_{dp3} = \left[ \int_{\frac{-SL}{2}}^{\frac{SL}{2}} \frac{1}{2} C_d \rho D_p \left[ \left( \frac{\pi H}{T} \right) e^{-h_o k} \sin(kx - \omega t) + \frac{(d - h_o) e^{-kh_o} U_c - U_v}{d} \right] \right] \quad (3.317)$$

$$\times \left[ \frac{\pi H}{T} e^{-h_o k} \sin(kx - \omega t) + \frac{(d - h_o) e^{-kh_o} U_c - U_v}{d} \right] x dy$$

$$\Rightarrow MV_{dp3} = \left[ \begin{array}{c} \frac{1}{2} C_d \rho D_p \left[ \left( \frac{\pi H}{T} \right) e^{-h_o k} \sin(k \times (-Pb/3) - \omega t) \right. \\ \left. + \frac{(d - h_o) e^{-kh_o} U_c - U_v}{d} \right] \\ \times \left[ \frac{\pi H}{T} e^{-h_o k} \sin(k \times (-Pb/3) - \omega t) \right. \\ \left. + \frac{(d - h_o) e^{-kh_o} U_c - U_v}{d} \right] \end{array} \right] S_L \times \frac{pb}{3} \quad (3.318)$$



$$MV_{dp1} + MV_{dp2} = 2 \int_{-\frac{2Sb}{3}}^{\frac{2Sb}{3}} \frac{1}{2} C_d \rho D_p \frac{4 \omega H}{3 \pi} \left[ \begin{array}{l} \frac{\pi H}{T} e^{-2kh_o} \sin(kx - \omega t) \\ + \frac{(d - h_o) e^{-kh_o} U_c}{d} \\ - 2e^{-kh_o} U_v \end{array} \right] \times -x \frac{\sin^2 \alpha}{\cos \alpha} dx \quad (3.319)$$

$$= \left[ \frac{4}{3} C_d \rho D_p \frac{\omega H}{\pi} \left[ \begin{array}{l} \frac{\pi H}{T} e^{-2kh_o} \left[ \frac{-x \cos(kx - \omega t)}{k} + \frac{\sin(kx - \omega t)}{k^2} \right] \\ + \frac{(d - h_o) x^2 e^{-kh_o} U_c}{2d} - \frac{2x^2 e^{-kh_o}}{2} U_v \end{array} \right] \right]_{x=-\frac{2Sb}{3}}^{x=\frac{2Sb}{3}} \frac{-\sin^2 \alpha}{\cos \alpha} \quad (3.320)$$

So total heave pitching moment on hull will be

$$MV_p = (MV_{ip1} + MV_{ip2} + MV_{ip3} + MV_{dp1} + MV_{dp2} + MV_{dp3}) \quad (3.321)$$

For calculating vertical pitch moment on columns, the exposed base of the corner columns of the triangular TLP experience a hydrostatic pressure which has no contribution to the pitch moment, when the integration is taken to the still waterline. However, there is a dynamic pressure variation due to the passage of the waves whose net contribution is non zero. The associated pitching moment arising from this is given by Eqn. (3.172).

$$\Rightarrow x = -\frac{Pb}{3} \rightarrow MV_{c4} + MV_{c5} \quad (3.322)$$

$$x = \frac{2Pb}{3} \rightarrow MV_{c6}$$

So total heave pitching moment on columns will be

$$MV_c = (MV_{c4} + MV_{c5} + MV_{c6}) \quad (3.323)$$

So total heave pitching moment on TLP will be

$$MV = (MV_p + MV_c) \quad (3.324)$$

So total pitching moment on TLP will be

$$F_{51} = (MV + MH) \quad (3.325)$$

### 3.4 Solution of the Equation of Motion in the Time Domain

Wave loading constitutes the primary loading on offshore structures.

The equations of motion of these structures are coupled and nonlinear as following

$$[m]\{x''(t + \Delta t)\} + [c]\{x'(t + \Delta t)\} + [k]\{x(t + \Delta t)\} = \{F_o(t + \Delta t)\} \quad (3.326)$$

The right hand side of Eqn. (3.326) is nonlinearly coupled, because of the presence of structural displacement, velocity and acceleration.

Therefore, the force vector should be updated each time step to account for the change in the tether tension. To achieve this response variation a time domain analysis is carried out for this purpose. Newmark's  $\beta$  time integration procedure is used in a step wise manner.

The velocity and displacement at time  $(t+\Delta t)$  can be expressed as

$$x'(t + \Delta t) = x'(t) + [(1 - \gamma)\Delta t]x''(t) + \gamma(\Delta t)x''(t + \Delta t) \quad (3.327)$$

$$x(t + \Delta t) = [x(t) + (\Delta t)x' + [(0.5 - \beta)(\Delta t)^2]x''(t) + [\beta(\Delta t)^2]x''(t + \Delta t)] \quad (3.328)$$

The parameters  $\beta$  and  $\gamma$  define the variation of acceleration  $x''$  over time step  $\Delta t$  and determine the stability and accuracy characteristics of the method. Typical selection for  $\gamma$  is  $\frac{1}{2}$  and  $\frac{1}{6} \leq \beta \leq \frac{1}{4}$  is satisfactory from all points of view, including accuracy.

The two special cases of Newmark's method that are commonly used are:

- 1) Average acceleration method in which the value of  $\gamma$  is  $\frac{1}{2}$ ,  $\beta = \frac{1}{4}$  where, this method is unconditionally stable.
- 2) Linear acceleration method in which the value of  $\gamma$  is  $\frac{1}{2}$ ,  $\beta = \frac{1}{6}$  where, this method is conditionally stable. The method of average acceleration will be used in this study.

The procedure of this method is summarized as solving Eqn. (3.328) for  $x''(t + \Delta t)$  in terms of  $x(t + \Delta t)$  and then substituting for  $x''(t + \Delta t)$  into Eqn. (3.327) we obtain equations for  $x''(t + \Delta t)$  and  $x'(t + \Delta t)$ , each in terms of unknown  $x(t + \Delta t)$  only. These two relations for  $x'(t + \Delta t)$  and  $x''(t + \Delta t)$  are substituted into Eqn. (3.326) to solve for

$x(t + \Delta t)$  after which, using Eqn. (3.327) and Eqn. (3.328),  $x''(t + \Delta t)$  and  $x'(t + \Delta t)$  can also be calculated at each step. The following values are updated

- a) The stiffness coefficients which varies with tether tension,
- b) The added mass which varies with sea surface fluctuations,
- c) The evaluation of wave forces at the instantaneous position of the displaced structure,
- d) The surge induced heave response.

## Chapter 4

### CASE STUDY

#### 4.1 Introduction

This chapter discusses the responses of the square and triangular TLPs due to a unidirectional wave in the surge direction. Main response parameters are shown as follows

- 1) Surge, heave and pitch responses of square TLP due to a unidirectional wave in the surge direction.
- 2) The change in tension in tether for square tension leg platform subjected to surge hydrodynamic force for different wave heights and wave periods.
- 3) The surge, heave and pitch responses of a triangular TLP due to a unidirectional wave in surge direction.
- 4) The change in tension in tether for triangular tension leg platform subjected to surge hydrodynamic force for different wave heights and wave periods.

In this numerical study the two test models are the same in the sense that they have the same weight and total tension force and the same draft length and overall dimensions. However, different columns and pontoon diameters were estimated to fix the same draft length as following

$$D_{r(\text{square})} = D_{r(\text{triangle})} \quad (4.1)$$

$$\left(\frac{F_B}{\rho g \pi} - D_{p(\text{square})}^2 S\right) / D_{c(\text{square})}^2 = \left(\frac{4F_B}{3\rho g \pi} - D_{p(\text{triangle})}^2 S\right) / D_{c(\text{triangle})}^2 \quad (4.2)$$

assume;

$$D_c = 2D_p \quad (4.3)$$

where; the weight of the platform and the total tension force in tethers will be the same for square and triangle TLPs. So total buoyancy force ( $F_B$ ) is the same for both, also both have the same length. So ( $S$ ) is the same for both platforms. Also when we

design TLP, we assume that columns diameter is twice the pontoon diameter in both of square and triangle TLP so that when we put this into consideration we find that

$$D_c^2 [4D_r + S]_{Square} = .75D_c^2 [4D_r + S]_{triangle} \quad (4.4)$$

$$D_{c(square)}^2 = .75D_{c(triangle)}^2 \quad (4.5)$$

$$D_{p(square)}^2 = .75D_{p(triangle)}^2 \quad (4.6)$$

The forgoing model properties are different than those of Chandrasekaran and Jain, 2002a; 2002b where they assumed that both models have the same weight and dimension which is questionable.

Table 4.1: Geometric properties of the square TLP and load data

Water properties		Platform properties			
Gravity acceleration (m/sec <sup>2</sup> )	9.81	Platform weight (KN),W	280000	Center of gravity above the sea level (m), H <sub>C</sub>	6.03
Water weight density (kN/m <sup>3</sup> )	10.06	Platform length (m), 2a	66.22	Tether stiffness (KN/m),γ	80000
Inertia coefficient, C <sub>m</sub>	2	Platform width (m), 2b	66.22	Tether length (m), L	569
Drag coefficient, C <sub>d</sub>	1	Platform radius of gyration in x-directions (m), r <sub>x</sub>	32.1	Platform radius of gyration in y-directions (m), r <sub>y</sub>	32.1
Current velocity (m/sec),U <sub>c</sub>	0	Platform radius of gyration in z-directions (m), r <sub>z</sub>	33	Water depth (m),d	600
Wave period (sec), T	8, 10, 12.5, and 15	Tether total force (KN),T <sub>t</sub>	160000	Diameter of pontoon (m), D <sub>p</sub>	9.03
Wave height (m), H	8, 10 and 12	Diameter of columns (m), D <sub>c</sub>	18.06	Draft(m),D <sub>r</sub>	31
				Damping ratio, ζ	5%

Table 4.2: Geometric properties of the triangular TLP and load data

Water properties		Platform properties			
Gravity acceleration (m/sec <sup>2</sup> )	9.81	Platform weight (KN),W	280000	Center of gravity above the sea level (m), H <sub>c</sub>	6.03
Water weight density (kN/m <sup>3</sup> )	10.06	Platform length (m), Pl	66.22	Tether stiffness (KN/m), $\gamma$	80000
Inertia coefficient, C <sub>m</sub>	2			Tether length (m), L	569
Drag coefficient, C <sub>d</sub>	1	Platform radius of gyration in x-directions (m), r <sub>x</sub>	32.1	Platform radius of gyration in y-directions (m), r <sub>y</sub>	32.1
Current velocity (m/sec),U <sub>c</sub>	0	Platform radius of gyration in z-directions (m), r <sub>z</sub>	33	Water depth (m),d	600
Wave period (sec), T	8,10, 12.5 and 15	Tether total force (KN),T <sub>t</sub>	160000	Diameter of pontoon (m), D <sub>p</sub>	11
Wave height (m), H	8, 10 and 12	Diameter of columns (m), D <sub>c</sub>	20	Draft(m),D <sub>r</sub>	31
				Damping ratio, $\zeta$	5%

Table 4.3: Calculated natural structural periods for different analysis cases (in seconds) for the four-legged tension leg platforms

Analysis Case	DOF					
	Surge	Sway	Heave	Roll	Pitch	Yaw
Coupled	97.099	97.099	2.218	3.126	3.126	86.047
Uncoupled	97.067	97.067	2.218	3.125	3.125	86.047

Table 4.4: Calculated natural structural periods for different analysis cases (in seconds) for the three-legged tension leg platforms

Analysis Case	DOF					
	Surge	Sway	Heave	Roll	Pitch	Yaw
Coupled	97.2453	97.2549	2.4913	2.9978	3.0521	62.7296
Uncoupled	97.2057	97.2057	2.5262	3.3773	3.3893	62.9697

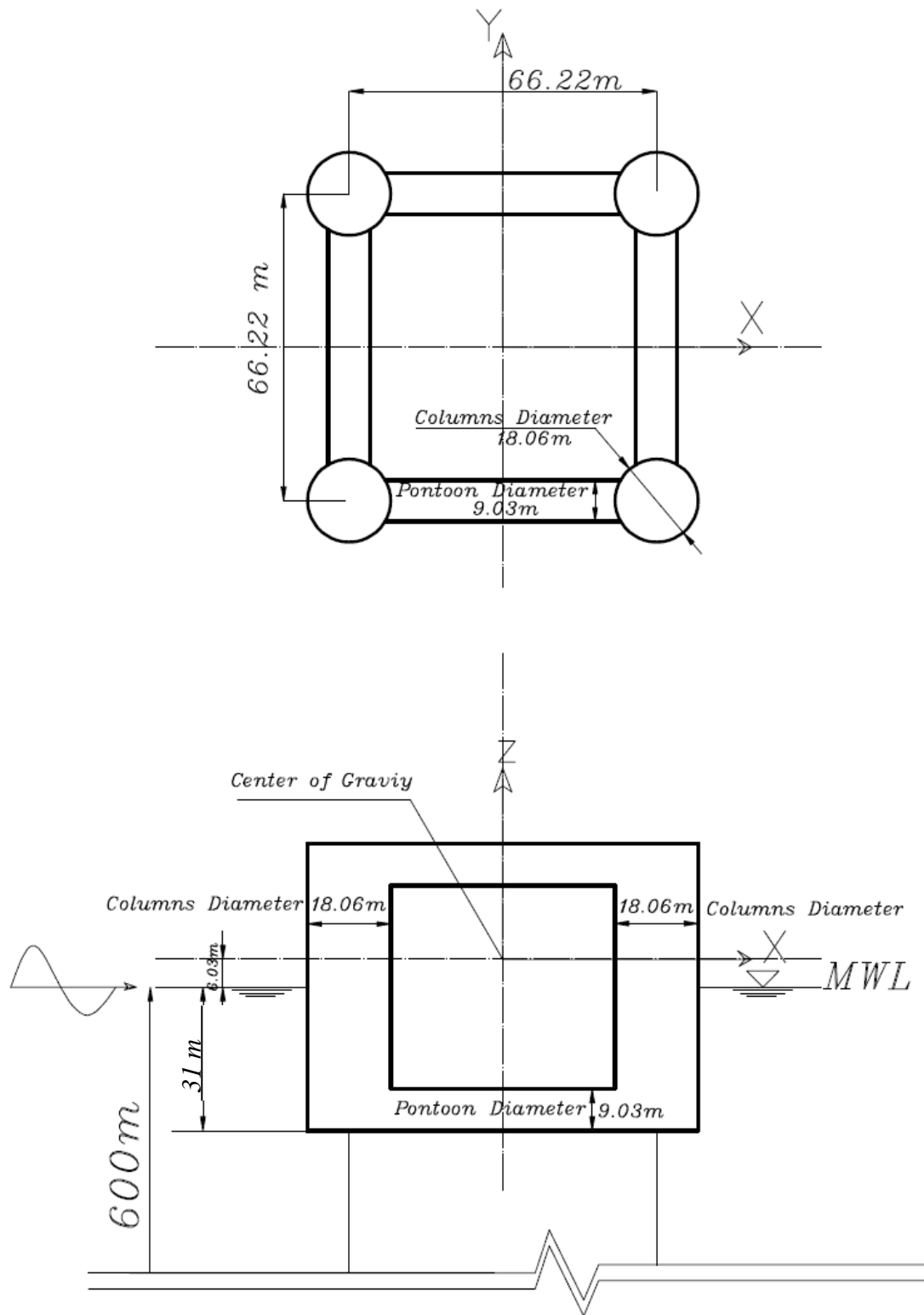


Figure 4.1: Layout of the studied square TLP case.

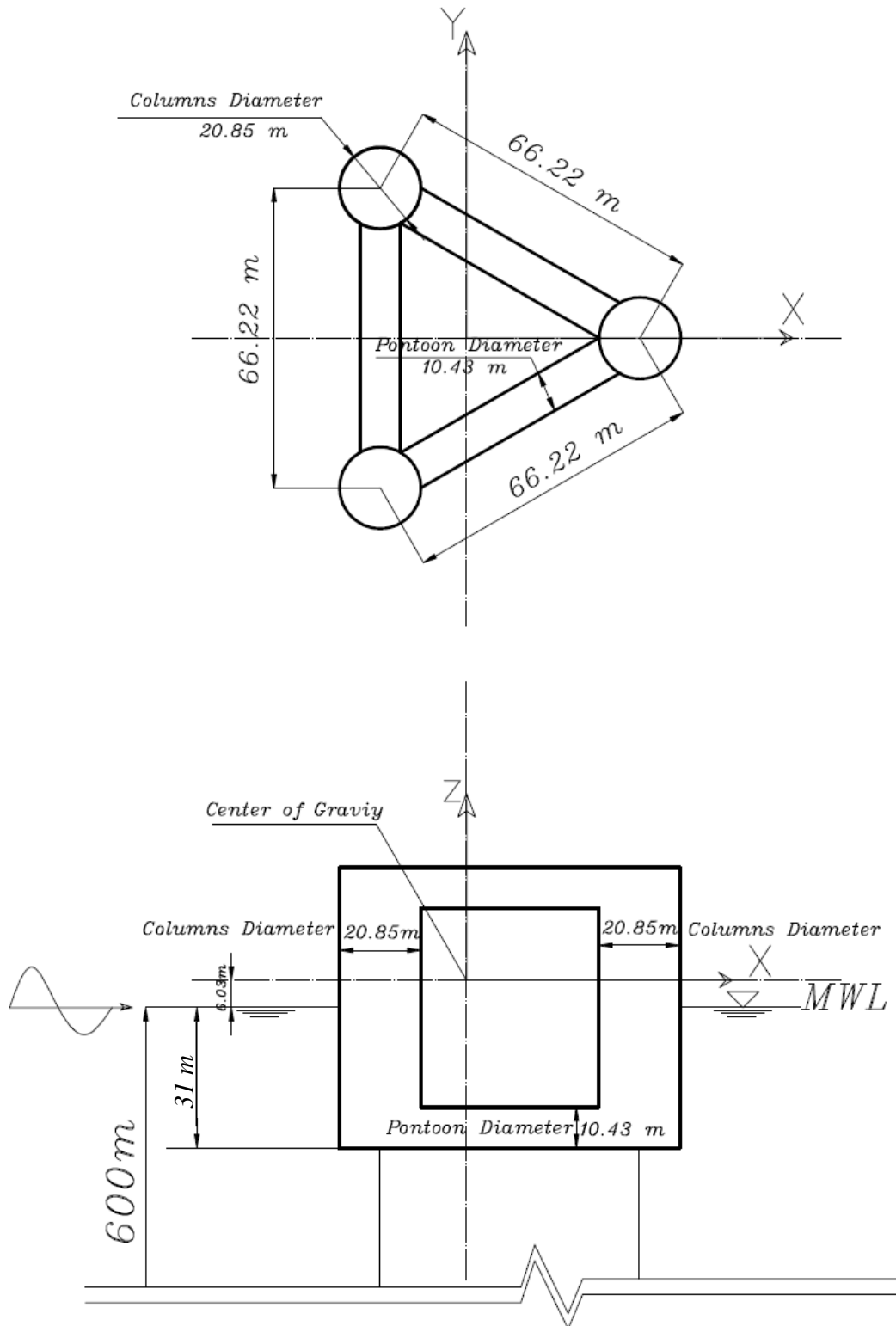


Figure 4.2: Layout of the studied Triangular TLP case.



## 4.2 Discussions

A numerical scheme was developed using MATLAB software where solution based on Newmark's beta method was obtained. A major concern was about the effect of the coupling of degrees of freedom and about its role in influencing response behaviors. Thus, numerical studies for evaluating the coupled and uncoupled responses of the square and triangular TLP under regular waves have been carried out. Coupling of various degrees-of-freedom was taken into consideration by considering the off-diagonal terms in stiffness matrix  $[K]$ . On the other hand, these off-diagonal terms were neglected to study the uncoupling effect. Wave forces were taken to be acting in the direction of surge degree-of-freedom. The geometric properties of the square and triangular TLP are shown in Figures 4.1 and 4.2 respectively. Moreover, the geometric and hydrodynamic data considered for force evaluation are given in Table 4.1 and table 4.2, respectively (Jain, A. K., 1990).

Tables 4.3 and 4.4 show the coupled and the uncoupled natural time periods of square TLP and triangular TLP, respectively. It is seen that coupling has insignificant effect on natural time periods. It is also observed that TLPs have very long period of vibration associated with motions in the horizontal plane (say 60 to 100 seconds). Since typical wave spectral peaks are between 6 to 15 seconds, resonant response in these degrees of freedom is unlikely to occur.

The natural periods in vertical plane in heave, roll and pitch are observed to be in the range of 2 to 4 seconds which is consistent with typical TLP's. While this range is below the periods of typical storm waves, everyday waves do have some energy in this range (the lowest wave period for most geographical locations is about 3 seconds). Thus, wave-excited vibrations can cause high-cycle fatigue of tethers and eventually instability of the platform. One alternative to this problem is to increase the moored stiffness as to further lower the natural periods in heave, roll and pitch movement. The other alternative is to install damping devices in the tethers to mitigate vertical motion.

Time histories of the coupled and the uncoupled responses are shown in Figures. 4.3 to 4.13. Before going into detailed discussion for each response it is clear from the

figures that for squared TLP, the coupling has no effect on response in the surge and heave directions where, it has negligible effect on pitch direction. On the other hand, for triangular TLP, while coupling has a non significant effect on the surge, the heave, and tether tension force, it has a significant effect on the pitch response in which ignoring the coupling effect will lead to overestimation of the pitch response.

## **4.2.1 Response for Square TLP**

### **4.2.1.1 Surge Response**

The time histories of the surge responses for the square TLP are shown in Figure 4.3. It is observed that, for a specific wave period, the amplitude of oscillations increases as the wave height increases. Moreover, for short wave periods (up to 10 sec), the system responds in small amplitude oscillations about a displaced position that is inversely proportional to the wave period and directly proportional to wave height. On the other hand, for relatively long wave period (12.5 or 15 sec.), the system tends to respond in high oscillations amplitude about its original position. The amplitude of oscillations increases with the increase in the wave period, which is expected because as the wave period increases, it becomes closer to the surge period of vibration (about 97 sec.). Moreover, the effect of wave height becomes more pronounced for shorter wave periods. In all cases, the surge response seems to have periodic oscillations that have the same exciting wave period. Finally, the transient state takes about 40-80 seconds where the stationary state begins.

### **4.2.1.2 Heave Response**

The time histories of the coupled and the uncoupled heave responses for the square TLP are shown in Figure 4.4. As expected, the response in the heave direction has very small values compared to that of the surge direction. This is attributed to the relatively high stiffness of the tethers in this direction together with the fact that the excitation is indirect in this case. Moreover, the heave response is directly proportional to the wave period and to a less extent to wave height. Also, the transient state takes about 10

seconds where the stationary state begins and the motion is almost periodic. The heave response appears to have a mean value of nearly zero.

#### **4.2.1.3 Pitch Response**

The time histories of the coupled and the uncoupled pitch responses for squared TLP are shown in Figure 4.5. It is clear that as the wave period increases the response becomes closer to being periodic in nature. For short wave periods (less than 10 sec.), a higher mode contribution to the response seems to take place. For long wave periods (12.5 and 15 sec.), the higher mode contribution vanishes after one or two cycles and we have a one period response (wave period) as in the surge and heave cases. Moreover, the transient state takes about 20 seconds before the stationary state begins.

To get an insight into the behavior for the short wave period cases, the response spectra for wave height of 8.0 m and wave period of 6, 8, and 10 sec was obtained and the results are shown in Figure 4.6. Clearly there are three distinct peaks. These are the exciting wave period, a period doubling case in which the spectra have peaks at half the exciting wave periods, and a third peak that is at about one third of the exciting wave period. This particular peak may indicate contribution of the pitch mode of vibration (about 3.1 sec.).

#### **4.2.1.4 Tether Tension Force Response**

The time histories of the tether tension force responses for the square TLP are shown in Figure 4.7. It is observed that, for a specific wave period, the amplitude of forces increases as the wave height increases. Moreover, for short wave periods (less than 10 sec), the forces oscillate about a non zero mean value that is inversely proportional to the wave period and directly proportional to wave height. On the other hand, for relatively long wave period (12.5 or 15 sec.), the forces tend to oscillate about a nearly zero value. The effect of wave height is observed to be more pronounced for shorter wave periods.

Lastly, to gain a conceptual view of the stability and periodicity of the dynamic behavior of the structure, the phase plane for wave periods of 10 and 15 sec are plotted in Figure 4.8. It is observed that the steady state behavior of the structure is periodic and stable.

## **4.2.2 Response of Triangular TLP**

### **4.2.2.1 Surge Response**

The time histories of the surge responses for the triangular TLP are shown in Figure 4.9. It is observed that, for a specific wave period, the amplitude of oscillations slightly increases as the wave height increases. Moreover, for short wave periods (up to 10 sec), the system responds in small amplitude oscillations about a displaced position that is inversely proportional to the wave period and directly proportional to wave height. On the other hand, for relatively long wave period (12.5 or 15 sec.), the system tends to respond in high oscillations amplitude about its original position. The amplitude of oscillations increases with the increase in the wave period, which is expected because as the wave period increases, it becomes closer to the surge period of vibration (about 97 sec.). Moreover, the effect of wave height becomes more pronounced for shorter wave periods. In all cases, the surge response seems to have periodic oscillations that have the same exciting wave period. Finally, the transient state takes about 140-160 seconds for short wave period (6 and 8 sec); whereas it takes about 80 sec for longer wave periods. After that the stationary state begins. Finally, it is observed that coupling has insignificant effect on the surge response. This is attributed to the fact that the loading is symmetrical in this case.

### **4.2.2.2 Heave Response**

The time histories of the coupled and the uncoupled heave responses for the triangular TLP are shown in Figure 4.10. As expected, the response in the heave direction has very small values compared to that of the surge direction. This is attributed to the relatively high stiffness of the tethers in this direction together with the fact that the excitation is indirect in this case. Moreover, the heave response is directly proportional to

the wave period and to a less extent to wave height. Also, the transient state takes about 10 seconds where the stationary state begins and the motion is almost periodic. Contribution from heave degree of freedom seems to take place. Finally, coupling seems to have a minor effect on the response of the TLP.

#### **4.2.2.3 Pitch Response**

The time histories of the coupled and the uncoupled pitch responses for triangular TLP are shown in Figure 4.11. It is clear that coupling has a significant effect on the pitch response. This is due to the fact that the structure is not symmetrical in this particular response where two legs exist at the left hand side while only one leg exists at the right hand side. The uncoupled response overestimates the values the pitch response.

It also observed that as the wave period increases the response becomes closer to being periodic in nature. For short wave periods (less than 10 sec.), a higher mode contribution to the response appears to take place. For long wave periods (12.5 and 15 sec.), the higher mode contribution vanishes after one or two cycles and we have a one period response (wave period) as in the surge and heave cases. Moreover, the transient state takes about 10 seconds before the stationary state begins. Finally, as the wave period increases, the pitch response decreases. This behavior is more pronounced in the coupled case.

#### **4.2.2.4 Tether Tension Force Response**

The time histories of the tether tension force responses for the triangular TLP are shown in Figure 4.12. It is observed that, for a specific wave period, the amplitude of the forces increase as the wave height increases. Moreover, for short wave periods (less than 8 sec), the transient state exhibits high tension forces in the tethers. This force is inversely proportional to wave period and directly proportional to wave height. On the other hand, for relatively long wave period (12.5 or 15 sec.), the forces become very smaller and have a mean value of nearly zero. Moreover, the effect of wave height is more pronounced for shorter wave periods. Finally, the transient state takes about 160

seconds for short wave period of 6 sec. it reduces significantly to 60 sec for wave period of 8 sec. for longer wave periods the transient state vanishes after less than 20 sec.

Lastly, to gain a conceptual view of the stability and periodicity of the dynamic behavior of the structure, the phase plane for wave periods of 10 and 15 sec are plotted in Figure 4.13. It is observed that the steady state behavior of the structure is periodic and stable.

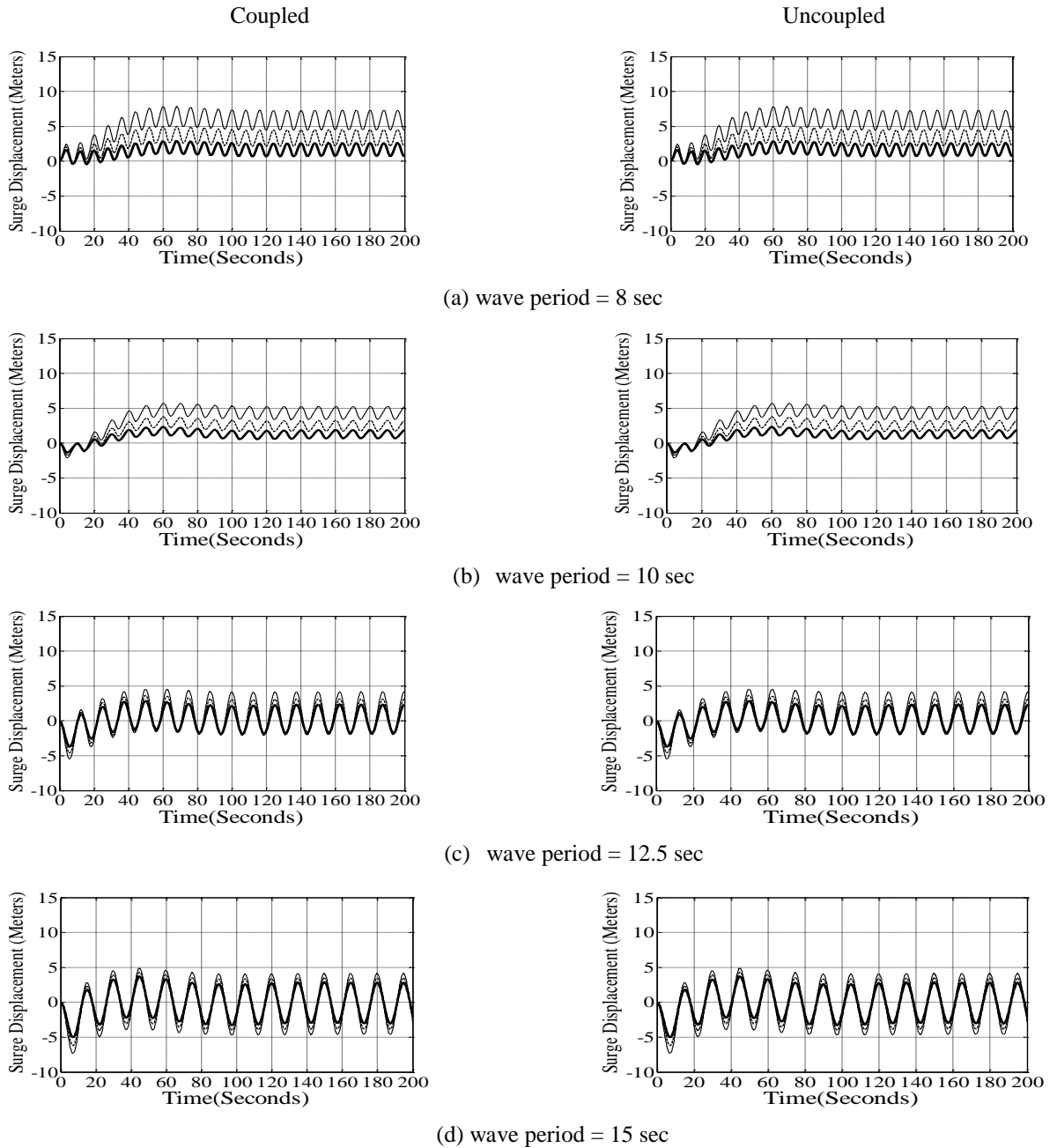


Figure 4.3. Surge response of square TLP for (a) wave period = 8 sec; (b) wave period = 10 sec; (c) wave period = 12.5 sec; (d) wave period = 15 sec.

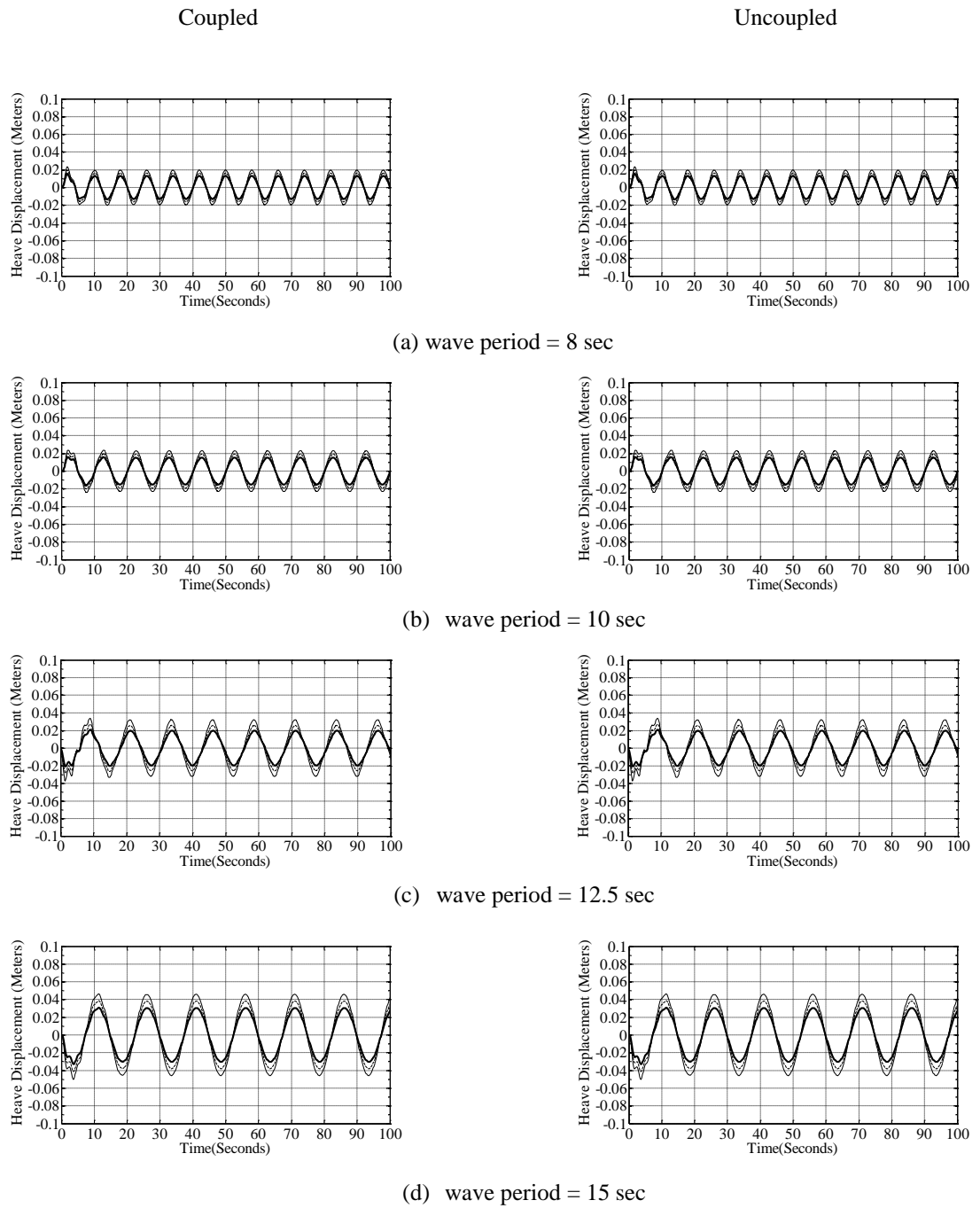


Figure 4.4. Heave response of square TLP for (a) wave period = 8 sec; wave period = 10 sec; (c) wave period = 12.5 sec; (d) wave period = 15 sec.



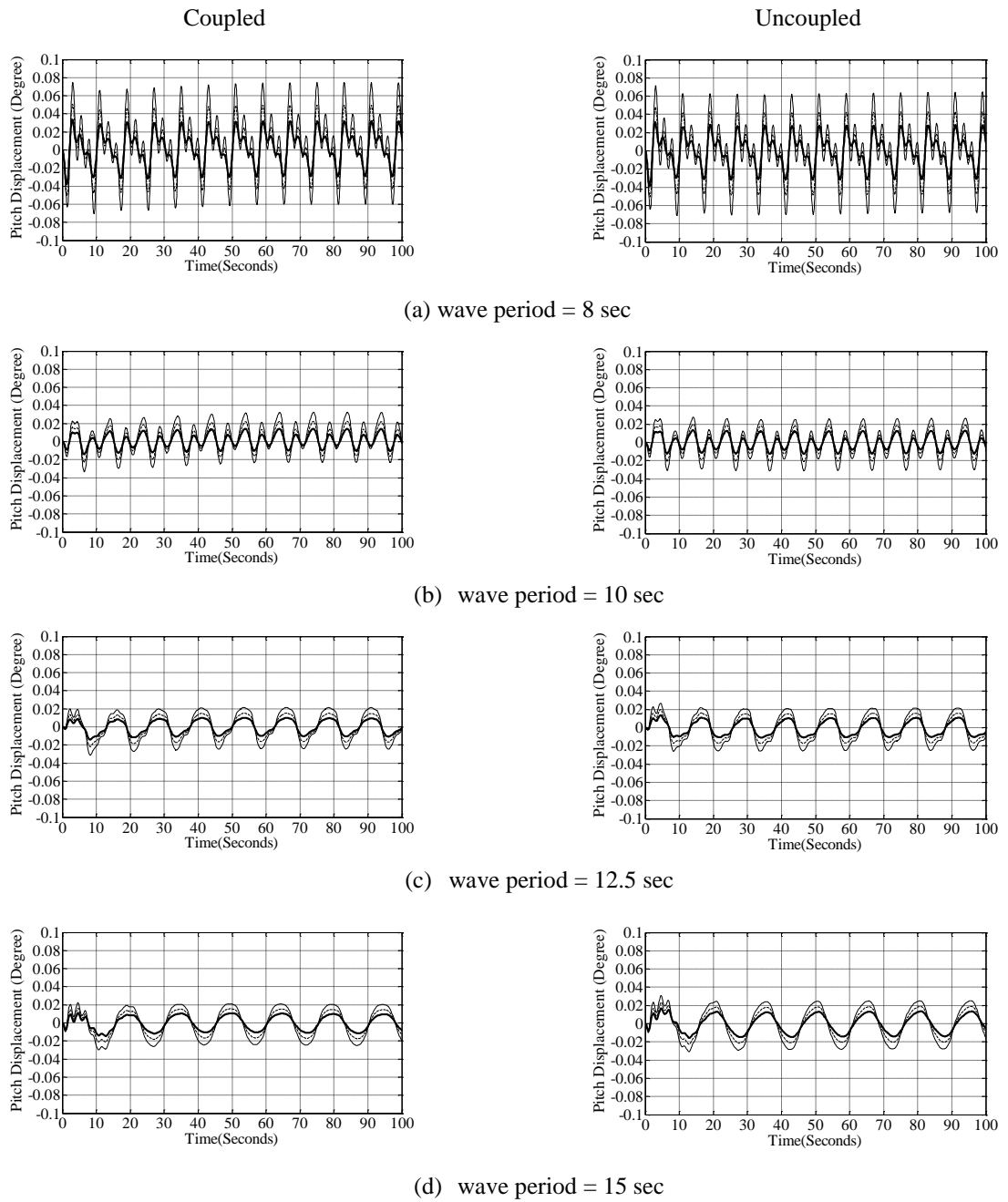


Figure 4.5. Pitch response of square TLP for (a) wave period = 8 sec; (b) wave period = 10 sec; (c) wave period = 12.5 sec; (d) wave period = 15 sec.

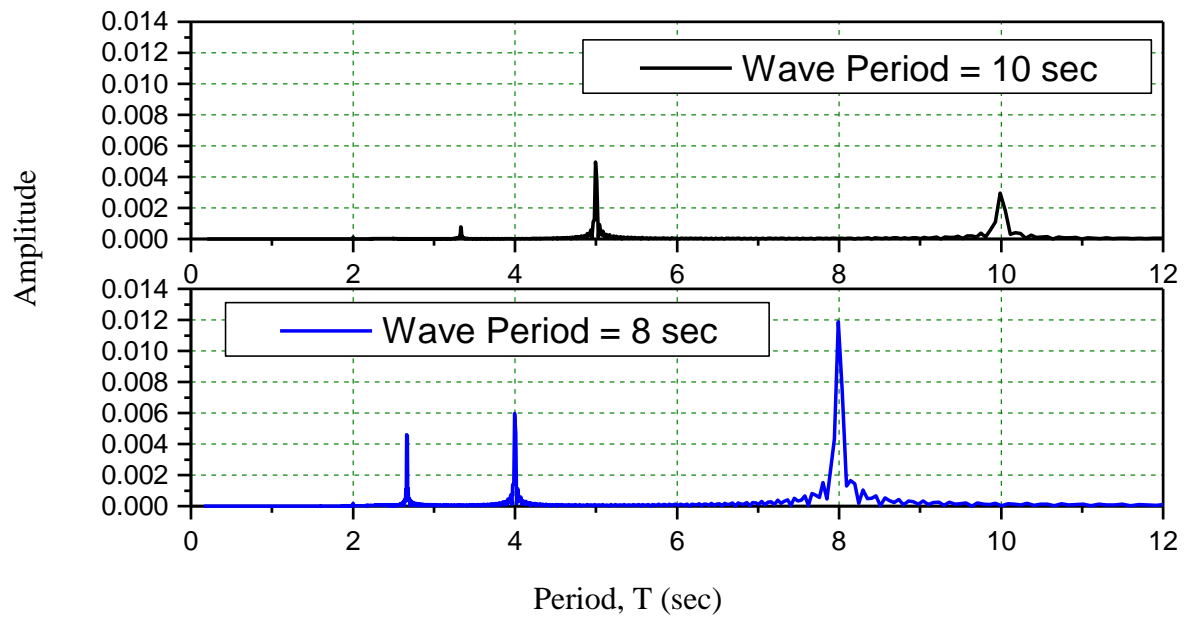


Figure 4.6. Response Spectrum for pitch motion of square TLP for different wave periods (wave height = 8.0m).

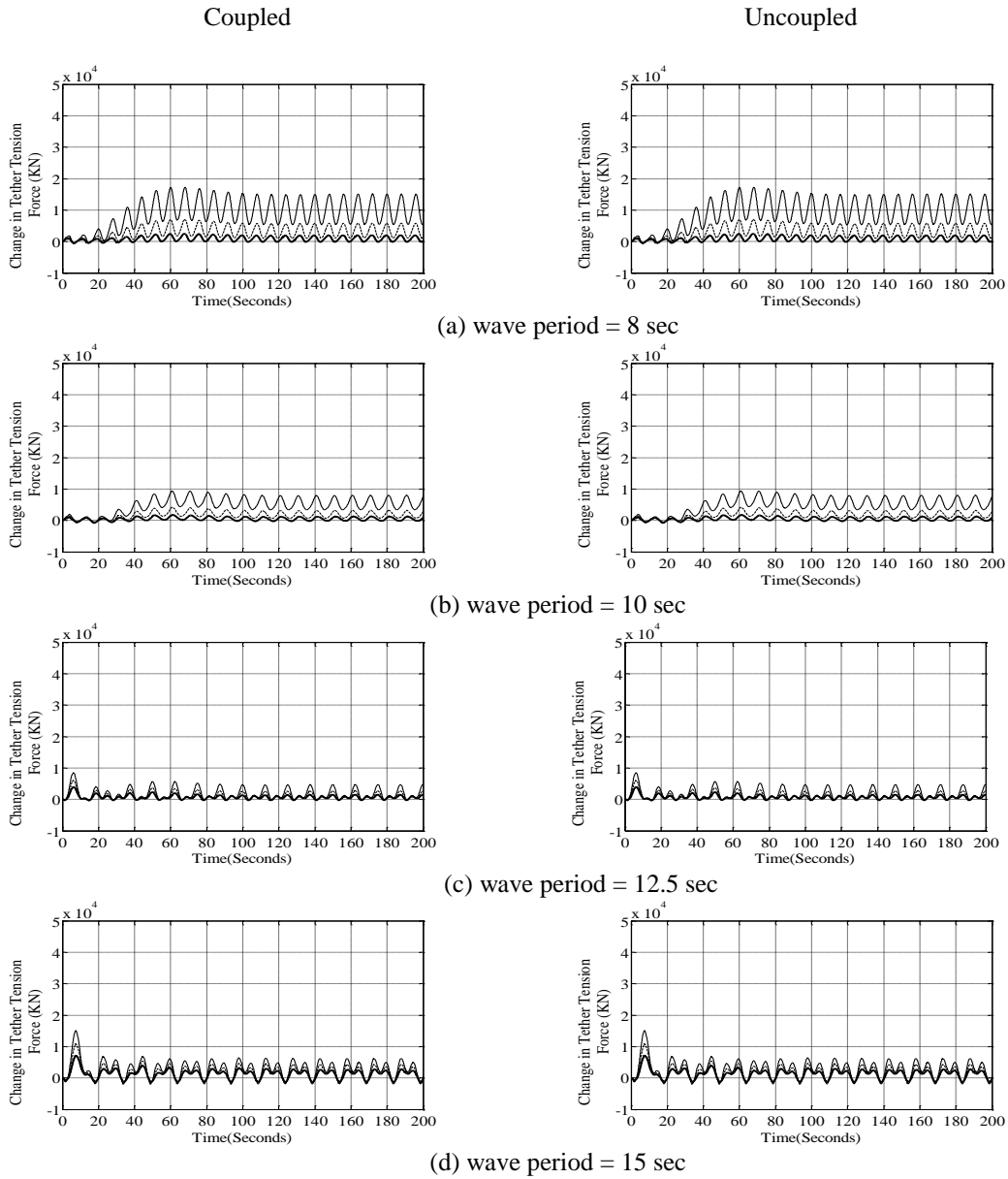


Figure 4.7. Tether tension force response of square TLP for (a) wave period = 8 sec; (b) wave period = 10 sec; (c) wave period = 12.5 sec; (d) wave period = 15 sec.

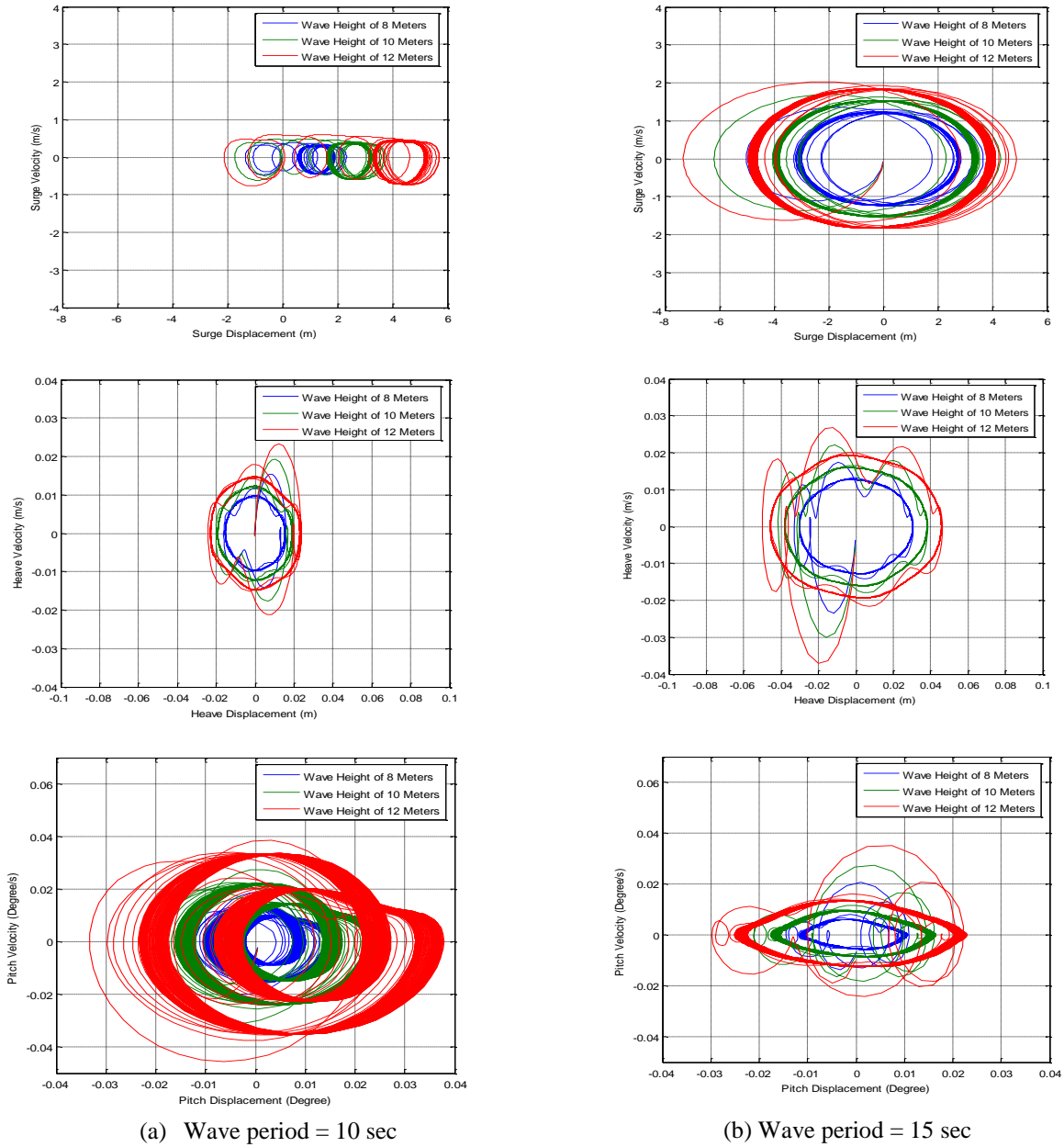
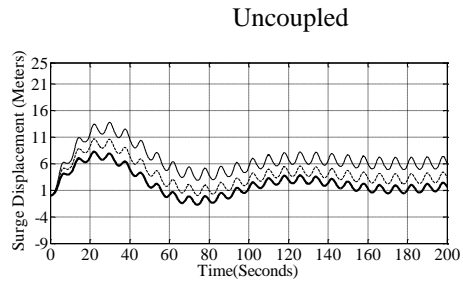
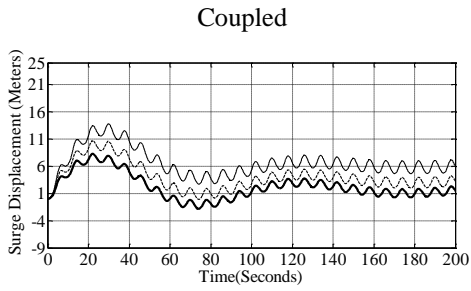
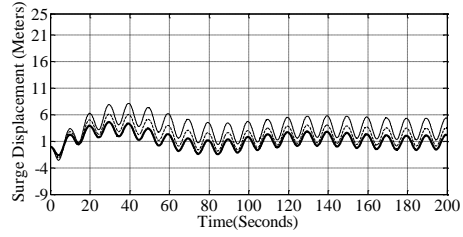
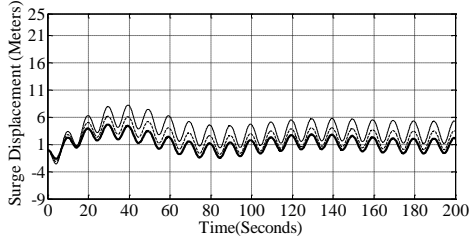


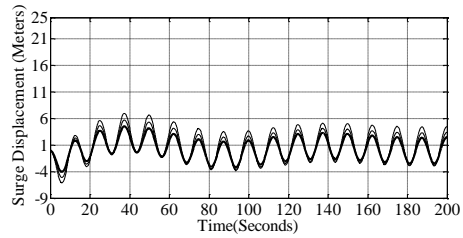
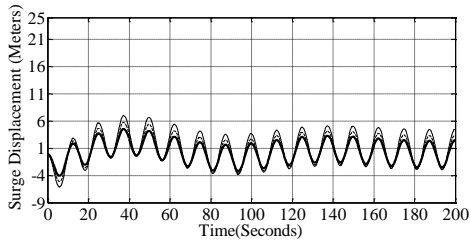
Figure 4.8. Phase plane for coupled motion of square TLP (a) Wave period = 10 sec; (b) Wave period = 15 sec.



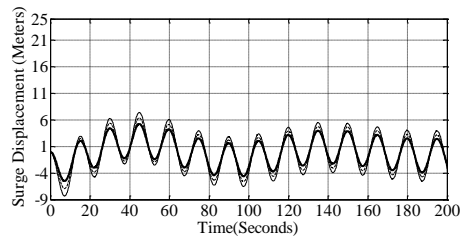
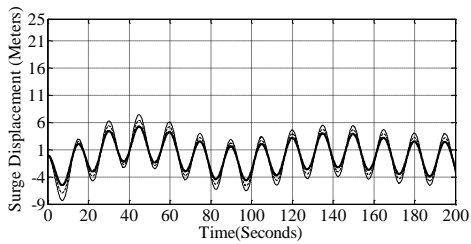
(a) wave period = 8 sec



(b) wave period = 10 sec



(c) wave period = 12.5 sec



(d) wave period = 15 sec

Figure 4.9. Surge response of triangular TLP for (a) wave period = 8 sec; (b) wave period = 10 sec; (c) wave period = 12.5 sec; (d) wave period = 15 sec.

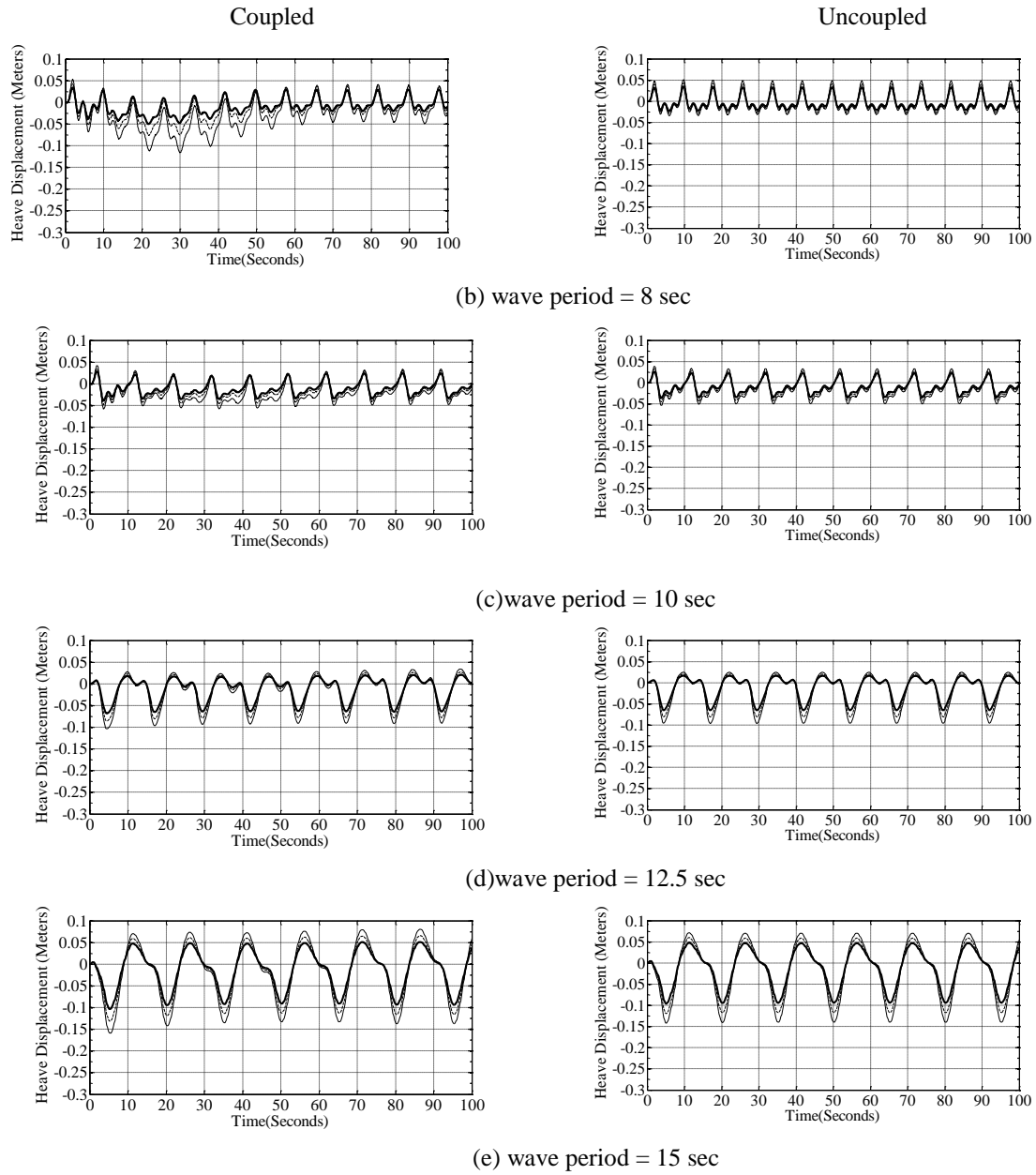
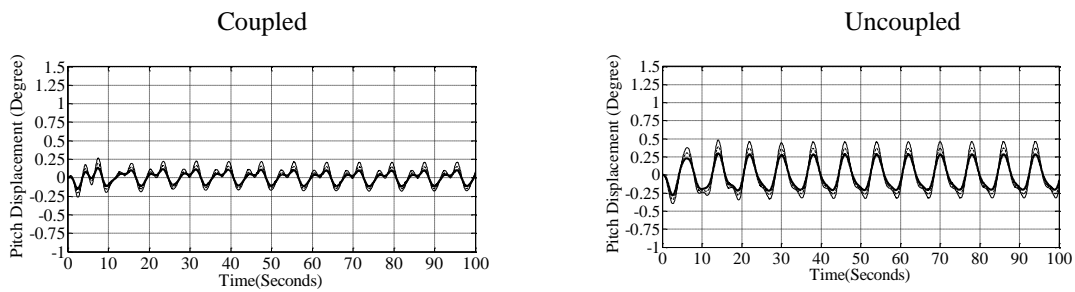
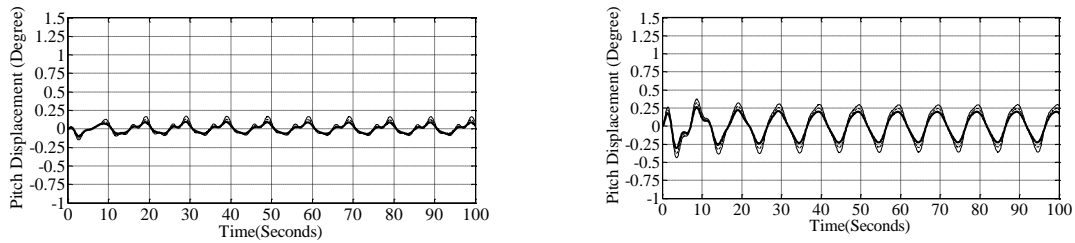


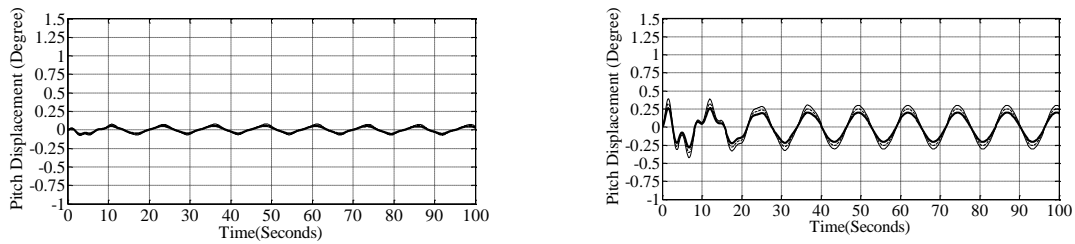
Figure 4.10. Heave response of triangular TLP for (b) wave period = 8 sec; (c) wave period = 10 sec; (d) wave period = 12.5 sec; (e) wave period = 15 sec.



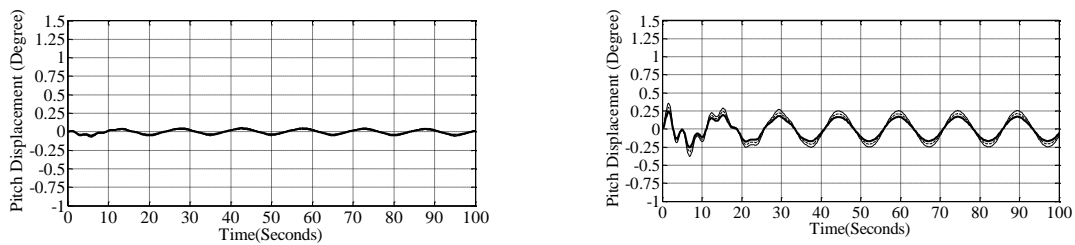
(b) wave period = 8 sec



(c) wave period = 10 sec



(d) wave period = 12.5 sec



(e) wave period = 15 sec

Figure 4.11. Pitch response of triangular TLP for (b) wave period = 8 sec; (c) wave period = 10 sec; (d) wave period = 12.5 sec; (e) wave period = 15 sec.

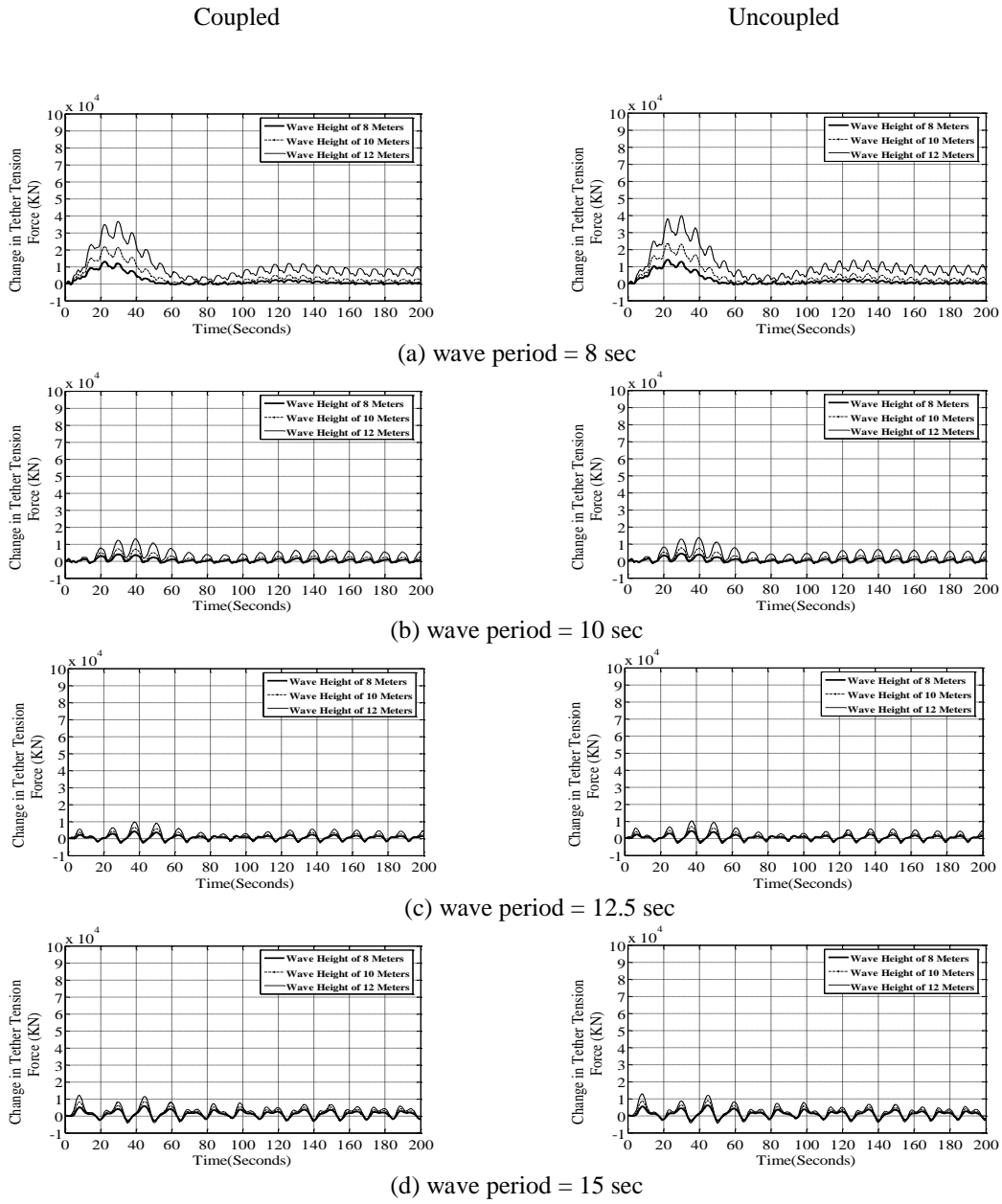


Figure 4.12. Tether tension force response of triangular TLP for (a) wave period = 8 sec; (b) wave period = 10 sec; (c) wave period = 12.5 sec; (d) wave period = 15 sec.



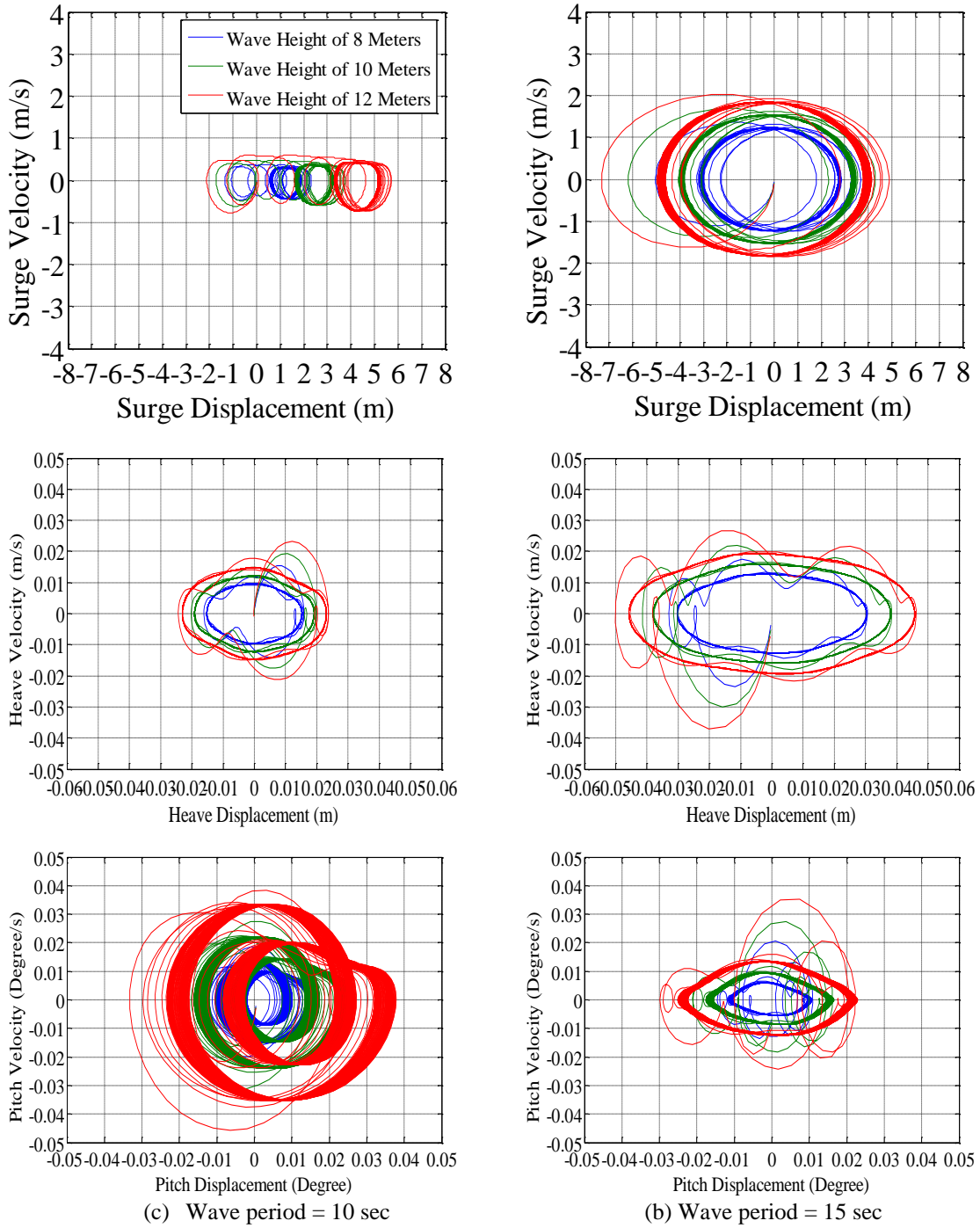


Figure 4.13. Phase plane for coupled motion of triangular TLP (a) Wave period = 10 sec; (b) Wave period = 15 sec.

## Chapter 5

### CONCLUSIONS AND RECOMENDITIONS

#### 5.1 Introduction

The present study investigates the dynamic response of square and triangular TLP under hydrodynamic forces in the surge direction considering all degrees of freedom of the system. A numerical dynamic model for the TLP was written where Morison's equation with water particle kinematics using Airy's linear wave theory was used. The scope of the work was to accurately model the TLP system considering added mass coefficients and nonlinearity in the system together with the coupling between various degrees of freedom. Results for the time histories for the affected degrees of freedom have been presented.

The TLP can be modeled as a rigid body with six degrees of freedom, which can be conveniently divided into two categories: those controlled by the stiffness of tethers, and those controlled by the buoyancy. The former category includes motion in the vertical plane and consists of heave, roll and pitch; whereas the latter comprises the horizontal motions of surge, sway and yaw. The natural periods of motion in the horizontal plane are high, whereas in the vertical plane the periods are low. Generally, the surge motion is predominantly high for head seas due to the combined actions of wind, waves and currents. However, due to coupling among various degrees of freedom and relatively low damping of hydrodynamic origin in the vertical plane motion, a complete analysis of a six degree-of-freedom system subjected to wind, waves and currents is desirable.

## 5.2 Conclusion

Based on the results shown in this thesis, the following conclusions can be drawn:

### a) For Square TLP

- Coupling between various degrees of freedom has no effect on the surge or the heave responses, and has an insignificant effect on the pitch response.
- TLP's have very long period of vibration (80 to 100 seconds) associated with motions in the horizontal plane, surge, sway and yaw. Since typical wave spectral peaks are between 6 to 15 seconds, resonant response in these degrees of freedom is unlikely to occur.
- For short wave periods (less than 10 sec.), the surge response consists of small amplitude oscillations about a displaced position that is inversely proportional to the wave period and directly proportional to wave height. On the other hand, for relatively long wave period (12.5 or 15 sec.), the system tends to respond in high oscillations amplitude about its original position.
- The heave response is directly proportional to the wave period and to a less extent to wave height.
- For short wave periods (less than 10 sec.), a higher mode contribution to the pitch response accompanied by period doubling appears to take place.
- The phase plane shows that the steady state behavior of the structure is periodic and stable.

### b) For Triangular TLP

- While coupling has a non significant effect on the surge, the heave, and tether tension force, it has a significant effect on the pitch response in which ignoring the coupling effect will lead to overestimation of the pitch response.

- TLP's have very long period of vibration (60 to 100 seconds) associated with motions in the horizontal plane, surge, sway and yaw. Since typical wave spectral peaks are between 6 to 15 seconds, resonant response in these degrees of freedom is unlikely to occur.
- For short wave periods (less than 10 sec), the system responds in small amplitude oscillations about a displaced position that is inversely proportional to the wave period and directly proportional to wave height. On the other hand, for relatively long wave period (12.5 or 15 sec.), the system tends to respond in high oscillations amplitude about its original position.
- The heave response is directly proportional to the wave period and to a less extent to wave height.
- For short wave periods (less than 10 sec.), a higher mode contribution to the pitch response appears to take place. For long wave periods (12.5 and 15 sec.), the higher mode contribution vanishes after one or two cycles and we have a one period response (wave period) as in the surge and heave cases.
- For short wave periods (less than 10 sec), the transient state exhibits high tension forces in the tethers. On the other hand, for relatively long wave period (12.5 or 15 sec.), the forces become very smaller and have a mean value of nearly zero.
- The phase plane shows that the steady state behavior of the structure is periodic and stable.
- The heave response will be highly underestimated if the coupling effect between various degrees-of-freedom is ignored in the analysis of TLP.
- While the general trend of the square and triangular TLP is similar, the triangular TLP response is generally higher than the square TLP.

### **5.3 Recommendations**

It is recommended that a further study should take place considering the following

1. Irregular wave models.
2. Higher order wave models.
3. Oblique wave direction.
4. TLP with wind turbine to study the behavior of coupled system and its stability due to the exerted force from the wind turbine. So we can view the feasibility of this coupled system for producing clean renewable energy (electricity).

## REFERENCES

1. Ahmad, N. Islam, A. Ali, "Wind-induced Response of Tension Leg Platform", *Journal of Wind Engineering and Industrial Aerodynamics*, vol. 72, 225-240, 1997.
2. Ahmad, S., "Stochastic TLP response under long crested random sea. *Journal of Computers and Structures*", 61(6): 975-993. [Doi: 10.1016/0045-7949(96)00188-5], 1996.
3. Ahmed, S., Bhaskar sengupta, A. Ali, "Nonlinear dynamic response of tension leg platform tether under offshore environmental conditions", *Ocean engineering*, vol. 30, 232-241, 1990.
4. Angelides, D. C., Chen, C., Will, S. A., "Dynamic Response of Tension Leg Platform". *Proceedings of BOSS*, 2:100-120, 1982.
5. Bhattachatya, S. K., Anitha, J., Idichandy, V. G., 2004, "Experimental and numerical study of coupled dynamic response of a mini-tension leg platform", *Journal of Offshore Mechanics and Arctic Engineering*, 126 (4), pp. 318–330.
6. Bhattacharjee, S., "filter approaches to stochastic dynamic analysis of compliant offshore platforms", Huston, Texas, March 1990.
7. Chandrasekaran, S. and Roy, A., 2005, "Phase space study of offshore structures subjected to non-linear hydrodynamic loading", *Proceedings of the International Conference on Structural Engineering*, SEC 2005, Indian Institute of Science, Bangalore.
8. Chakrabarti, S. K., "Discussion of dynamics of single point moorings in deep water", *Journal of Waterways, Harbour and Coastal Engineering Division*, *Transactions of ASCE* 97 (WN3), pp.558–590, 1971.
9. Chakrabarti, S. K., "Hydrodynamics of Offshore Structures ", Springer-Verlag N. Y., 1987.
10. Chan K. Yang, M. H. Kim, 2010, "Transient effects of tendon disconnection of a TLP by hull–tendon–riser coupled dynamic analysis", *Ocean Engineering* 37 (2010) 667–677.

11. Chandrasekaran, S., Jain, A. K., "Dynamic behavior of square and triangular offshore tension leg platforms under regular wave loads", *Ocean Engineering*, 29(3):279-313[doi:10.1016/S0029-8018(00)00076-7], 2002a.
12. Chandrasekaran, S., Jain, A. K., "Triangular configuration tension leg platform behavior under random sea wave loads", *Ocean Engineering*, 29(15):1895-1928. [doi:10.1016/S0029-8018(01)00111-1], 2002b.
13. Chandrasekaran, S., A. K. Jain, A. Gupta, A. Srivastava, "Response behaviour of triangular tension leg platforms under impact loading", *Ocean Engineering* 34 (2007) 45–53.
14. Chandrasekaran, S., A. K. Jain, Anupam Gupta, " Influence of wave approach angle on TLP's response", *Ocean Engineering* 34 (2007) 1322–1327.
15. Chopra, A. K., **Dynamics of structures**, Prentice Hall, 1995.
16. Dean, R. G., A. Dalrymple, R. A., **Water wave mechanics for engineers & scientists**, World scientific, Volume2, 1984.
17. Denis. J. P. F. and Heaf, N. J, "A Comparison between linear and nonlinear response of a proposed Tension Leg Production Platform", *Proceedings of the Offshore Technology Conference, OTC 3555*, pp. 1743-1754, 1979.
18. Duggal, A. S., Niedzwecki, J. M., 1995, "Dynamic response of a single flexible cylinder in waves", *Journal of OMAE* 117, 99–104.
19. Faltinsen, O. M., van Hooff, R. W., Fylling, I. J., Teigen, P. S.," Theoretical and Experimental Investigations of Tension Leg Platform Behavior", *Proceedings of BOSS*, 1:411-423, 1982.
20. Hahn, G. D., 1994, "Influences of wave stretching on the response of wave-excited offshore platforms", *International Journal of Ocean Engineering* 21 (6), 507–517.
21. Hogben, N., B. L. Miller, J. W. Searle, and G. Ward, "Estimation of Fluid Loading on Offshore Structures," *Proc. of the Inst. of civil Engineers*, vol. 63, part 2, pp. 515-462, 1977.
22. Huse, E. and Utnes, T., 1994," Spring Damping of Tension Leg Platforms", *Proceedings of the Offshore Technology Conference, OTC 7446*, 2, pp. 259-267.

23. Jain, A. K., "Nonlinear dynamic response of tension leg platform", *Ocean engineering*, vol. 30, 222-231, 1990.
24. Jain, A. K., "Nonlinear coupled response of offshore tension leg platforms to regular wave forces", *Ocean engineering*, vol. 24, 577-592, 1997.
25. Jain, A. K., A.M.Asce, M.Iscope and S.Chandrasekaran, "Aerodynamic effects on offshore tension leg platforms", *Ocean engineering*, vol. 31, 147-155, 1990.
26. Joseph, A., Lalu Mangal and Precy Sara George, 2009, "Coupled Dynamic Response of a Three-Columns Mini Tlp", *Ocean Engineering* 33 (2009) 620–634
27. Kareem, A., 1987, "Dynamic Response of structures under stochastic environmental Loads ", *J. stuct. Engr., ASCE*, vol.14, No.1, pp1-8.
28. Kareem, A. and Li, Y. S., 1992, " Wind-excited surge Responses of Tension Leg platform: frequency-domain approach, "*J. Engr. Mechanics*, vol.119, No.1, pp161-183.
29. Ketabdari, M. J. and Ardakani, H. A., 2005, "Nonlinear response analysis of a sea star offshore tension leg platform in six degrees of freedom", *WIT Transactions on the Built Environment* 84.
30. Kirk, C. L. and E. U. Etok, "Dynamic Response of Tethered Production Platform in a Random Sea-State", *Proceedings on Behavior of Offshore Structures*, Boss 1977, pp.139-164, MIT, Boston, 1979.
31. Kurian, V. J., M. A. Gasim, S. P. Narayanan, V. Kalaikumar, 2008, "Response of Square and Triangular TLPs Subjected to Random Waves", *ICCBT-C-12*-pp.133-140.
32. Kurian, V. J., M. A. Gasim, S. P. Narayanan, V. Kalaikumar, 2008, "Parametric Study of TLPs Subjected to Random Waves", *ICCBT-C-19*-pp.213-222.
33. Lee, C. P., 1994," Draggged surge motion of a tension leg structure", *International Journal of Ocean Engineering* 21 (3), 311–328.
34. Li, Y. S. and Kareem, A., 1993, "Multivariate Hermite Expansion of Hydrodynamic Drag Loads on Tension Leg Platform", *Journal of the Engineering Mechanics*, vol.119, No.1, pp.91-112.



35. Lyons, G. J., Patel, M. H., Sarohia, S., 1983," Theory and model test data for tether forces on tensioned buoyant platforms", In: Proceedings of the Offshore Technology Conference, OTC No. 4643, pp.533–544.
36. Lee, H. H. and Wang, P. W., 2000, "Analytical solution on the surge motion of tension leg twin platform structural systems", *Ocean Engineering*, vol. 27, pp. 393–415.
37. Mekha, B. B., Johnson, C. P., Roesset, J. M., 1994, "Effects of different wave free surface approximations on the response of a TLP in deep water", In: Proceedings of the Fourth ISOPE, Osaka, pp. 105–115.
38. Morgan, J. R. and Malaeb, D. , "Dynamic Analysis of Tension Leg Platforms", Proceedings of the Second international Offshore Mechanics and Arctic Engineering symposium. U.S.A., paper no. 4, pp. 31-37, 1983.
39. Morison, J. R. and et.al, "The Force Exerted by Surface Waves on Piles", Petroleum Transaction, ASME, vol.189, pp.149-154, 1950.
40. Munkejord, T., 1996, "The Heidrun TLP and concept development for deep water", In: Proceedings of ISOPE, Los Angeles, pp. 1–11.
41. Natvig, B. J., Vogel, H., 1995," TLP design philosophy—past, present, future", In: Proceedings of ISOPE, The Hague, pp. 64–69.
42. Paulling, J. R., Horton, E.E., 1970," Analysis of the tension leg stable platform", In: Proceedings of the Offshore Technology Conference, OTC No. 1263, pp. 379–390.
43. Patel, M. H., 1989,"Dynamic of Offshore Structures", Butterworth, London.
44. Penzien, J., 1976, "Structural Dynamics of Fixed Offshore Structures", Behavior of Offshore Structures, Proceeding, 1ST Int. Conf., v. 1.
45. Spanos, P. D., Agarwal, V. K., 1984," Response of a simple TLP model to wave forces calculated at displaced position", *Journal of Energy Resources Technology* 106, 437–443.
46. Stokes, G. G., "On the Theory of Oscillatory Waves", *Trans. Of the Cambridge Philosophical Society*, vol. 8, pp.441-455, 1847.

47. Tabeshpour, M. R., Seif, M. S., Golafshani, A. A., 2004, "Vertical Response of TLP with the Effect of Added Mass Fluctuation", 16th Symposium on Theory and Practice of Ship Building. Croatia.
48. Tabeshpour, M. R., Golafshani, A. A., and Seif, M.S., 2006, " Simple Model for Exact Heave Motion of Tension Leg Platform" WSEAS Transactions on Applied Mathematics, vol. 5, pp. 500- 506.
49. Tabeshpour, M. R., Golafshani, A. A., and Seif, M.S., (2005), "The effect of added mass fluctuation on vertical vibration of a TLP", International Journal of Engineering, vol. 18, No 3.
50. Tabeshpour, M. R., B. Ataie Ashtiani, M. S. Seif and A. A.Golafshani, (2006) "Wave Interaction Pitch Response of Tension Leg Structures", 13th International Congress on Sound and Vibration, Austria, Vienna.
51. Tan, S. G. and De Boom, W. C., "The Wave Induced Motions of a Tension Leg Platform in Deep Water", Proceedings of the Offshore Technology Conference, OTC 4074, pp. 89-98, 1983.
52. Taudin, P., "Dynamic Response of Flexible Offshore Structures to Regular Waves", Proceedings of the Offshore Technology Conference. OTC, 3160, pp. 975-986, 1978.
53. Teigen, P. S., Naving, "The Response of a Tension Leg Platform in Short-Crested Waves", Proceedings of the Offshore Technology Conference, Paper No. 4642, p.525-532, 1983.
54. Vickery, P. J., "Wind and wave loads on a Tension leg platform: Theory and experiment", the university of Western Ontario, June 1988.
55. Wheeler, J. D., "Method for Calculating Forces Produced by Irregular Waves", J. of Petroleum Technology, vol. 22, pp. 359-367, 1969.
56. Y. M. Low, 2010, "Influence of the setdown of a tension leg platform on the extreme airgap Response", Applied Ocean Research 32 (2010) 11\_19
57. Y. M. Low, "Frequency domain analysis of a tension leg platform with statistical linearization of the tendon restoring forces", Marine Structures 22 (2009) 480–503

## APPENDIX A

### Newmark's $\beta$ method

The algorithm based on Newmark's  $\beta$  method for solving the equation of motion is given below:

#### First : initial calculations

Step 1. Calculate the stiffness matrix  $[K]$ , the damping matrix  $[C]$ , the mass matrix  $[M]$ , the initial displacement vector  $\{X_o\}$ , and the initial velocity vector  $\{X'_o\}$  is given as the known input data.

Step 2. The force vector  $\{F(t)\}$  is calculated.

Step 3. The initial acceleration vector is then calculated as

$$[m]\{x_o''\} = \{F_o(t)\} - [c]\{x_o'\} - [k_o]\{x_o\} \Rightarrow \{x_o''\}$$

Step 3. Select the time step  $\Delta t$

Step 5. Calculate the method coefficients as

$$[a_1] = \frac{4}{\Delta t}[m] + 2[c], [a_2] = 2[m], a_3 = \frac{4}{\Delta t^2}, a_4 = \frac{4}{\Delta t}, a_5 = \frac{2}{\Delta t}$$

#### second : calculations for each time step

step 6. Calculate the new stiffness matrix  $[\bar{k}]$  and the new force  $\{F(t + \Delta t)\}$

Step 7. Calculate the difference in force.  $\{\Delta F\}$

$$\{\Delta F\} = \{F(t + \Delta t)\} - \{F(t)\}$$

Step 8. Calculate  $\{\hat{\Delta F}\} = \{\Delta F\} + [a_1]\{x_o'\} + [a_2]\{x_o''\}$

Step 9. Calculate the tangent of stiffness matrix

$$[\hat{k}] = [\bar{k}] + a_5[c] + a_3[m]$$

Step 10. Solve to get the difference in displacement as

$$\{\Delta x\} = [\hat{k}]^{-1}\{\hat{\Delta F}\}$$

Step 11. Then we can get the difference in velocity  $\{\Delta x'\}$  and acceleration  $\{\Delta x''\}$  as

$$\{\Delta x'\} = a_5\{\Delta x\} - 2\{x'(t)\}$$

$$\{\Delta x''\} = a_3\{\Delta x\} - a_4\{x'(t)\} - 2\{x''(t)\}$$

Step12. Now we can get the new displacement  $\{x(t + \Delta t)\}$ , velocity  $\{x^\bullet(t + \Delta t)\}$  and acceleration  $\{x^{\bullet\bullet}(t + \Delta t)\}$  as

$$\{x(t + \Delta t)\} = \{x(t)\} + \{\Delta x(t)\}$$

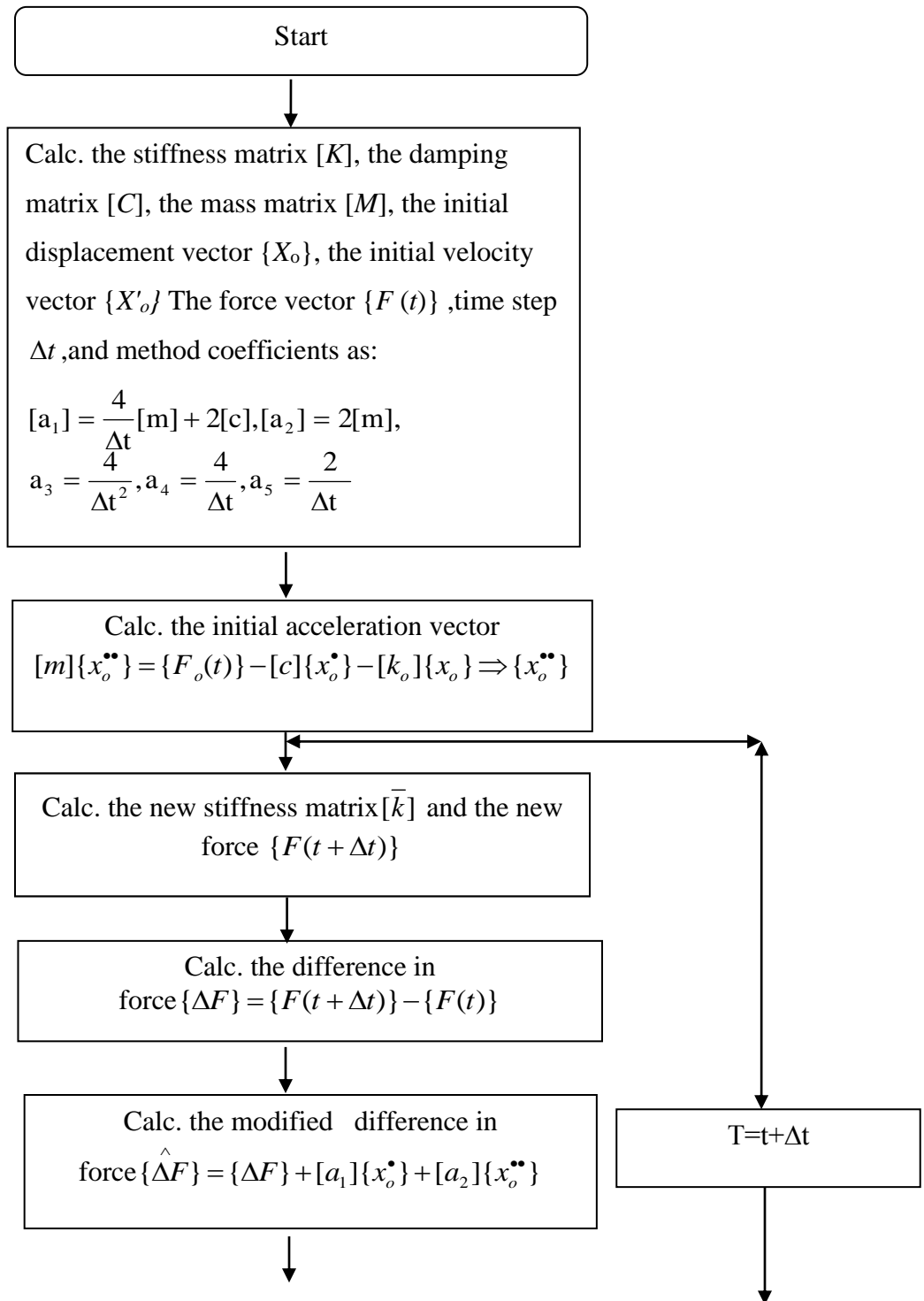
$$\{x^\bullet(t + \Delta t)\} = \{x^\bullet(t)\} + \{\Delta x^\bullet(t)\}$$

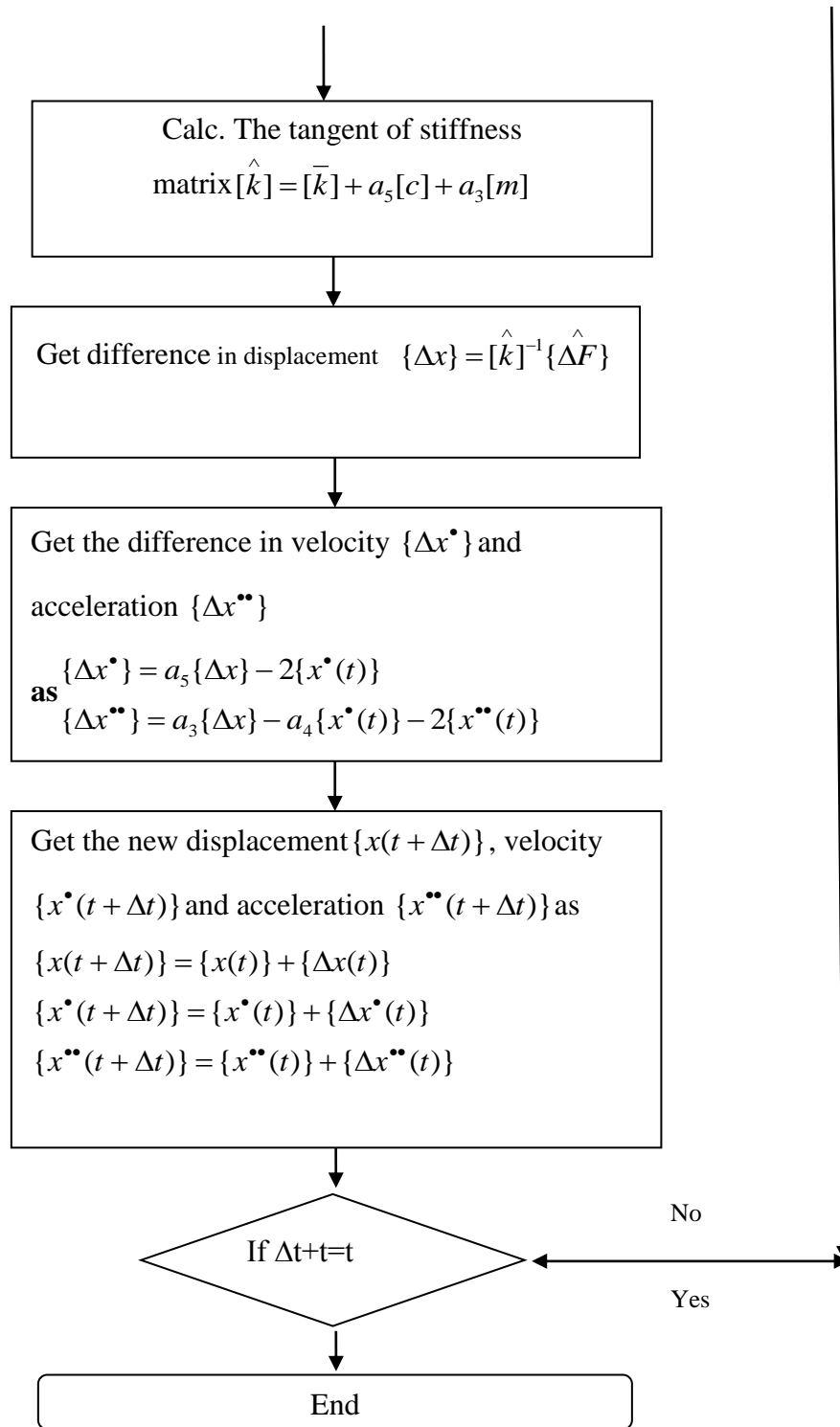
$$\{x^{\bullet\bullet}(t + \Delta t)\} = \{x^{\bullet\bullet}(t)\} + \{\Delta x^{\bullet\bullet}(t)\}$$

Step13. Repetition for the next time step. Replace  $t$  by  $(t + \Delta t)$  and implement steps 6 to 12 for the next time step

## APPENDIX B

### Program flow chart





## **VITA**

### **Amr Ramadan Ibrahim Ali Elgamal**

1El-Rahman mosque St., El Khosos, Cairo

Cairo, Egypt.

Postal Code: 13518

Mobile (+2) 010 0941720

Home (+2) 0229266741

Eng\_amrramadan@yahoo.com

**Structural Administrator**

**Civil Engineer**

### **EDUCATION:**

- 2004, Benha University, Higher Institute Of Technology, Cairo ,  
Egypt.
- B.Sc. Civil Engineering.
- General grade: Very Good with honor degree (80%).(*first student*)
- Project grade:Excellent (99%)

### **Language Skills:**

- ✓ Arabic: mother tongue.
- ✓ English: Very Good command of both written and spoken English language.

### **JOB EXPERIENCE:**

#### **"Teaching"**

- at" B.H.I.T "as structure mechanics adminstrator from 2005 until now and teach alot of subjects like "steel structures design, concrete structure design, strength of material, materials,soil mechanics and foundations".
- at "15 MAY INSTITUTE" 2006-2007.

-at "MODERN ACADEMY" 2007-2008.

### **"RESEARCH"**

- Finishing from graduate courses for master degree.
- Going on preparing experimental work for master degree in the point "*the Hydrodynamic Characteristics of ATension leg platform*".
- Helping in preparing technical papers in "dynamic response of bridges".

### **"Concrete structures design"**

- at "*EWAN,ELTHIATE,NWARA*, design groups in El-Tgmoa El-khams" (many villas and building) Design and site supervision.
- at "*DAR ELANSHA*, design groups in El-Manil" (many villas and building) Design and site supervision.
- at "*EMAC GROUPS* ", design water supply station at Tami El-Amid.
- at "*HISSHAM HAGAGA GROUPS*", design some parts of American university in El-Tgmoa El-khams.
- at "*EHAf GROUPS*", design Sefore town in Sharm El-Shikh.
- at" *MAS GROUPS IN BENHA* ", design a lot of building and tanks.
- at" *EGYPTIAN FOR MALLS*", site supervision at a lot of building in El-Tgmoa El-khams.
- at" *KAFR EL-SHIKH UNION FOR CONSTRUCYION*", site supervision at a lot of building in MADI (repairing and constructions).
- at" *Enviro civic* ", site supervision at alot of building in October and Alex.
- at" *El-safa*" site supervision at alot of building in october and alex.
- at "Benha university "as concrete designer, do report for building and technical office engineer.



## "Steel structure design"

-at" *MAS GROUPS IN BENHA* "design some factories and garage (truss and frames).

-at" *icon* "design some factories and garage (truss and frames).

### **CERTIFICATES:**

<b>Sap2000v.11.04</b> <b>"2d , 3d , static and dynamics"</b>
<b>Etab v.9.5</b> <b>"2d , 3d , static and dynamics"</b>
<b>Safe v.8</b>
<b>Primavera 3</b>
<b>Staadwin 2007</b> <b>"2d , 3d , static and dynamics"</b>
<b>Autocad 2008</b> <b>"2d , 3d"</b>
<b>Ansys 10</b>
<b>Matlap</b>
<b>Fluent in office 2007 word,Excel</b>
<i>Currently studying ABACUS6.7. And preparing for more...</i>

### **INTERESTS:**

Playing Chess,, football, travelling, browsing the web and reading.

**PERSONAL INFORMATION:**

Date of birth: September 07, 1982

Gender: Male

Marital status: Married

Military service: served a year from 2005 to 2006 with honor  
grade.

## المخلص

فى الأونة الاخيرة زاد الاهتمام بدراسة الاستجابة الديناميكية للمنصات البحرية تحت تأثير قوى الامواج لحساب الاستجابة الديناميكية للمنصات البحرية الموجودة فى المياه العميقة (القوى الهيدروديناميكية) التى تحتاج الى اخذ العديد من العوامل فى الاعتبار التى لا نستطيع تحديدها بدقة لأن بها الكثير من العوامل الغير محددة. هذه العوامل الغير محددة لها علاقة بخصائص المنشأ وتحديد الأحمال الناتجة عن الموجات العشوائية للبحر. ولذا فانه من الشائع عمل نموذج رياضى مبسط للحصول على المعلومات الهامة للإستجابة الديناميكية.

من بين هذه المنصات **المنصات ذات الارجل المشدودة** هى اساسا عبارة عن منشأ طافى مربوط بعناصر رابطة. هذه الروابط سابقة الاجهاد "مشدودة مسبقا" نتيجة لتأثير قوى الطفو على المنشأ. وهذا النوع من المنصات البحرية بة ستة درجات من الحرية ثلاث درجات ازاحة فى اتجاه المحاور الثلاث للحركة ( اثنتين فى المستوى الافقى وواحد فى المستوى الراسى) وثلاث درجات دوران حول المحاور الفراغية الثلاثة. وتعتبر اكثر الازاحات تأثيرا فى الاستجابة الديناميكية للمنصة هى الموجودة فى المستوى الافقى حيث ان المنصة مشدودة وذات جساءة عالية فى المستوى الراسى ولذا الازاحة فى المستوى الراسى يمكن اهمالها. وكلما تحركت المنصة أفقيا فإن المركبة الافقية لقوى الشد فى الروابط تعمل على منع الحركة وارجاع المنصة إلى وضعها الاصلى.

ان حساب القوى الهيدروديناميكية نتيجة لقوى الموجات فى العناصر الإنشائية للمنصة ذات الارجل المشدودة حيوى من الناحية الاقتصادية والأمنة للتصميم.

العديد من الأبحاث قدمت العديد من الطرق والأساليب لحساب القوى والخصائص الديناميكية المنقولة لكل من المنصات البحرية المستطيلة والمثلثة الشكل فى الأعماق المختلفة.

فى هذه الرسالة تم عمل تحليل ديناميكى لكلا من المنصات البحرية ذات الارجل المشدوده المثلثة والمستطيله تحت تأثير قوى فى اتجاه واحد هو اتجاه المحور الطولى.

نتيجة التغير فى الموجه من حيث الارتفاع والزمن الدورى فى حالة وجود ارتباط بين درجات الحرية وفى عدم وجوده.

ولقد تم حساب القوى على العناصر باستخدام معادلة "مورسن" المعدله وباستخدام النظرية الموجية الخطية "ايرى" وتم حساب الاستجابة الديناميكية باستخدام طريقة " نيومارك بيتا التكاملية" فى المدى الزمنى.

ومن النتائج لوحظ ان الارتباط بين درجات الحرية المختلفة يؤثر بشده على سلوك المنصات البحرية ذات الارجل المشدوده كما لوحظ ان الاستجابة الديناميكية للمنصات البحرية المثلثة اكبر من الاستجابة البحرية للمنصات المستطيله.

فى النهاية نوصى بضرورة الاخذ فى الاعتبار فى الابحاث المستقبلية كلا من الموجات العشوائية والقوى المائله وتأثير تربيئة الرياح على المنصات البحرية.

وقد اشتملت هذه الرسالة على خمسة ابواب كالتالى :

**الباب الاول:** يحتوى هذا الباب على مقدمة عن المنصات البحرية والتعرف على انواعها المختلفه وخصوصا المنصات البحرية المشدوده كما تم عمل مسح لعدد من الابحاث السابقة.

**الباب الثانى:** يحتوى على مقدمة عن الموجات البحرية ونظرياته المختلفه وخصوصا الخطية " نظرية أبرى " كما نبين القوى المؤثره على المنشآت المعرضة لقوى هيدروديناميكية وكيفية حسابها عن طريق " معادلة مورسن".

**الباب الثالث:** يحتوى على تفصيل موضح للمنصات البحرية المشدوده سواء المثلثة او المستطيله من حيث كيفية حساب الكتلة والجسائة والقوى ومعامل الترخيم وفى النهاية كيفية عمل التحليل الرياضى باستخدام " طريقة نيومارك بيتا".

**الباب الرابع:** يحتوى على النموذج محل الدراسه والنتائج والتعليق عليها.

**الباب الخامس:** ويحتوى على النتائج والتوصيات الواجب توافرها فى الابحاث المستقبلية.

وافق الاستاذ الدكتور / نائب رئيس جامعة بنها على تشكيل لجنة مناقشة والحكم من  
السادة :-

- ١- أ.د/ السيد سعد عبد السلام أستاذ بقسم الهندسة المدنية – جامعة الزقازيق "ممتحن خارجي ورئيسا"
- ٢- أ.د/ محمد عباس قطب أستاذ بقسم الهندسة البحرية – جامعة الاسكندرية "ممتحن خارجي"
- ٣- أ.م.د/ اشرف محمد ابو ريان أستاذ مساعد بقسم الهندسة المدنية – المعهد العالى – جامعة بنها "مشرفا رئيسيا"
- ٤- أ.م.د/ ايمن احمد سليمه أستاذ مساعد بقسم الهندسة الإنشائية – كلية الهندسة – جامعة طنطا " مشرف"

لفحص الرسالة المقدمة من المهندس / عمرو رمضان ابراهيم على الجمال  
للحصول على درجة الماجستير فى تكنولوجيا الهندسة المدنية

وكيل المعهد للدراسات العليا  
أ.د / محمد انور راضى

الدراسات العليا

# السلوك الديناميكي للمنصات البحرية ذات الارجل المشدودة المعرضة للقوى الهيدروديناميكية

رسالة مقدمة من

المهندس / عمرو رمضان ابراهيم على الجمال  
إلى المعهد العالي للتكنولوجيا - جامعة بنها

كجزء من متطلبات الحصول علي درجة الماجستير  
في تكنولوجيا الهندسة المدنية

اعتمدت و أجزت من السادة الممتحنين

( ممتحناً خارجياً و رئيساً )

.....

أ.د./ السيد سعد عبد السلام  
أستاذ بقسم الهندسة المدنية – جامعة الزقازيق

( ممتحناً خارجياً و عضواً )

.....

أ.د./ محمد عباس قطب  
أستاذ بقسم الهندسة البحرية – جامعة الإسكندرية

( مشرفاً و عضواً )

.....

أ.م.د/ أشرف محمد أبوريان  
أستاذ بقسم تك الهندسة المدنية بالمعهد العالي للتكنولوجيا- جامعة بنها

( مشرفاً و عضواً )

.....

أ.م.د/ أيمن أحمد سليمة  
أستاذ مساعد بقسم الهندسة الإنشائية - جامعة طنطا

( رئيس القسم )

.....

اعتمدت من قسم تكنولوجيا الهندسة المدنية  
أ.م.د/ أحمد حسن عبد الكريم

( وكيل المعهد للدراسات العليا )

.....

اعتمدت من الدراسات العليا  
أ.د./ محمد انور راضى



جامعة بنها  
المعهد العالي للتكنولوجيا

# السلوك الديناميكي للمنصات البحرية ذات الارجل المشدودة المعرضة للقوى الهيدروديناميكية

رسالة مقدمة من

عمرو رمضان ابراهيم على الجمال

المعيد بقسم الهندسة المدنية – المعهد العالي للتكنولوجيا – جامعة بنها

كجزء من  
متطلبات الحصول علي درجة

الماجستير  
في  
تكنولوجيا الهندسة المدنية

تحت إشراف

أ.م.د/ أيمن أحمد سليمة  
أستاذ مساعد بقسم الهندسة الإنشائية  
كلية الهندسة  
جامعة طنطا

أ.م.د/ أشرف محمد أبوريان  
أستاذ مساعد بقسم الهندسة المدنية  
المعهد العالي للتكنولوجيا  
جامعة بنها

ابريل ٢٠١١